2005

A study of effects of aggregate on concrete rheology

Jiong Hu
Iowa State University

A study of effects of aggregate on concrete rheology

by

Jiong Hu

A dissertation submitted to the graduate faculty

in partial fulfillment of the requirements for the degree of

DOCTOR OF PHILOSOPHY

Major: Civil Engineering (Civil Engineering Materials)

Program of Study Committee:
Kejin Wang, Major Professor
James K. Cable
Halil Ceylan
Kristen P. Constant
David J. White

Iowa State University

Ames, Iowa

2005

Graduate College
Iowa State University

This is to certify that the doctoral dissertation of

Jiong Hu

has met the dissertation requirements of Iowa State University

Signature was redacted for privacy.

Committee Member

Signature was redacted for privacy.

Committee Member

Signature was redacted for privacy.

Committee Member

Signature was redacted for privacy.

Committee Member

Signature was redacted for privacy.

Major Professor

Signature was redacted for privacy.

For the Major Program

TABLE OF CONTENTS

LIST OF FIGURES

LIST OF TABLES

ABSTRACT

Concrete rheology is important because it affects the workability and uniformity of fresh concrete as well as the properties of the hardened concrete. In this dissertation, new models for predicting mortar and concrete rheological properties were developed.

The present study includes both experimental and modeling work. In the experimental study, mortar and concrete specimens were prepared with consideration of three factors: paste or mortar rheology, aggregate properties, and aggregate content. The aggregate properties were characterized with the uncompacted void content and friction angle. Effects of these aggregate properties on mortar and concrete rheology were studied using a Brookfield and portable IBB rheometer, respectively. Using the artificial neural network as a tool to analyze the test data, the relative degree of importance of the factors that influence mortar and concrete rheological behavior were evaluated, and the important factors were then considered in the proposed models. The experimental results indicated that aggregate with low uncompacted void content generally provided the concrete with low yield stress and viscosity, while aggregate with high friction angle generally resulted in high yield stress and viscosity.

In the modeling study, concrete was considered as a two-phase material, consisting of mortar and coarse aggregate. Mortar and concrete rheological behavior was assumed mainly controlled by (1) the excess paste/mortar thickness of fine/coarse aggregate, and (2) the friction between the aggregate particles. The excess paste/mortar thickness and aggregate friction were calculated and used to develop functions that relate to mortar and concrete rheology. Statistical analyses were performed on the test data to obtain specific relationships between the concrete rheology parameters and the paste/mortar properties as well as the excess paste/mortar thickness in the concrete. The modeling results demonstrated that the predicted concrete rheological parameters had very good correlations with the measured results. It is expected that the developed models can be used not only for concrete rheology prediction but also for designing concrete mixtures with improved rheology.

Keywords: aggregate, mortar, concrete, rheology, modeling

CHAPTER 1. INTRODUCTION

In present study, the rheology of a series of paste, mortar, and concrete mixtures with different aggregates are measured by paste/mortar and concrete rheometers, respectively. Based on the experimental results, two-phase theory, and the excess thickness theory, new models has been developed to predict mortar and concrete rheology considering the effect of aggregate including size, gradation, shape and surface texture. The developed models can directly help the concrete industry to predict concrete rheology from mix design, and more importantly, to design concrete mixtures to obtain desired flowability.

1.1 Background

Fresh concrete properties, especially workability, significantly affect transporting, placing, and compacting concrete; thus, these properties have significant effects on the quality and cost of concrete construction. They also potentially determine certain hardened concrete properties, such as uniformity, strength and durability. One particularly important fresh concrete property is workability. Based on the American Concrete Institute (ACI) (ACI Committee 116, 2000), workability is defined as "the property of freshly mixed concrete or mortar that determines the ease with which it can be mixed, placed, consolidated, and finished to a homogenous condition". Concrete must have proper flowability, or rheology, in order to obtain desirable workability. The rheology of concrete is a quantitative property that describes concrete deformation and flow. Concrete rheology also provides important information on other aspects of concrete workability, such as segregation resistance. Research has shown that a suitable range of rheology is helpful to prevent segregation (Assaad et al., 2004; Petrou et al., 2000a, 2000b). The rheology study can also determine the design in pumped concrete. The fluidity of the vibrated concrete, determined from the rate of efflux from the pipe, is controlled by the peak velocity of the vibration and influenced by the rheology of the unvibrated concrete (Banfill et al., 1999).

Concrete is one of the most widely used building materials. The importance of studying concrete rheology has been understood for many years, because the ease of flow and

placement can significantly reduce costs and allow more flexibility in architectural and structural design. The rheology of concrete can be affected by different factors: mix proportions, characteristics of the cement, aggregate properties, amount and type of admixtures, time, temperature, and mixing condition. Among all these factors, aggregate properties are the most important because the aggregate normally occupies up to 70-80 percent of the total concrete volume of concrete. The flowability of concrete can be significantly changed by using different aggregates. The aggregate directly affects the flowability of concrete through interparticle forces (such as interlocking and friction of solid particles) and the movement of solid and liquid phases inside fresh concrete mixtures. Several factors, such as size, type, gradation and texture of aggregates, also affect the properties of fresh concrete. The study of the effect of aggregate on concrete rheology is still very limited, and no efficient concrete rheology model considering the effect of aggregate had been developed so far.

Various models have been developed to predict the rheological parameters of concrete from the composition, but the application of existing models are often restricted due to one or more of the following reasons:

- Some models are empirical models, which are not suitable for common situations. Most of the existing models do not have enough theoretical analysis or the derivation is too complicated, involving a tremendous and impractical amount of calculation and computer simulation.
- Some of the models are not directly related to rheological parameters, due to the limitation of rheology measurement equipment.
- Some of the models just relate to one parameter of rheology, which is insufficient to reflect the flowability of concrete.
- Aggregate properties, including shape and texture, are rarely included in the models.

1.2 Objectives

The goal of this study is to develop a model to predict concrete rheological properties based on paste rheology, aggregate properties and mix design parameters. Three objectives of present research are:

1. To determine parameters that characterize aggregate properties;
2. To quantitatively study aggregate effect on concrete rheology; and
3. To develop rheology model for prediction of concrete rheological behavior.

1.3 Research Approach

In order to ensure a successful model, the overall research strategy schematically outlined below in Figure 1-1 was used in present research.

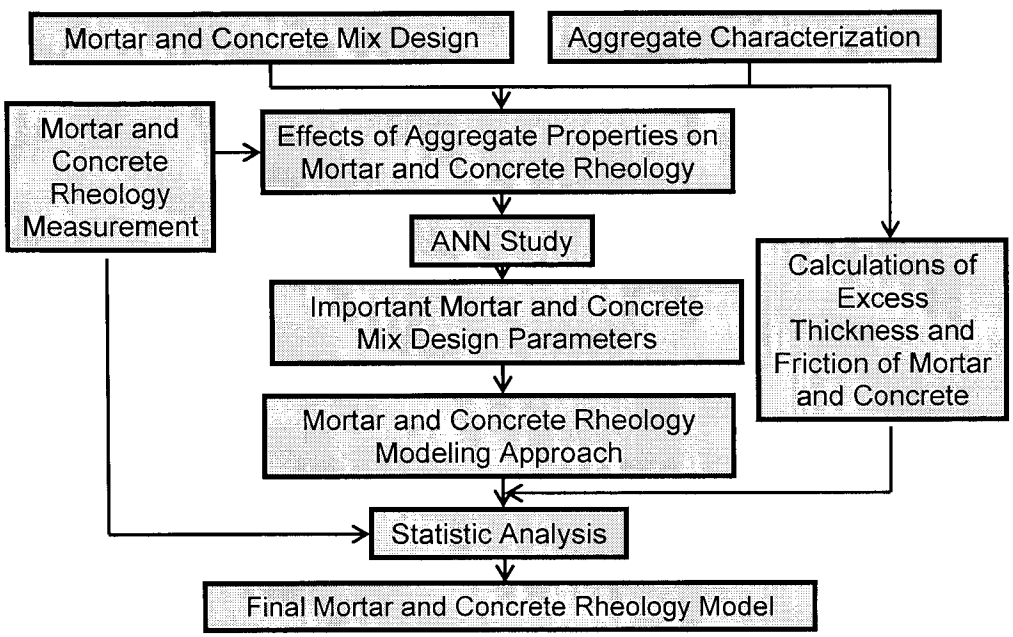

Figure 1-1 Flowchart of concrete rheology model development

Different mortar and concrete materials, including type I/II Portland cement, fine aggregate (type, size and gradation), and coarse aggregate (size and gradation) were selected for this study. According to factorial mix design, specimens with different mortar and concrete mixes

were prepared in a consideration of three factors: paste or mortar rheology properties, aggregate gradation and aggregate content. Different sizes (fineness), gradations, shapes and surface textures of fine and coarse aggregate were characterized according to both uncompacted void content test and friction angle test. The effect of aggregate properties of on mortar and concrete rheological properties were measured by a Brookfield and a portable IBB rheometer, respectively. Based on the test data, the importance of factors that influence mortar and concrete rheology were evaluated by artificial neural network (ANN) analysis. According to the excess paste theory and consider concrete as a two-phase material of mortar and coarse aggregate, the excess paste thickness of fine aggregate, and excess mortar thickness of coarse aggregate were calculated based on mortar and concrete mix design and aggregate characterization. The rheology contributed from spacing and paste or mortar rheology was then calculated based on microstruction of mortar and concrete related to excess thickness. The rheology contributed from aggregate friction was calculated based on the measured fine aggregate friction angle. Together with the measured matrix (paste or mortar) rheology from identical mix design and by comparison with actual measured mortar and concrete rheology, the mortar and concrete rheology model was finalized according to statistical regression analysis.

1.4 Scope of Dissertation

Nine chapters, including the experimental work and modeling, are presented in this dissertation. The experimental studies include aggregate characterization and rheology measurements of paste, mortar, and concrete. The modeling includes the rheology models for both mortar and concrete.

Chapter 2 contains a literature review, which serves to provide the necessary background and terminology on concrete rheology. The utilization of different equipment for concrete workability measurement, especially the rheometer, will be summarized. The factors that influence concrete rheology, especially aggregate effect, will also be reviewed. This section will further provide a summary of current models to predict concrete rheology from mix composition, especially considering the aggregate effects.

In Chapter 3, the laboratory work is described. The lab methods, including the measurement of aggregate properties, cement paste, mortar and concrete rheology, are presented. The materials information for the different mixtures are all presented in this chapter as well. All of the test procedures are listed and the experimental program design is described.

Chapter 4 summarizes the information collected during the aggregate testing phase of this study. Fine aggregate and coarse aggregate properties are presented and analyzed.

Chapter 5 presents the experimental study of the effect of water-to-cement ratio (w/c) and mixing procedure on cement paste rheological performance. Statistical equations for the effect of w/c on rheological parameters of cement pastes are also developed.

Chapter 6 concentrates on the mortar rheology study. Two kinds of fine aggregate (limestone and riversand) and a wide range of w/c and sand-to-cement ratio (s/c) for mortar mix design are used. The effect of fine aggregate size, type and gradation are studied through the rheology tests.

In Chapter 7, the results of the concrete rheology study are presented. In this chapter, coarse aggregate proportion, size and gradation are studied using the concrete rheometer and the slump test.

In Chapter 8, models are developed to predict mortar and concrete rheology from aggregate properties. Certain parameters, including excess paste and mortar thickness and aggregate friction angle, are considered in the model. Theoretical and statistical analysis is used during this stage.

Finally, Chapter 9 provides a summary of this research, offers overall conclusions from this study, and provides recommendations for future research.

Eight appendices are included at the end of the dissertation, which contain some additional results obtained during this study and the ANN and statistical analysis used in the model development stages.

CHAPTER 2. LITERATURE REVIEW

2.1 Introduction

Concrete is a composite material composed of a coarse granular material (the aggregate) embedded in a matrix of material (the cement paste) that fills the space between the aggregate particles and glues them together. Fresh concrete properties, such as workability, are important mainly because they can affect the choice of equipment for handling and consolidation and also influence the properties of hardened concrete.

Concrete workability is often used to describe different aspects of fresh concrete, such as: consistency, flowability, mobility, pumpability, compactibility, finishability, and harshness. These terms are qualitative and subjective, and therefore the term of concrete rheology was applied to describe concrete flowability.

Gjorv (1998) reported that the measurement of the rheological parameters could be used to evaluate the flowability and the compatibility of the fresh concrete. Yen et al. (1999) found that the application of a rheological method could provide more stable results than any other test method in describing the flowability of concrete. Noguchi et al. (1999) had also successfully used a rheological approach to assess the ability of self-consolidating concrete (SCC) to pass between reinforcing bars according to the clearance between them, the volume of aggregate and the rheological properties of matrix. Martys and Ferraris (2003) used dissipative particle dynamics (DPD) models to simulate the complex concrete flow inside a coaxial rheometer and between rebars.

Viscosity is an important rheological parameter in determining the tendency for coarse aggregates to segregate (Tang et al., 2001). In general, fresh concrete made with mortar with high viscosity may reduce flowability, but low viscosity may cause aggregate segregation. The fact that the viscosity of concrete can be directly related to the resistance to segregation is extremely important in SCC. A suitable range of viscosity is required to produce SCC (Assadd et al., 2004; Bonen and Shah, 2005). Saak recommended that there should be a

rheological self-flow zone (SFZ), which can be determined by the theoretical segregation limit (Saak et al., 2001). A numerical approach has also been developed to determine viscosity-dependent segregation in fresh concrete (Bilgil et al., 2005). Rheology parameters can also be helpful in SCC design when considering the segregation effects. Petrou et al. (2000a) studied the effect of mortar rheology on aggregate settlement. Ravindrarajah et al. (2003) found that partially replacing aggregate with fly ash could produce SCC with low segregation potential. Ho et al. (2002) showed that limestone powder can be successfully used to control the segregation potential and deformability of fresh SCC, while a higher dosage of superplasticizer was used to achieve similar flow properties.

Banfill et al. (1999) used the parameter of viscosity to determine fluidity of concrete in pump concrete, and the relationship between the rheology of unvibrated fresh concrete and its flow under vibration in a vertical pipe apparatus was established. Concrete rheology can also be used in some special applications; for example, Pfeuffer and Kusterle (2001) established a correlation between the rheological characteristics and the rebound of dry-mix shotcrete, which allowed a simple, fast assessment to be made of the effect of individual admixtures or additives in minimizing rebound in the laboratory before conducting any spray experiments at construction site.

A literature review focuses on the factors affecting concrete rheology (especially aggregate effects), concrete rheology measurement and models is presented in this chapter. Proposed factors and theories usable for a modeling study are found at the end of this chapter.

2.2 Fundamentals of Concrete Rheology

2.2.1 Basic Principles of Rheology

Rheology is the science of the deformation and flow of matter, and the emphasis on flow means that it is concerned with the relationships between stress, strain, rate of strain, and time. Concrete in its fresh state can be considered as a fluid and therefore the basic principles of rheology can be applied to this material (Barnes et al., 1989).

The simplest fluid is one that obeys Newton's law of viscous flow, which can be described as:

$$\tau = \eta\dot{\gamma} \qquad \textbf{Equation 2-1}$$

In this equation τ is the shear stress (Pa), η is the coefficient of viscosity (Pa·s), and $\dot{\gamma}$ is the rate of shear (shear rate) or the velocity gradient (s^{-1}).

The flow behavior of any fluid requires the measurement of the relationship between shear stress and shear strain rate of the material, which is normally called the flow curve. As shown in Figure 2-1 (a), the Newtonian liquid described in Equation 2-1 can be represented with a plot of the shear rate versus the shear stress that has a straight line passing through the origin, with a slope of η.

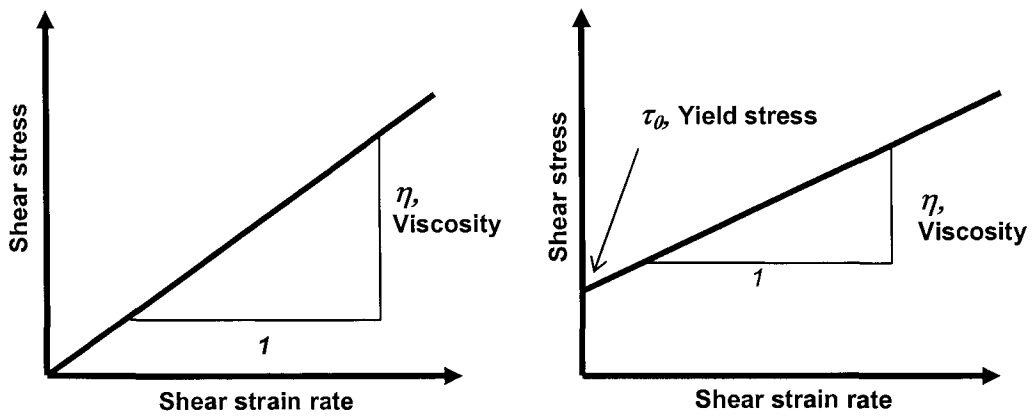

(a) Newtonian model **(b) Bingham model**

Figure 2-1 Newtonian model and Bingham model

For a very diluted suspension of solids in a liquid, there is no interparticle force; and the effect of small increases in the amount of suspended solid is merely to increase the coefficient of viscosity. Nevertheless, concrete has to be considered as a very concentrated suspension, in which the volume ratio of solids-to-water would be as high as around 4.5:1. For such concentrated materials, there are forces acting between the particles. This does not merely change the viscosity, but actually changes the type of flow. Tattersall and Banfill (1983) carried out systematic investigations in the rheology of concrete. They found that

there was a linear relationship between torque and the rotation speed of the viscometer after a certain torque had been exceeded. They stated that concrete flow could be expressed by the Bingham model. As seen in Figure 2-1 (b), concrete has a yield stress, which indicate the minimum stress to start a flow of a material. The material obeys Bingham model and can be written as:

$$\tau = \tau_0 + \eta\dot{\gamma} \qquad \textbf{Equation 2-2}$$

In this equation τ_0 is the yield stress (Pa) and η is the plastic viscosity (Pa·s).

Both parameters should be used in order to fully describe the rheology of the materials that obeys Bingham's model, because some materials may have the same viscosity but different yield stresses or the same yield stress but different viscosities.

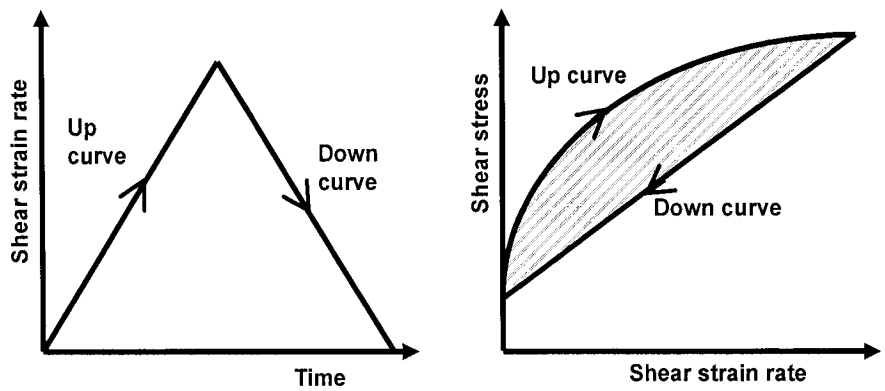

(a) Shear rate vs. time **(b) Shear rate vs. shear stress**

Figure 2-2 Thixotrophy behavior and hysteresis loop

Another important parameter of rheology is thixotrophy. As shown in Figure 2-2, a thixotropic fluid undergoes a decrease in viscosity with time, while it is subjected to constant shearing. The shear rate was first increased to a certain value, then immediately decreased to the starting point. The "down" curve as shown in Figure 2-2 lies beneath "up" curve. This "hysteresis loop", the area between the up and down curves (as shown in the shade area in Figure 2-2 (b)), is caused by the decrease in the fluid's viscosity with increasing time of shearing resulting from the material's structural breakdown. Generally, the larger the "hysteresis loop" area, the higher degree that the material structure is broken down (Banfill,

2003). Some thixotropic fluids, if allowed to stand undisturbed for a while, can regain their initial viscosity, while others can not. This behavior is due to interparticle attraction and weak bonds.

2.2.2 Flow Curve Equations

A great deal of research has been conducted to study the flow behavior of cementitious materials. Figure 2-3 shows the most commonly used types of curves that express the stress and shear rate relationship of cementitious materials.

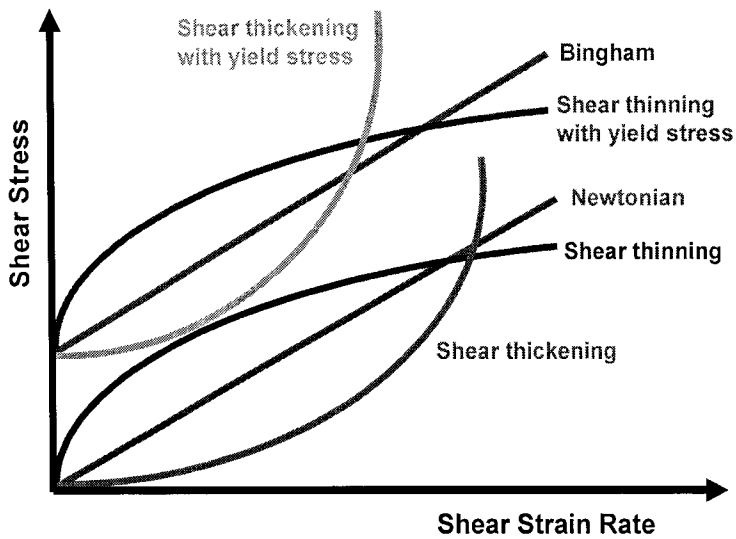

Figure 2-3 Common used flow curves (after Ferraris and de Larrard, 1998)

As shown in this figure, Newtonian liquid has a constant viscosity. A Bingham material needs to overcome the yield stress to initial flow, and its plastic viscosity is also constant. In a shear thickening material, viscosity increases continuously with shear rate, while viscosity decreases continuously with shear rate. In the material having shear thinning with yield stress, viscosity decreases with shear rate once the yield stress has been exceeded.

The flow curves can be described with various relationships between shear stress and shear rate as summarized in Table 2-1. The Power equation can be used to describe shear thinning ($n<1$) or shear thickening ($n>1$) behavior. The Herschel-Bulkley equation can be used for the case of shear thinning or shear thickening with yield stress.

Table 2-1 Equations relating shear stress and shear rate

Model	Equation	Reference
Newtonian	$\tau = \eta\dot{\gamma}$	Ferraris, 1999; Papo, 1988
Power equation	$\tau = A\dot{\gamma}^n$	Ferraris, 1999;
Bingham	$\tau = \tau_0 + \eta\dot{\gamma}$	Ferraris, 1999; Nehdi and Rahman, 2004
Herschel-Bulkley	$\tau = \tau_0 + K\dot{\gamma}^n$	Ferraris, 1999; Papo, 1988; Nehdi and Rahman, 2004
Modified Bingham	$\tau = \tau_0 + \eta\dot{\gamma}^{n_1} + A\dot{\gamma}^{n_2}$ $\tau = \tau_0 + \eta\dot{\gamma} + A\dot{\gamma}^2$	Ferraris, 1999 Nehdi and Rahman, 2004
Casson	$\tau = \tau_0 + \eta_\infty\dot{\gamma} + 2(\sqrt{\tau_0\eta_\infty})\sqrt{\dot{\gamma}}$	Papo, 1988; Nehdi and Rahman, 2004; Papo and Piani, 2004a
Generalized Casson	$\tau^m = {\tau_0}^m + [\eta_\infty\dot{\gamma}]^m$	Papo and Piani, 2004a
Papo-Piani	$\tau = \tau_0 + \eta_\infty\dot{\gamma} + K\dot{\gamma}^n$	Papo and Piani, 2004a
De Kee	$\tau = \tau_0 + \eta\dot{\gamma}e^{-\alpha\dot{\gamma}}$	Yahia and Khayat, 2001
Yahia-Khayat	$\tau = \tau_0 + 2(\sqrt{\tau_0\eta_\infty})\sqrt{\dot{\gamma}e^{-\alpha\dot{\gamma}}}$	Yahia and Khayat, 2001
Vom Berg	$\tau = \tau_0 + B\sinh^{-1}(\dot{\gamma}/C)$	Ferraris, 1999; Papo, 1988
Ostwald-De Waele		
Eyring	$\tau = a\dot{\gamma} + B\sinh^{-1}(\dot{\gamma}/C)$	Ferraris, 1999; Papo, 1988
Robertson-Stiff	$\tau = a(\dot{\gamma} + C)^b$	Ferraris, 1999; Papo, 1988; Jones and Taylor, 1977
Atzeni	$\dot{\gamma} = \alpha\tau^2 + \beta\tau + \delta$	Ferraris, 1999; Papo, 1988
Williamson	$\tau = \eta_\infty\dot{\gamma} + \tau_f\frac{\dot{\gamma}}{\dot{\gamma} + \Gamma}$	Papo, 1988
Sisko-Ellis	$\tau = a\dot{\gamma} + b\dot{\gamma}^c$ (c<1) $\eta = \eta_\infty + K\dot{\gamma}^{n-1}$	Papo, 1988; Atzeni et al., 1985; Nehdi, 2004
Shangraw-Grim-Mattocks	$\tau = \tau_0 + \eta_\infty\dot{\gamma} + \alpha_1[1 - \exp(-\alpha_2\dot{\gamma})]$	Papo, 1988

Variable definitions:

τ = shear stress (Pa), $\dot{\gamma}$ = shear rate (s^{-1}), τ_0 = yield stress (Pa), η = viscosity (Pa·s), τ_f = intercept of the asymptote of the flow curve with the τ axis (Pa), η_∞ = viscosity at infinite shear rate (Pa·s), Γ = parameter which governs the deviation from Binghamian behavior (s^{-1}), A, a, B, b, C, c, K, M, n_1, n_2, α, α_1, α_2, β, δ = constants

Several researchers have compared the equations describing flow curves of cementitious materials (Atzeni et al., 1985; Papo, 1988; Nehdi and Rahman, 2004). All of the relationships

listed in Table 2-1 (except Newton model) used at least two parameters to describe the flow. Struble and de Larrard (1998) found that concentrated suspensions such as concrete processes yield stress. Those equations that have a term of yield stress (such as the Bingham model, Herschel-Bulkley model, and Casson model, etc.) have a physical basis, while some equations contain more than two parameters (such as the Herschel-Bulkley equation, which has an exponent term "*n*") without exact physical meanings.

Different models may only suitable for certain range of material or measurement. Some researchers stated that the Herschel-Bulkley model is more suitable than the Bingham model for certain concretes like SCC (de Larrard et al., 1998). Atzeni et al. (1985) compared the rheological properties of Portland cement pastes using different mathematical models; and he found that the best results were obtained with Eyring's equation, Herschel-Bulkley's equation and the parabolic equation, while Vom Berg's model only holds for low shears. Jones and Taylor (1977) stated that the Robertson-Stiff model might be used to predict the relationship for the whole range of w/c considered while the Herschel-Bulkley model can only predict shear stress shear and rate data for a limited range of w/c. However, fresh concrete, including cement paste and mortar, is most commonly described using the Bingham model because the flow of most concrete follows this equation fairly well (Tattersall and Banfill, 1983) and the two parameters in Bingham model; yield stress and viscosity, can be measured independently.

Various factors may affect the shape of the flow curve of cementitious materials, including testing equipment, testing time, experiment duration and procedure (Shaughness and Clark, 1988; Banfill and Saunders, 1981; Roy and Asaga, 1979). The shear thickening phenomenon can also occur simultaneously with shear thinning (Vom Berg, 1979). When more networks in the material are destroyed, the shear resistance between the flow layers of the material is lower. Thus, the apparent viscosity decreases and shear thinning behavior is observed.

2.2.3 Rheology of Cement-Based Materials

Table 2-2 shows the normal range of rheological parameters of cementitious materials based on the Bingham model. From cement paste to concrete, the yield stress and plastic viscosity increases as the particle size increases. Tattersall and Banfill (1983) pointed out that this was because the aggregate could resist stresses without deformation. Since the aggregate occupies up to 70-80% of concrete volume, the yield stress of concrete is higher then cement paste which has no aggregate inside. Concrete yield stress also increases with aggregate content. Due to the increased interparticle contact and surface interlocking, the plastic viscosity of concrete increases when the particle size increases. It is also partly due to the incapability of the aggregate to be sheared. When concrete is subjected to a shear stress, since the solid aggregate particles can not deform, the shear rate within the solid aggregate particles is zero. As a result, in order to have a certain shear rate in the whole composite, the shear rate in paste is higher compared to the material with just pure cement paste. This higher shear rate results in a higher stress and resistance to flow in the paste that in turn accounts for the increase in measured plastic viscosity of the bulk material.

Table 2-2 Rheological parameters of cementitious material (adopted from Banfill, 2003)

Material	Paste	Mortar	SCC	Flowable Concrete	Pavement Concrete
Yield Stress (Pa)	10-100	80-400	50-200	400	500-2000
Plastic Viscosity (Pa·s)	0.01-1	1-3	20-100	20	50-100

2.3 Test Method Relate to Workability of Concrete

The choosing of suitable rheology measurement methods is very important, because the success of a concrete rheology model in a large degree depends upon whether the test methods can completely and accurately reflect the rheology performance of concrete. A large number of workability tests have been proposed over the years since the early 20th century. Koehler and Fowler (2003) summarized previously developed equipments, and up to 61 different test methods for measuring concrete workability were described in the report.

However, most of the test methods are empirical, and only a few of them have been incorporated into standards, the rest have received very limited use.

With the exception of the most widely used slump test, which can only measure the consistency of concrete, most of the other tests have in general failed to gain common acceptance. Even with the increase in understanding of concrete rheology, the slump test remains the predominately used test method for measuring concrete workability. As mentioned, concrete workability can be best characterized in terms of the rheological parameters in the Bingham equation. The flow of a granular material like concrete is defined by at least two parameters for instance yield stress and plastic viscosity as defined by the Bingham equation. However, the measurements are not easy to obtain although the theory exists. While there are many tests to characterize the flow of concrete, not many give results in fundamental units and therefore the measured rheological properties of concretes, using different tests, cannot be directly compared. New tests have recently been developed which attempt to characterize concrete using a more elementary approach. While not all researchers agree on which test is the most appropriate for the wide range of concretes in use today, it is generally agreed that tests which can give results in fundamental units which can be used on construction site are needed.

2.3.1 Principles of Workability Measurement

The term workability is broadly defined, which includes the properties of placing, compacting and finishing. No single test method measures all aspects of workability. Numerous test methods have been developed since the 1920s, but the principle of measuring concrete flow curves in terms of shear stress and shear rate was not established until concrete was considered as Bingham material (Tattersall and Banfill, 1983). Many of the new test methods developed since the establishment of concrete as a Bingham fluid have attempted to measure yield stress and plastic viscosity. The large number of workability test methods can be divided into categories based on several different classification schemes. Tattersall (1991) broadly splits the assessment of workability into three classes, as shown in Table 2-3. The majority of workability test methods fall into Class II and Class III.

Table 2-3 Classes of workability measurement (adopted from Tattersall, 1991)

	Examples	Definition
Class I: Qualitative	Workability, Flowability, Compactability, Finishability, Pumpability, etc.	To be used only in a general descriptive way without any attempt to quantify
Class II: Quantitative Empirical	Slump, Compacting Factor, Vebe Time, Flow Table Spread, etc.	To be used as a simple quantitative statement of behavior in a particular set of circumstances
Class III: Quantitative Fundamental	Viscosity, Mobility, Fluidity, Yield Value, etc.	To be used strictly in conformity with standard definitions

In order to properly define the rheology of concrete, both yield stress and viscosity must be measured. The existing test methods for concrete can also be divided into two categories as shown in Table 2-4 in regard to whether the output of the experiment gives one or two of these parameters according to Ferraris (1999).

In Table 2-4, a single-factor test can measure only one of the factors of rheological parameters and therefore provides an incomplete description of workability. For example, the slump test only provides information of the yield stress. Two-factor tests, which can measure multiple points on the flow curve, normally by varying the shear rate, can provide a more complete description of concrete rheology. Single-factor tests are generally intended to be simple and rapid; though they do not provide information on both yield stress and viscosity. The tradeoff between single-factor tests and two-factor tests is usually that single-factor tests are simpler (although they are less complete). Single-factor tests may sometimes be appropriate for certain type of concrete mix or a certain application even though the test can not fully measure fundamental rheological parameters. Single-factor tests generally fall into Class II of Tattersall's scheme, which can provide a direct or indirect measurement of yield stress, plastic viscosity, or some other property; whereas two-factor tests fall into Class III, which can typically measure yield stress and plastic viscosity, or closely related values.

Table 2-4 Single and multi-factor workability tests (after Ferraris, 1999[1])

	Test methods
One-factor tests	Slump, flow table test (DIN), penetrating rod (Kelly ball, Vicat, Wigmore test), K-slump test, turning tube viscometer, Ve-Be time or remolding test, LCL apparatus; vibration testing apparatus; filling ability (flow cone, Orimet apparatus)
Two-factors tests	Two-point test, Bertta apparatus, BTRHEOM rheometer, modified slump cone test, IBB rheometer, vibration slope apparatus (VSA), BML viscometer, ICAR

2.3.2 Category and Descriptions of Test Methods

Workability test methods can also be classified in terms of the type of measurement principle during the test. The National Institute of Standards and Technology (NIST) divided existing rheology test methods into four broad categories (Hackley and Ferraris, 2001). The definitions of the four categories are listed in Table 2-5.

Table 2-5 NIST categorization of concrete rheology test methods (adopted from Hackley and Ferraris, 2001)

Category	Definition
Confined Flow Tests	The material flows under its own weight or under an applied pressure through a narrow orifice.
Free Flow Tests	The material either flows under its own weight, without any confinement or an object penetrates the material by gravitational settling.
Vibration Tests	The material flows under the influence of applied vibration. The vibration is applied by using a vibrating table, dropping the base supporting the material, an external vibrator, or an internal vibrator.
Rotational Rheometers	The material is sheared between two parallel surfaces, one or both of which are rotating.

The NIST categorization method is most consistent with the current understanding of concrete rheology and workability. Confined flow, free flow, and vibration test methods

[1] Additional information were added based on latest development

generally attempt to simulate flow conditions of concrete in field placement, while rotational rheometers attempt to apply the general rheological concepts and directly earn rheological parameters of concrete. It should also be documented that some existing test methods, especially those tests for low slump concrete, do not directly measure the flow properties of concrete and, therefore, do not fit into any of the above four categories. The results of these tests can still give meaningful information on concrete workability. In this section, each category of test methods is described in general terms. The rotational rheometers are then described.

(1). Confined flow tests

Most of the confined flow test methods are only appropriate for SCC, and are not suitable for low-to-moderate slump concretes, because their flowability is insufficient to allow materials to readily flow under confined conditions and produce meaningful results. Some tests that incorporate vibration (which imparts energy into the concrete and produces flow in low flowability concrete) are classified as vibration tests, such as Vibra-John test (Wang and Hu, 2005).

The compaction factor test measures the degree of compaction resulting from the application of standard amount of work (Bartos, 1992). The K-slump test measures the amount of concrete that can be flow into the probe with a hollow center when it was inserted into concrete; this test was found to be directly related to the slump test (Ferraris, 1999). The filling ability test measures the capability of concrete to flow into a form, while the L-Box test estimates the time required for a concrete to flow within a certain range inside an L-shape tube (Bui et al., 2002a).

(2). Free flow tests

Free flow test methods are usually simple to perform and provide a clear and direct result which generally relates to yield stress. The slump cone test is the most widely used workability test method in the lab and field for its repeatability and simplicity. A slump test (ASTM C143) is performed based on the deformation of concrete under self weight, which is

decided by the stress from gravity of concrete, and it was found to be related to yield stress. Schowalter and Christensen (1998) confirmed that a simple analysis based upon the Bingham model correlates slump data for a wide variety of materials, including concrete. Saak et al. (2004) state that a fundamental relationship exists between yield stress and slump, which is independent of the material under study and largely independent of cone geometry. As shown in Figure 2-4, Murata and Kikukawa (1992) developed equations to quantify related slump values with the yield stress of concrete (Equation 2-3).

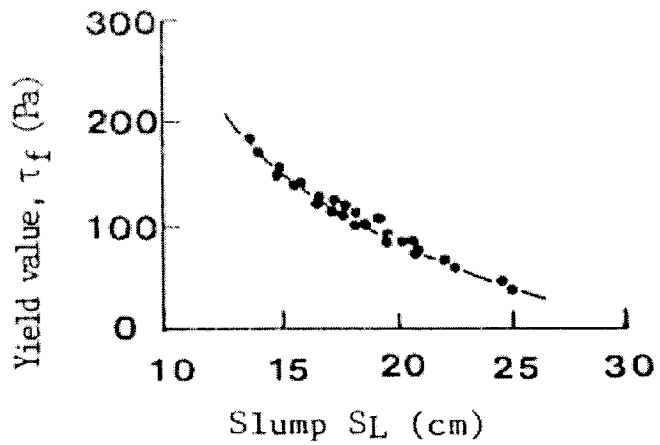

Figure 2-4 Slump value and yield stress (adopted from Murata and Kikukawa, 1992)

$$\tau_f = -4.83 \log S_L + 7.29 \qquad \textbf{Equation 2-3}$$

Where t_f is the yield stress (Pa) and S_L is the slump (cm).

Some models were also developed to simulate the shape of the concrete cone after the slump test according to the yield stress from the conical slump test by tools such as finite element analysis (Pashias et al., 1996; Schowalter and Christensen, 1998; Tanigawa et al., 1986). However, it was found that the slump test is only suitable for certain ranges—it is not appropriate for measuring concrete with too low or too high slump (Zain et al., 1999). Other research claimed that slump test is not sufficient to reflect the rheology of concrete. An example was shown by Tattersall (1991) in Figure 2-5. Two concretes had the same slump, but one was suitable for piping and the other was not because it had a much higher viscosity value caused by the angularity of the aggregate. Since slump is largely unaffected by viscosity, the slump test cannot pick up the difference between these two concretes.

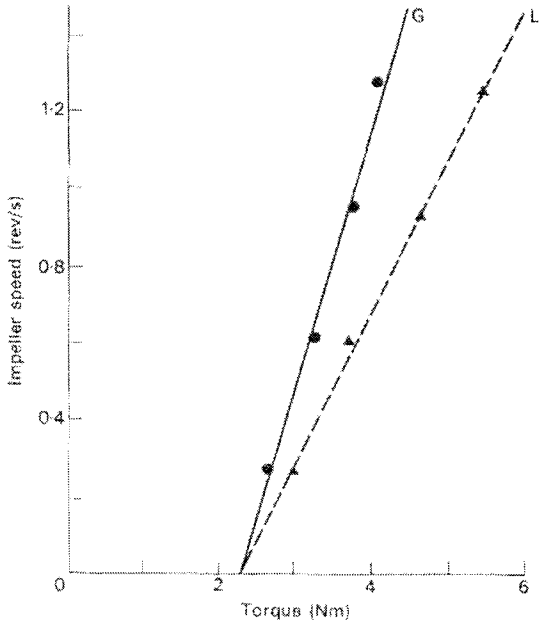

Figure 2-5 Different concretes with same slump (adopted from Tattersall, 1991)

Penetrating rod tests, such as Kelly ball, Vicat and Wigmore, measure the depth of penetration of object (Powers, 1968; Bartos, 1992; Wong et al., 2001). Some researchers claimed that these tests only compare the applied stress with the yield stress of concrete and sometimes can not give a direct result. Furthermore, the time required to perform these tests is substantially longer than other tests because the settling distance can not be recorded until the concrete harden (Bui et al., 2002a).

The flow table test measures the spread of concrete when it is dropped a predetermined number of times on a metal sheet. The result is considered to be related to viscosity because dropping on the metal sheet subjects the concrete to a stress larger than the yield stress (Tattersall, 1991). Ferraris and de Larrard (1998) developed a modified slump test, which measures the time for a plate to slide down to certain distance in addition to slump value. It was intended for use as a field test to measure both yield stress and viscosity; however, it was found that this test is only suitable for concrete of a limited range of workability.

(3). Vibration tests

The Vebe (Ve-Be) consistometer measures the capability of concrete to change shape under vibration. Bartos (1992) reported that the Vebe consistometer is a suitable test for determining differences in consistency of very dry mixes, but it may be difficult to determine the end point of the test. The remolding test (Powers, 1968) is similar to the Vebe test, which measures the remolding effort use the number of drops required to remold the concrete to the shape of the outer cylinder. The LCL apparatus determines the time it takes for concrete to flow into a new form. This test was found to be suitable only for concretes with low and moderate workability. The Vibra-John test (Wang and Hu, 2005) is similar to the L-box test; which measures the ability of concrete to flow through an opening under vibration. The vibration slope apparatus (VSA) was designed for estimating both yield stress and viscosity of low slump concrete, which measures concrete flow from chute in certain angle under vibration; however, the equipment itself and data analysis method is still being verified (Koehler et al., 2004; Wang et al., 2005).

(4). Rotational rheometers

Many attempts have been made to adapt traditional rotational rheometers to measure the workability of concrete. Rotational rheometers apply shear stress to concrete under different shear rates in order to discover the flow curve and measure the fundamental rheological parameters including yield stress and viscosity. Various equipment have been developed based on different principles, including the coaxial rheometer, vane rheometer and parallel plate rheometer. The size of this equipment varies from a mixing truck to a portable device. Details regarding these rheometers will be discussed in next section.

(5). Other methods

As discussed, some measurement methods was developed to estimate the workability of dry concrete, which is not directly related to concrete flow. Ritchie (1962) used a triaxial test method to study the properties of fresh concrete and found that the angle of internal friction and the apparent cohesion can be discovered through the test. He also stated that the viscosity

of the mix may be recorded in terms of the initial yield and the plastic viscosity characteristics of matrix; however, the cohesion is possibly best measured by direct tension.

Li et al. (2004a) developed a shear box test to determine the fluidity of concrete using direct shear test method. Results shows the test results of the yield stress for three types of highly fluid cementitious materials under different mean normal stresses. It was found that the yield stress of high fluidity concrete in the fresh state, which results from its interfriction, increases linearly with the normal stress applied on the shear plane.

Amer et al. (2004) used gyratory compaction to study the density and mechanical properties of roller-compacted concrete (RCC). The gyratory compactor produced specimens with mechanical properties consistent with those achieved in the field, and the gyratory compactor may be used to substitute other methods presently used for preparing RCC specimens such as the modified Vebe apparatus, the vibrating table, and the vibrating hammer.

2.3.3 Rotational Concrete Rheometers

Rheometer technology is based on theories from hydraulic science and stems from models. Limited understanding of concrete rheology and the relatively high cost restrict the development of this equipment. However, in the last couple of decades, several instruments have been developed for concrete use, which employ different rotational geometry, including rotating vanes, coaxial cylinders and parallel plates.

(1) Vane rheometer

Tattersall (1973) first developed the two-point rheometer based on the fact that fresh concrete behaves as a Bingham material and therefore measurements on at least two rates of shear are needed to characterize it. The two-point device developed by Tattersall is the origin of most of the other concrete rheometers. Some researchers improve the test by modifying the two point test (Wallevik and Gjorv, 1990; Domone et al., 1999). However, the device's size limits its use in the field. The ICAR rheometer was developed by Koehler and Fowler (2004), which is a portable rheometer with small size that is approximately the size of a drill and can

be operated by hand or positioned above a standard container. Attempts had also been made to measure the workability of fresh concrete using a mixing truck (Amziane et al., 2005). Although the plastic viscosity determined by the truck measurement was found to not correlate with plastic viscosity measured by the ICAR rheometer well, the yield stress did correlate well with the measured slump and the ICAR rheometer results. The IBB rheometer is an instrument with an H-shaped impeller controlled by computer. Using a DC motor; the impeller is capable of rotating in planetary motion, which is more accurate compared to other impellers and keeps acting on materials in same shearing plane. The portable version of IBB rheometer was developed recently for site use (Ferraris and Brower, 2004).

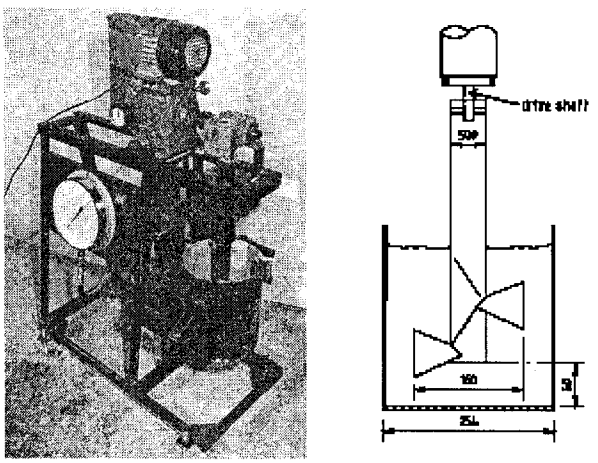

(a) Two point test (Adopted from Tattersall, 1991 and Ferraris, 2004)

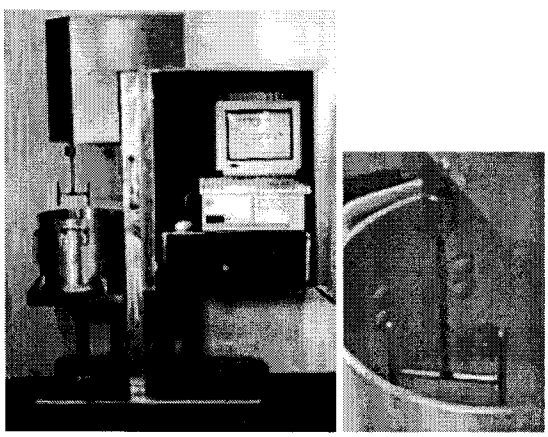

(c) IBB rheometer (Adopted from Ferraris and Brower, 2004)

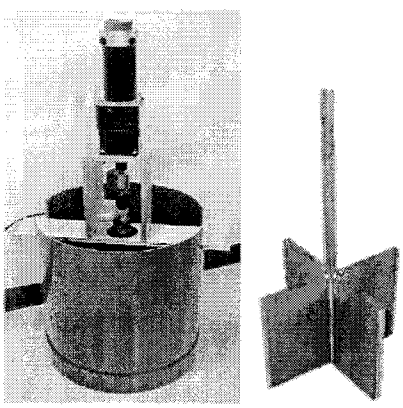

(b) ICAR rheometer and vane (Adopted from Amziane et al., 2005)

Figure 2-6 Vane concrete rheometers

The differences between the equipment and the impellers used in different rheometers are shown in Figure 2-6. The rotational concrete rheometer had been widely used to estimate workability of concrete of a wide range from 2 inch slump to SCC. Wallevik and Gjorv (1990) pointed out two main problems with the original two-point workability test apparatus, namely the segregation of the concrete during testing and the difficulties in operating the equipment. These problems also apply to other rotational vane rheometers. In addition to that, because of the complicated flow pattern, the device must be calibrated.

(2). Coaxial rheometer

The BML viscometer was developed in Norway in 1987 based on both the Power and Wiler plastometer and Tattersall two-point device (Gjorv, 1998; Geiker et al., 2002a). A large-scale field coaxial cylinder rheometer, CEMAGREF, which was originally developed to measure mud-flow rheology has also been applied in measuring concrete rheology (Coussot and Piau, 1995).

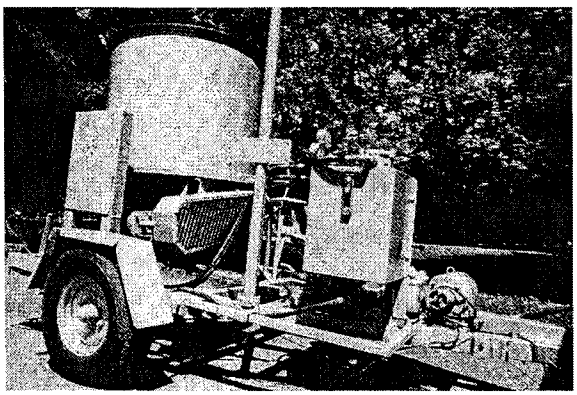

(a) CEMAGREF rheometer (Adopted from Coussot and Piau, 1995)

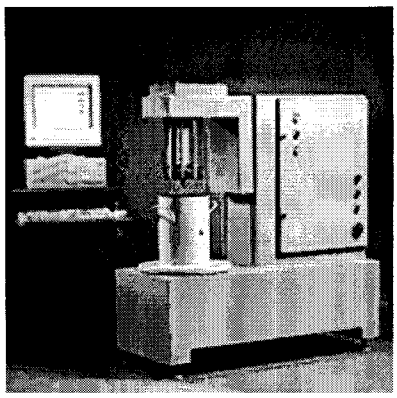

(b) BML rheometer (Adopted from Ferraris and Brower, 2004)

Figure 2-7 Coaxial concrete rheometers

These two devices are shown in the following Figure 2-7. Compared to the rotational vane rheometer, the flow pattern of material while testing is simpler and it is relatively easy to interpret the results. However, the device requires huge dimensions for a desirable linear flow gradient between the shearing surfaces. For example, the CEMAGREF has a 1.2m diameter, 0.2m gap, and a sample volume of $0.5m^3$, which greatly limits their use. Besides, a

problem was found that the shearing zone between the inner and outer cylinders has a tendency to dilate, which results in artificially low measurements of torque. In addition, the device is too large to be used outside of a lab.

(3). Parallel plate rheometer

The BTRHEOM rheometer was developed in France (de Larrard et al., 1997; Hu and de Larrard, 1996), which is a parallel plate rheometer capable of measuring the yield stress and viscosity of moderate-to-highly fluid concrete mixtures. The device includes a vibrator to consolidate the concrete and is capable of measuring the effect of vibration on the rheological parameters (de Larrard et al., 1997). The UIUC rheometer was built in University of Illinois at Urbana-Champaign (UIUC) based on BTRHEOM. Figure 2-8 showed the difference of these two rheometers. The major changes of UIUC rheometers are to reduce the difficulties involved in the installation and cleaning of the apparatus during the experiments.

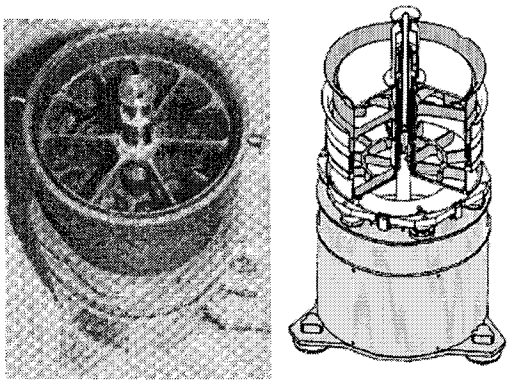

(a) BTRHEOM rheometer(Adopted from de Larrard et al., 1997)

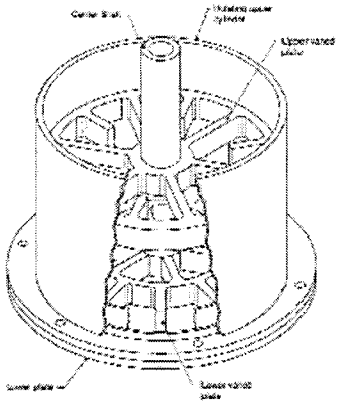

(b) UIUC rheometer (Adopted from Ferraris and Brower, 2004)

Figure 2-8 Parallel-plate concrete rheometers

The devices of the parallel-plate concrete rheometer are able to measure yield stress, plastic viscosity, and yield stress at rest or dilatanacy of concrete. A model has also been proposed for predicting the plastic viscosity of HPC from the mixture proportions using the data from BTRHEOM rheometer. It was reported that the comparison with the experimental results is satisfactory (Hu and de Larrard, 1996). However, the device is complex and expensive for

everyday field use. In additional to that, the device is only suitable for concrete with slumps greater than 4 inches, the limitation of measuring range constrained the application of these rheometers.

Papo (1988) reported that the results achieved from different researchers do not agree either qualitatively or quantitatively because of the different mix conditions as well as different experimental techniques, procedures and instruments employed. Two phases of international tests, phase I in LCPC (France) on 2000, phase II in MBT (USA) in 2003, had been performed to compare the different concrete rheometers. Various rheometers including the BML, BTRHEOM, CEMAGREF, IBB and two-point were considered, while mixtures with a wide range of yield stress and viscosity were used. It was found that purpose to correlate pairs of rheometers can be established, specifically, the ranking is similar by all rheometers and there is a high degree of correlation exists between rheometers. However, the absolute values of rheological parameters are very different; therefore, it was recommend that relative viscosity be used as a practical method to compare different rheometers (Ferraris and Brower, 2004; 2001). Additionally, these two comparisons showed that it is necessary to develop reference materials in order to learn the absolute rheological value and improve the accuracy of concrete rheometers. The selection of reference materials are currently under discussion by ACI 236A commettee.

2.3.4 Typical Rheometer Test Results

Initially, the most commonly used rheometers measured shear stress while the tested fluid is subjected to a controlled shear rate. The yield stress is determined by the maximum shear stress, which normally occurs at the early stage of testing. As shown in Figure 2-9 (a), the torque decreases with increasing velocity in a steady state (Coussot and Piau, 1995). Commercially available rheometers are designed for simpler, more homogenous liquids; they are not well suited for measuring fluid materials like fresh concrete that contains solid particles. Another kind of procedure is more oftenly used in concrete rheology measurement, which applies an increasing shear rate to the material, and records the shear stress at different shear rates. The flow curve as shown in Figure 2-9 (b) can be obtained through the test, and

the yield stress and viscosity can be calculated from the interception and slope of the curve respectively.

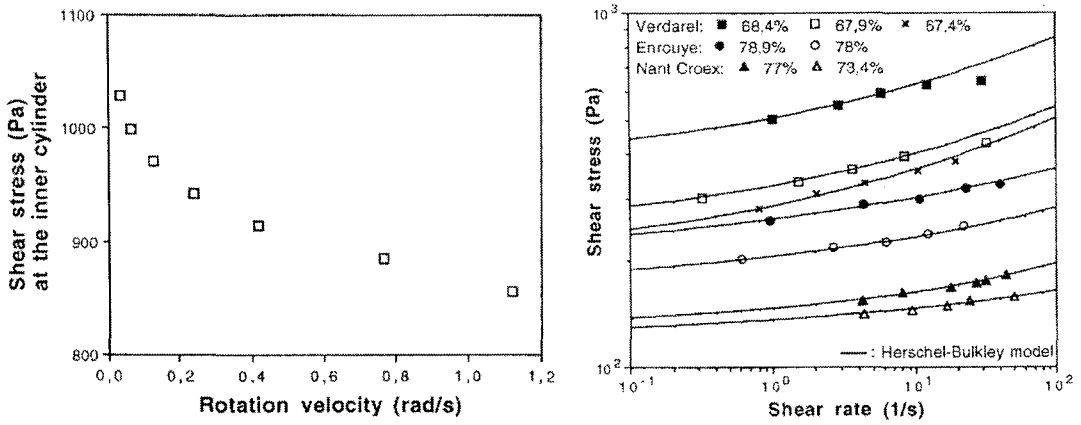

(a) Shear stress vs. time **(b) Shear stress vs. shear rate**

Figure 2-9 Typpical results from CEMAGREF rheometer (adopted from Coussot and Piau, 1995)

However, due to the complication within the flow pattern while testing because of the applied different shape of impeller, the shear rate in a mixer varies significantly from point to point. It is difficult to calculate exact value of shear stress and shear rate. Instead of shear stress and shear rate curve, the torque verse speed relation as shown in Figure 2-10 is more often learned through the test (Tattersall, 1976; Tattersall and Banfill, 1983). The equation as shown in Equation 2-4 is normally used:

$$T = G + HN \qquad \textbf{Equation 2-4}$$

In this equation, T is the torque act on impeller (Nm), N is the rotation speed (r/s), G is torque resistance (Nm) and H is flow resistance (Nm·s). It is generally agreed that an effective average shear rate exists that is proportional to the impeller speed, that the flow of concrete in the container is laminar, and the torque resistance can be related to yield stress while flow resistance can be related to viscosity (Tattersall, 1991). The value of G and H can be obtained through linear regression of the flow curves.

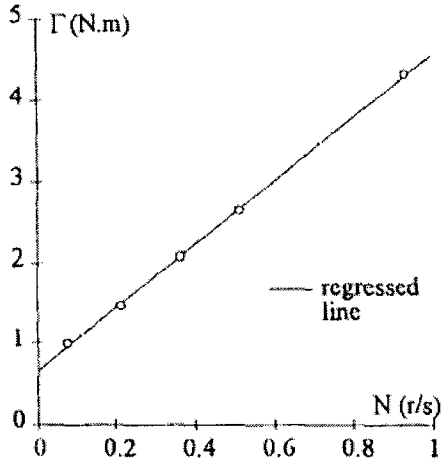

(a) Torque vs. impeller speed (Adopted from Hu and de Larrard, 1996)

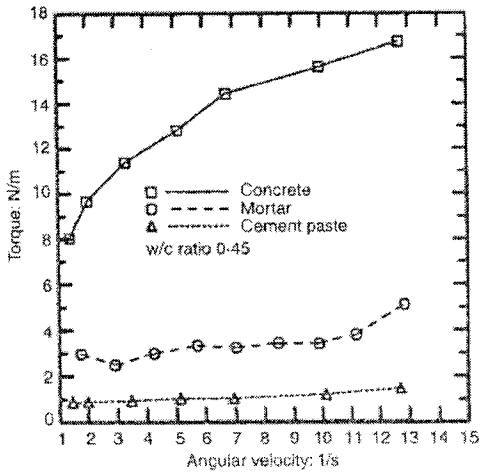

(b) Torque vs. angular velocity (Adopted from Struble et al., 2001)

Figure 2-10 Typical flow curves from concrete rheology test

Through the whole test process, an increase of shear rate (up curve) followed by a decreasing shear rate (down curve) is regularly used. As shown in Figure 2-11, the ascending curve did not approximate the Bingham model well. It has been recognized by researchers that a certain amount of time is necessary for cementitious materials to reach equilibrium state. The downward flow curves generally follow the Bingham model well, which is because the time to attain equilibrium at a given shear rate is shorter when going from a higher to a lower shear rate (Nehdi and Mindess, 1996). Hence, the down part of flow curve is generally used to calculate the parameters of flow and torque resistance.

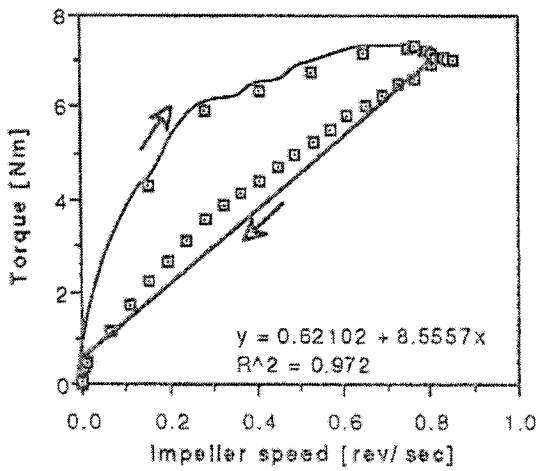

Figure 2-11 Down curves and up curves of a typical test result (adopted from Nehdi and Mindess, 1996)

2.4 Factors Affecting Concrete Rheology

Rheology is affected by all of the components of concrete and essentially every condition under which concrete is made. Factors including the amount of water, the properties and the amount of the cement, properties and proportion of fine and coarse aggregates, type and amount of mineral and chemical admixture, temperature of the concrete, mixing time and method, and the time since the water and cement made contact will be discussed in this section.

(1). Water content

Water content is the most important factor governing the rheology of concrete. Increasing the water content while keeping the proportions of the other constituents constant will decrease yield stress and viscosity of the concrete. However, increased water may lead to segregation and to bleeding. Due to equipment limitation, most research focuses on the effect of water content on rheology of cement, rather than concrete (Rosquoet et al., 2003; Svermova et al., 2003). Jones and Taylor (1977) showed an empirical equation that related the flow curves of a cement paste to its w/c. Banfill (1994) summarized previous results and showed that the increase of water content would result in higher slump and less Vebe time.

(2). Cement characteristics and content

The physical and chemical properties of cements are correlated to the rheological properties of cement pastes. Vom Berg (1979) studied the influence of specific surface area (SSA) and concentration of solids on the flow behavior of cement pastes. He found that the yield stress and plastic viscosity of cement paste increased as the cement fineness or the solids concentration increased, which reflects the dominance of the water cement interface in this system. The fineness of cement particles controls the balance of attractive and repulsive force between cement particles, which has a profound impact on the flow of concrete. At a given water content, low cement content tends to produce harsh mixtures with poor workability, while high cement content produces better cohesiveness.

(3). Aggregate

The particle size of aggregate influences the water requirement for a given slump of concrete. Very fine sands will require more water for a given consistency; on the other hand, they will produce harsh and unworkable concrete compared to coarser sands at same water content. The shape and texture of aggregate particles can also affect the rheology. Generally, the more nearly spherical the particles, the more workable the resulting concrete will be. The gradation and fine-to-coarse aggregate ratio will also provide concrete with different rheology. The effect of various properties of aggregate will be described in detail later.

(4). Chemical admixtures

Admixtures can change the yield stress and viscosity of concrete. The workability of concrete mixtures is commonly improved by air-entraining and water-reducing admixtures. An air entraining agent (AEA) typically increases paste volume and improves the consistency of the concrete while reducing bleeding and segregation. Chia and Zhang (2004) stated that adding AEA could reduce the plastic viscosity without changing yield stress, because they produced small bubbles of air which provided lubrication. Conversely, Struble and Jiang (2004) found that with increasing air content, the yield stress increased and the plastic viscosity decreased.

In fresh concrete, charged cement particles cling together and form flocs which trap water inside. After adding a water reducer (WR), the admixture molecules adsorbed solid surfaces, thus, dispersing flocs into individual grains and releasing trapped water for improving concrete workability (Kantro, 1980; Mehta and Monteiro, 1993; Papo and Piani, 2004b). Cry et al. (2000) studied the effect of high range water reducer (HRWR), or superplasticizer, on the rheology of cement paste. Shear thickening was observed when suspensions had a high solid concentration and when repulsive interactions are predominant. Chia and Zhang (2004) found that WR or HRWR will decrease yield stress but did not have a significant effect on the plastic viscosity. While the results of Golaszewski and Szwabowski (2004) showed that HRWR could considerably reduce yield stress value, it might increase viscosity. Perret et al. (2000) studied the effect of different cement and HRWR, and he found that diverse combinations of cement and HRWR provided pastes with different rheological behaviour.

Viscosity modifying admixtures (VMA) or viscosity enhancing admixtures (VEA) were commonly applied in SCC recently because they were found to be able to improve the stability of SCC (Lachemi et al., 2004a). A VMA is a water-soluble polymer that increases the viscosity and cohesion of cement-based materials. A VMA also increases the homogeneity of cement-based materials and leads to greater uniformity of hardened properties. In the case of flowable concrete with high slump (larger than 200mm), the addition of a VMA is shown to significantly increase the thixotrophy compared with similar concrete made without any VMA (Assaad et al., 2003). Khayat et al. (2002) found that these admixtures increase the yield value and viscosity rheological parameters. The yield value and plastic and apparent viscosities of cement grouts increased with increasing dosage of VMA while the apparent viscosity decreased more dramatically at low shear rates than that at high shear rates with increasing dosage of HRWR (Khayat and Yahia, 1997). The combined use of proper dosages of VMA and HRWR is shown to clearly contribute to creating high-performance cement paste that is highly fluid yet cohesive enough to reduce water dilution and enhance water retention (Lachemi et al., 2004b; Kamal, 1998).

Research had shown that the time of the addition of admixture also affects the properties of concrete. Ferraris et al. (2001) reported that the delayed addition of HRWR leads to a better dispersion of cement. Aiad (2003) and Aiad et al. (2002) claimed that the lower the amount of HRWR absorbed by cement paste, the lower amount of water needed for constant fluidity. Research had been performed to study the effects of different kinds of admixtures and of the timing of adding of different admixtures on fluidity and fluidity loss of fresh cement pastes. Results indicate that delaying the addition of naphthalene formaldehyde sulfonate (NFS) admixtures increases the cement paste workability when compared with adding them at the beginning of concrete mixing (Aiad et al., 2002).

(5). Supplementary Cementitious Materials (SCMs)

SCMs are widely used in order to improve strength, durability, and workability in concrete. Freshly mixed cementitious materials are generally more workable when fly ash is applied (Rudzinski, 1984). The major reason for this improving of workability is because of the

spherical particles and smooth surface texture which can act as small ball bearings to reduce interparticle friction. Experiment results also show that particle size distribution, density and particle morphologies of fly ash are the major factors affecting their fluidity (Li et al., 2004b).

Replacing some of the cement with fly ash will generally decrease yield stress, but may either increase or decrease the viscosity, depending on the properties of the mineral admixture and its interaction with the cement. For all cementitious mixtures, the SSA and particle size distribution (PSD) of the particles have the greatest influence on workability. Very finely divided mineral admixtures, such as silica fume, can have a very strong negative effect on water demand and hence workability, unless HRWR are used (Cry et al., 2000; Faroug et al., 1999; Park et al., 2005). However, the fact that silica fume increased the superplasticizer demand at a constant rheology while ground silica or limestone will not affect it significantly suggests that a high surface area is not the only parameter influencing the superplasticizer demand, and silica fume may have a strong affinity for multi-layer adsorption of superplasticizer molecules (Nehdi et al., 1998).

(6). Mixing

It was known that mixing conditions, especially mixing sequence and mixer type, also affect the rheological performance of cementitious materials. Results from Roy and Asaga (1979) showed that a change from the least severe to the most severe mixing procedure can cause both the yield stress and plastic viscosity to decrease by about 60%, while at the same time the width of the hysteresis loop decreased.

Yang and Jennings (1995) found that the rheological behaviors of cement paste are strongly influenced by mixing methods during the first two hours. Poorly mixed cement paste (mixed by hand) has more rapidly-increasing peak shear stresses than well-mixed cement paste (high energy blender). The agglomeration initially occurs in cement powder and later may remain in the paste due to insufficient mixing was considered to be responsible for the higher value and faster increase in peak stress.

Williams et al. (1999) investigated the effects of mixing shear rate on the yield stress and viscosity of cement paste by using a rheometer with different pre-shear rates. The results show that well-mixed pastes exhibit a decreased propensity for further structural breakdown and a low plastic viscosity; thus, they exhibit improved flowability. Ferraris et al. (2001) found that the Hobart mixer or blender may have different influences on the rheological properties of cement paste when different kinds of mineral admixtures were applied. Banfill also confirmed that the yield stress and plastic viscosity decrease as the duration of stirring time increase using a simple mechanical stirrer (Tattersall and Banfill, 1983).

(7). Time and environmental conditions

It is a well known fact that freshly mixed concrete loses flowability with time due to the process of hydration. The reduction in flowability is generally attributed to loss of water by evaporation or absorbed into aggregate, and from chemical reaction with the cementitious materials in early hydration reactions. Elevated temperatures increase the rate of water loss for the similar reason as time elapse.

Several researchers have studied the rheological performance through the hydration process. Petit et al. (2005) studied the influence of temperature and time on the evolution of the rheological properties. Lei (1997) studied the effects of hydration on both the microstructure and flow properties of fresh cement paste during the induction period. Different measurement methods were also applied; for example, Laboutet et al. (1998) used ultrasound methods for monitoring the rheology properties of cement, while Nachbaur et al. (2001) used a dynamic mode rheometer to study the evolution of the structure of cement and pure tricalcium silicate pastes from mixing up to setting and even after setting. Jiang and Roys (1993) studied the rheological properties of the paste as functions of hydration and setting. Struble and Lei (1995) use oscillatory rheology to study the change of yield stress through the setting process of cement paste, and it was found that yield stress increases slowly at first, then more rapidly. They stated that this rapid increase in yield stress occurs at the end of the induction period and corresponds to the initial setting.

(8). Vibration

When the concrete experienced vibration, the segregation resistance decreased with a decrease in both the yield stress and viscosity. However, it was reported by Chia and Zhang (2004) that the effect was more pronounced with the decrease in yield stress. Hu and de Larrard (1996) found that the vibration reduced the yield stress of fresh concrete to about half of that without vibration, but had little influenced the plastic viscosity.

De Larrard et al. (1997), Krstulovic and Juradin (1999) and Banfill et al. (1999) studied the effect of vibration on concrete rheology and fluidity using a BTRHEOM rheometer and vibration rheometer respectively and a vertical pipe apparatus . It was found that workability is proportional to the peak velocity of vibration up to a critical level, above which it does not further increase. The critical velocity is proportional to the yield value of the unvibrated concrete, and the peak workability was found to be inversely proportional to the plastic viscosity of the unvibrated concrete (Banfill et al., 1999).

Rheological parameters determine the workability of fresh concrete. A lower yield stress and plastic viscosity normally indicate a more fluid mix, while reducing the yield stress will lower the resistance to flow, and reducing viscosity will result in less cohesion and increased response during compaction by vibration. As mentioned, the rheological performance of cementitious materials is determined by various factors. Figure 2-12 summarizes the general finding of varying the proportions of concrete constituents on the Bingham constants. Increasing the water content whilst keeping the proportions of the other components constatn generally decreases yidld stress and viscosity in approximately similar proportions. Increase the paste content will nromally increase viscosity and decrease yield stress, which make the mix more easily start to flow but stickier. Adding a WR or HRWR decreases yield stress but leaves viscosity relatively constant. The small bubbles of air produced by AEA provide lubrication to reduce the plastic viscosity, but at relatively constant yield stress. Replacing some of the cement with SCMs will generally decrease yield stress, but may either increase or decrease viscosity, depending on the nature of them and the interaction with the cement.

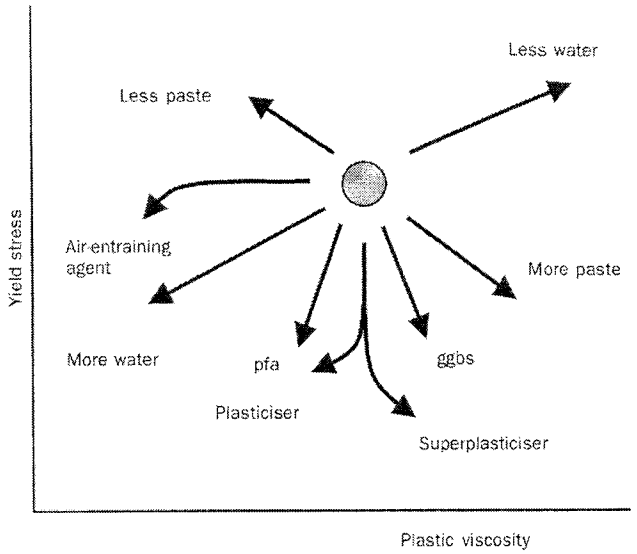

Figure 2-12 Effect of varying the proportions of concrete constituents on Bingham constants (adopted from Illston and Domone, 2001)

It is necessary to point out that these factors generally interact with each other so that changing the proportion of one component to produce a specific characteristic requires that other factors be adjusted to maintain workability. Limited research has been done on the effects from the combination of different components; for example, Xie et al. (2002) investigated utilizing both ultrapulverized fly ash (UPFA) and HRWR in order to develop high-strength SCC. Svermova et al. (2003) studied the combination effect of w/c, HRWR dosage, VMA dosage and the proportion of limestone powder as replacement of cement. Due to the limitation of space, these were not specifically discussed here.

2.5 Effects of Aggregate on Concrete Rheology

The flowability of concrete can be significantly changed by using different kinds of aggregate (Mehta and Monteiro, 1993). Most of the current research focused on paste and mortar rheology due to the complexity of concrete and the limitation of equipment. Research regarding the effects from the aggregate are still relative limited.

(1). Aggregate volume fraction

The amount of aggregate and the relative proportions of fine and coarse aggregate are two factors that significantly affect the concrete rheology. The increase in the fine aggregate/coarse aggregate ratio generally increases the water content required for a given workability. For a given w/c, increasing the aggregate/cement ratio generally results in decrease of workability; furthermore, more cement is needed when finer aggregate grading is used. The greater portion of fine aggregates in concrete provides larger surface area and requires a higher quantity of cement paste to coat all of the particles and to fill the interstitial spaces between particles. An excess of fine aggregate will result in a somewhat more permeable and less economical concrete, and the potential of drying shrinkage of hardened concrete will also increase although the mix is more workable. Alternatively, an increase in the relative coarse aggregate proportion will initially lead to a more workable, stronger, and cheaper concrete. However, there is an optimum coarse aggregate amount in considering workability. An excessively high amount of coarse aggregate results in a mix that is harsh, which means it is prone to segregation and difficult to finish. This will eventually lead to a weaker and less durable hardened concrete (Mindess et al., 2003).

Denis et al. (2002) studied the effect of coarse aggregate on the workability of sandcrete with two different mortar matrixes. The results confirmed the significant effect of coarse aggregate concentration on workability. Results from Geiker et al. (2002b) showed that the relative yield stress and relative viscosity, which were defined as the rheological parameters of concrete divided by the parameters of mortar, both significantly increased with the increase of coarse aggregate volume fraction, no matter what type of aggregate was used (Figure 2-13).

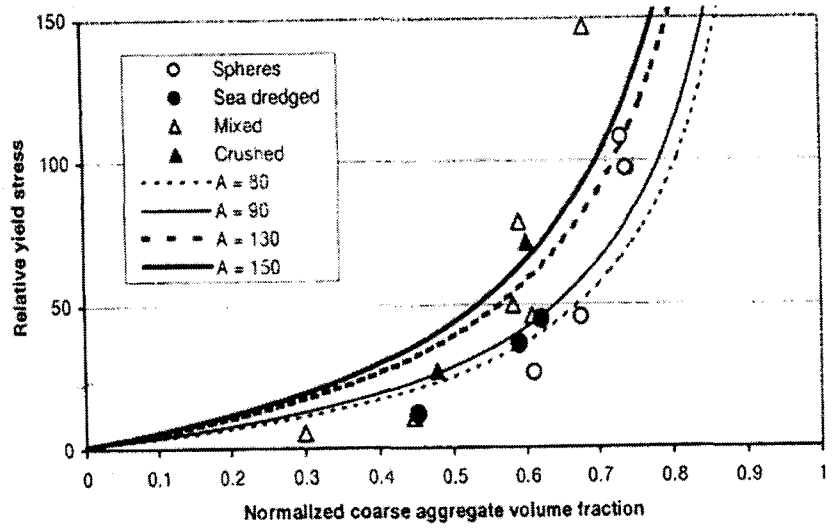

(a) Relative yield stress

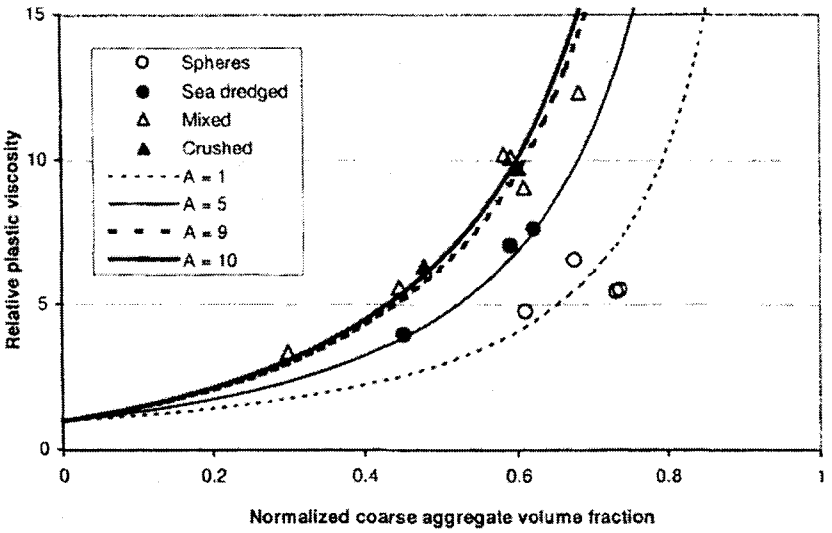

(b) Relative viscosity

Figure 2-13 Relative rheological parameters of concretes varying in amount and type of coarse aggregates (adopted from Geiker et al., 2002b)

(2). Particle size distribution

The particle size distribution, or gradation, of an aggregate is one of the most influential aggregate characteristics in determining how the concrete will perform as a pavement material. Gradation and the maximum size of aggregate in PCC affects the mix design as well as durability, porosity, workability, cement and water requirements, strength and shrinkage and durability of PCC. In order to obtain the proper workability of concrete, a

certain amount of cement paste will be required to fill up the space between aggregate, hence the gradation and size of aggregate will significantly affect the workability of concrete. Very fine sand or very coarse aggregate cannot produce the most satisfactory result. Aggregate that does not have a large deficiency or excess of any size and has a smooth grading curve is required to produce satisfactory and economical concrete (Mindess et al., 2003).

Aggregates by themselves can display different levels of "compactability", depending on the grading and the method of compaction used. A term of "coarse aggregate factor" is used to describe the compaction degree of coarse aggregate gradation, which is defined as the ratio of the amount of coarse aggregate in a unit volume of concrete to the amount of the same coarse aggregate compacted by the standard dry-rodding procedure into a mold of the same unit volume. This factor might be considered as the percent of maximum compacted density of the coarse aggregate in the concrete. Nichols (1982) found that the coarse aggregate factors are lower when the coarse aggregates size becomes smaller. As a result, decreasing maximum particle size normally requires an increase in the total fine aggregate content and a corresponding increase in water demand.

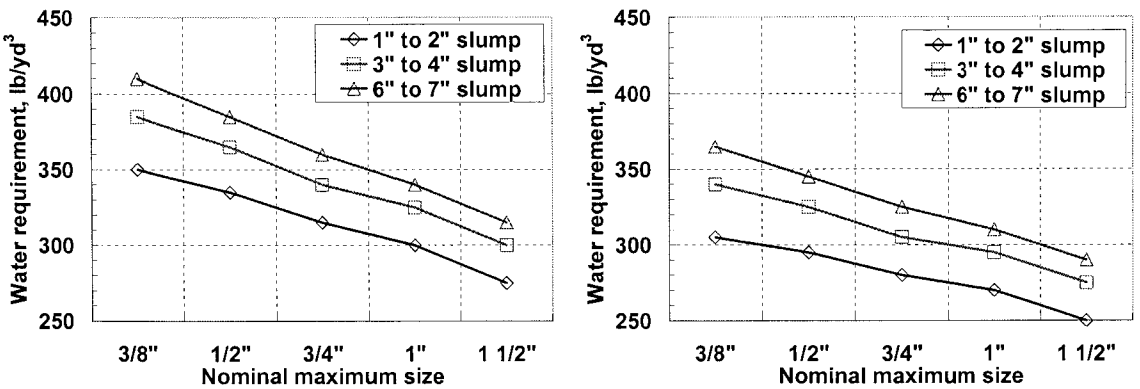

(a) Non-air entrained concrete **(b) Air-entrained concrete**

Figure 2-14 Effect of aggregate size on water requirement
(replot of data adopted from Mehta and Monteiro, 1993)

If a finer aggregate is substituted in a mixture, the water content typically must be increased to maintain the same workability because finer aggregate grading requires more cement to coat the particles. Mehta and Monteiro (1993) reported the approximate mixing water and air

content requirements for different slumps and nominal maximum sizes of aggregates. As shown in Figure 2-14, with the increase of aggregate size, the water demand for same slump decreases. However, note that increasing the maximum aggregate size (from 3/4" to 1.5") reduces the mixing water requirement but has an offsetting negative effect on concrete strength (Bloem and Gaynor, 1963). Larger size coarse aggregates are suffer greater effects during the vibration process than the smaller size aggregate (Safawi et al., 2004). Figure 2-14 also confirmed that the addition of AEA can improve concrete workability, which is consistant with the statement from section 2.4.

Graded aggregate offers a noticeable improvement in ability to fill the space between particles, so that an optimized aggregate blend results in a higher degree of packing and therefore requires lower amounts of paste. Research indicated that there is an optimum aggregate gradation that can produce the most effective w/c and highest strength. The optimum gradation should have the lowest possible surface area and void content per unit weight (Smith and Collis, 2001). The grading of fine and coarse aggregate that is suitable for manufacture of ordinary concrete is specified by a national standard (ASTM C33). The purpose of setting up these limits on grading is to get close to the optimum grading for economical concrete mixes in general construction practice.

Jamkar and Rao (2004) reported that for a given material, there exists a unique combination of coarse and fine aggregates that yield maximum workability, which implies that the volume of fine aggregate of a particular type and grading depends on the grading, shape and surface texture of coarse aggregate. Struble et al. (1998) found that both the yield stress and viscosity depends upon the amount and grading of the aggregate and properties of cement paste, which can both reach minimum values at an intermediate sand content. This behavior can be expected based on considerations of particle packing.

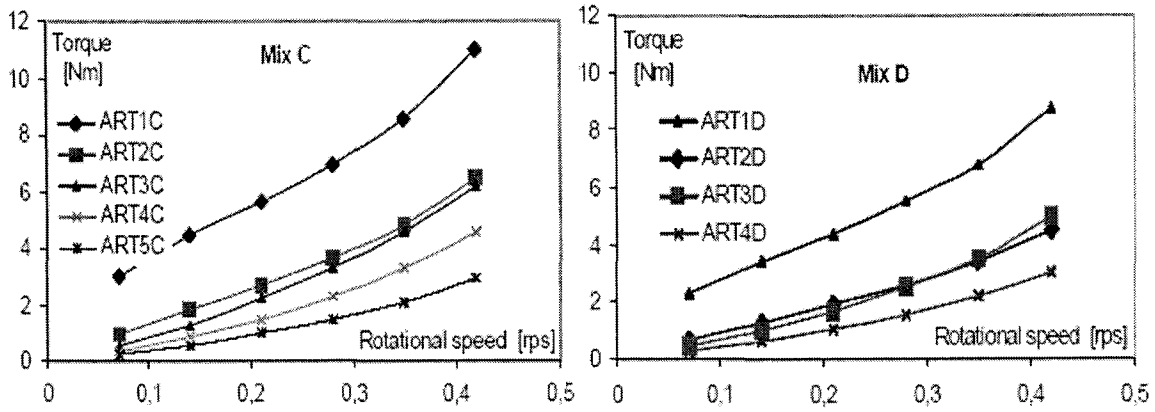

(a) Mix C **(b) Mix D**

Figure 2-15 Influence of gradation of artificial sands on the flow of mortars (adopted from Bager et al., 2004)

Bager et al. (2004) investigated the influence of artificial sands with different grading (ART1 through ART5 as shown in Figure 2-15) on the rheological parameters of self-compacting mortars in two different concrete mix design (Mix C and Mix D). The results shown in Figure 2-15 indicate that the gradation of aggregate influences the yield stress and the viscosity. The effect is different in various mix design; however, increased fineness generally leads to increases in both yield stress and viscosity.

(3) Particle shape and surface texture

Aggregate composed of spherical shapes with smooth surface textures is generally considered to be good for the workability of concrete. Rounded particles create lower degrees of particle-to-particle interlock than angular particles and thus provide better workability. Particles with smoother surfaces have a lower surface-to-volume ratio than rough surfaced particles and thus may be easier to coat with binder. Particles with rougher surfaces provide more area to which the cement paste can bond, which requires more sand, cement and water to provide adequate workability. However, the requirement for workability does not match the requirement of concrete strength. Angular, irregular shapes with rough surface texture aggregate have greater surface area for bonding with cement paste and have better interlock between aggregate particles which creates stronger concrete.

Malhotra (1964) studied the correlation between the particle shape and surface texture of fine aggregates and their water requirement. Research showed that crushed sands tend to have a higher water requirement than natural sands because of the higher angularity and differences in surface texture. Angular fine aggregate particles interlock and reduce the freedom of movement of particles in the fresh concrete. As a result, using angular fine aggregate (e.g., manufactured sand) increases the amount of fine aggregate that must be used for a given amount of coarse aggregate and generally requires that more water be added to achieve the workability obtained with rounded sand. Kosmatka et al. (2002) confirmed that the workability of fresh concrete and the bond between cement paste and a given aggregate is affected by particle shape and surface texture. It was found that water content must be increased to maintain workability if angular aggregate is substituted for rounded aggregate. Crushed aggregates having numerous flat or elongated particles will produce less workable concrete that requires higher mortar content and possibly higher paste content. Quiroga and Fowler (2004) systematically studied the effect of aggregates characteristics on the performance of PCC. Their research confirmed that aggregates blended with well-shaped, rounded, and smooth particles require less paste for a given slump than those blended with flat, elongated, angular, and rough particles.

As shown previously in Figure 2-13, Geiker et al. (2002b) used aggregates with different aspect ratios (A) to study the effect of fraction and shape of coarse aggregate on the rheology of concrete. The investigation indicated that the aspect ratio, angularity, and surface texture of aggregates affect the viscosity and yield stress differently, round and smaller aggregates results in lower rheological parameters. Particle shape is the shape of individual aggregate particle and surface texture is degree of roughness or irregularity of surface of an aggregate particle. There is no direct ASTM and AASHTO standard test or detailed definition for fine aggregate particle shape and surface texture. However, tests for the void content of bulk aggregate and the rate of flow through an orifice provide excellent empirical measurements indirectly related to particle shape characteristics (Wills, 1967). A fine aggregate angularity test (ASTM C1252) and void content of coarse aggregate test (ASTM C29) were generally used to estimate the surface and shape of aggregate particles, arising from the idea of "compactability" of aggregate.

Some researchers have developed different methods and parameters in order to estimate the shape and texture of aggregate. For example, the image analysis was developed by Persson (1998) and Dilek and Leming (2004), while Mora et al. (1998) and Kwan et al. (1999) used digital image processing (DIP) techniques. Garboczi et al. (2001) used x-ray computed tomography to acquire three-dimensional aggregate shape information. However, there is still a big gap until these methods are widely utilized, mainly because these methods require expensive equipment, large data bases, and complicated analysis method.

(4). Others

The porosity of aggregates can also affect workability. Normally less water will be available to provide workability if the aggregate can absorb a great deal of water. Absorption of mixing water causes a change in workability of fresh concrete, which usually happens within the first 5 to 10 minutes after mixing. This effect can reduce the medium slump to zero or a very low value, while the compactability of the concrete may be too low to permit full compaction and achieve the potentially high strength caused by the reduced free w/c of the mix. Low density aggregate tends to float in the fresh mix and rise to the surface. As a result, high workability mixes with light weight aggregate will segregate more easily than normal mixes of the same workability. On the other hand, the use of high density aggregate also increases the potential of segregation. The amount of limestone dust or quarry dust in an aggregate was also found to have significant effects on concrete workability. Celik and Marar (1996) reported that the slump and air content of fresh concrete decreased as the percentage of dust content increased. Ho et al. (2002) stated that mixes with quarry dust required a higher dosage of superplasticizer to achieve similar flow properties due to its shape and particle size distribution. Research also indicated that finer and better graded limestone dust significantly increases the deformability of the paste (Bosiljkov, 2003).

2.6 Modeling of Concrete Rheology

A successful model that can predict the rheological parameters of concrete from composition would be valuable because engineers may be able to predict fresh concrete properties with

this model. Using the model, engineers can also optimize mixture proportions at the mixture design stage. A great deal of work has been done relating concrete rheology parameters to its composition. The existing rheological models are summarized in the following categroies:

(1). Empirical model

Due to the limitation of test equipment, the rheological parameters can not always be learned. Some researchers try to correlate the particle concentration with the parameters from empirical tests, which are considered to be related to concrete rheology. Ouchi et al. (1999) adopted a simple evaluation method for the interaction using the mortar funnel test, in which funnel speeds (speed of materials passing through the funnel) of mortar with and without coarse aggregate (glass beads were used as model coarse aggregate in this research) are compared. It was claimed that the index for the interaction, which can be defined by the ratio of funnel speed of mortar with aggregate and without aggregate (R_{mb}/R_m), is similar to the idea of relative viscosity and yield stress. As shown in Figure 2-16, the volume content of coarse aggregate was found to be able to relate to R_{mb}/R_m. However, the application of this empirical model is very limited, not only because it is only suitable for specific equipment, but the applicable range of material is limited. As it was shown in Figure 2-16, the R_{mb}/R_m for high coarse aggregate content (for example, 30%) is not available, because the glass beads block the opening of the funnel.

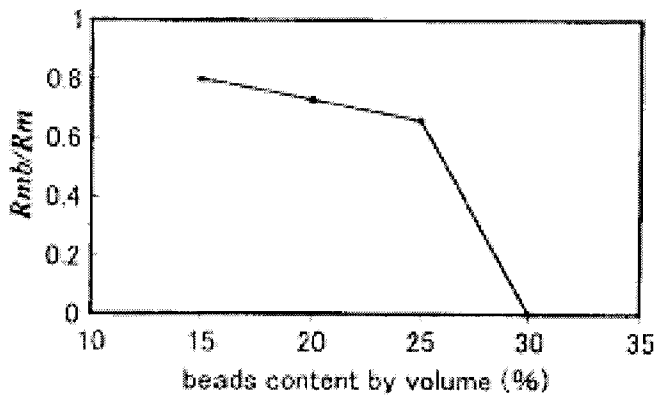

Figure 2-16 Relationship between R_{mb}/R_m and coarse aggregate content (adopted from Ouchi et al., 1999)

(2). Volume fraction model

Volume fraction models were used to predict the rheology of cementitious materials by relating aggregate volume percentage (volume fraction) to concrete rheology. The basic idea of this kind of model is that the viscosity of a composite increases with increasing volume of solids.

Einstein first deduced a model for the viscosity of a Newtonian fluid containing a low concentration of small rigid inclusions (Powers, 1968). He assumed that the disturbance propagated by the particle could spread without reflection and without interference from other disturbances (Equation 2-5).

$$\eta = \eta_0(1 + [\eta]\phi) \qquad \textbf{Equation 2-5}$$

In this equation η and η_0 are the viscosities (Pa·s) of the composite and suspending fluid respectively, $[\eta]$ is the intrinsic viscosity parameter (equals to 2.5 for spheres particles) and ϕ is the particle volume concentration. Practically, the effects of interferences that were not considered in the derivation are proven to be negligible for particle concentrations up to about 3% by volume (Powers, 1968). However, this model is valid for dilute suspension ($\phi<0.05$) only because the particle interaction can not be neglected after this limit (Hobbs, 1976).

Figure 2-17 illustrates the volume fraction of solids versus relative viscosity (viscosity of the composite divided by viscosity of the matrix) of the composite according to some experimental results reported in previous literature (Hu et al., 1995). It clearly shows that the viscosity of the composite will increase with the increasing of solid proportion.

A lot of models based on the idea of volume fraction have been developed to describe the rheological parameters of composites including cementitious materials, most of which analyzed fresh concrete as a paste/aggregate composite. These models generally attempt to infer the viscosity of the concrete from the paste viscosity by multiplying it by a function which takes the volume of granular phase into consideration. In order to calculate the

viscosity of multi-modal suspensions, the interactive calculation was performed in a consideration of the suspending fluid and particles. However, these models generally did not consider the inter-particle interactions, and simplified the particles into single size or a number of discrete classes.

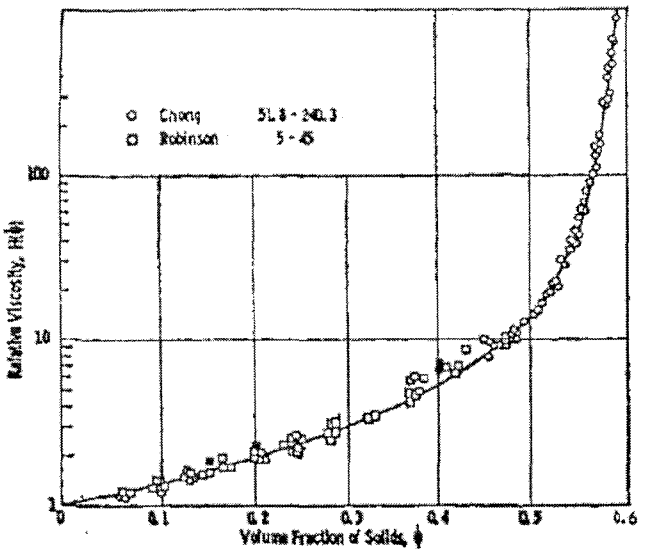

Figure 2-17 Solid concentration and relative viscosity (adopted from Hu et al., 1995)

(3). Maximum packing density model

With the development of concrete study, it was found that the rheology of concrete is not only determined by the volume fraction of aggregate, but is also related to the type of aggregate. By introducing a new parameter of maximum packing density of aggregate, Hobbs (1976) derived an equation to predict the viscosity of concrete based on the volume concentration of aggregate:

$$\eta_c = \eta_p \left[\frac{1 - \phi + 2.5\phi_{\max}\phi/(\phi_{\max} - \phi)}{1 + \phi} \right] \qquad \textbf{Equation 2-6}$$

In this equation, η_c and η_p are the viscosities (Pa·s) of concrete and paste respectively and ϕ_{max} is the maximum packing factor of particles. It was found that the equation can be used to describe the effect of both type and volume concentration of aggregate from previous data. The effect of aggregate volume concentration on concrete viscosity using aggregates with

different maximum packing density is shown in Figure 2-18. Roshavelov's research (2005) further confirmed the effect of maximum packing density by successfully calculating the viscosity of fresh mixes as a function of volume fraction of solids, normalized with respect to their maximum packing values.

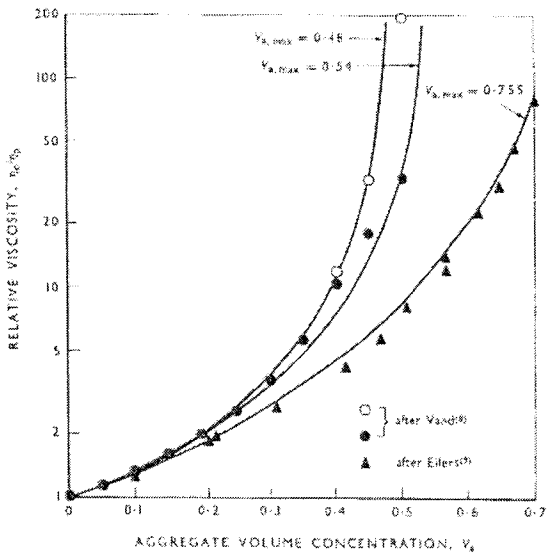

Figure 2-18 Relation between relative viscosity and aggregate volume concentration (adopted from Hobbs, 1976)[1]

According to Hobbs (1976), the rheological equation for a concrete mixture containing rigid aggregate particles in a Bingham paste was further derived and given by:

$$\tau_c = \tau_{0p}\left[1+\frac{1.5\phi_{\max}\phi+\phi^2}{\phi_{\max}-\phi}\right]+\eta_p\left[1+\frac{2.5\phi_{\max}\phi}{(1-\phi)(\phi_{\max}-\phi)}\right]\dot{\gamma}_c \qquad \textbf{Equation 2-7}$$

In this equation τ_c is the shear stress of concrete(Pa), τ_{0p} is the yield stress of concrete (Pa), and $\dot{\gamma}_c$ is the shear rate inside concrete (s^{-1}). According to the theory, increasing the volume fraction of aggregate can therefore increase the yield stress and plastic viscosity of concrete. The equation can be reduced to Einstein's equation when there is no yields stress ($\tau_{0p}=0$) and the concentration is extreme low ($\phi \rightarrow 0$).

[1] Here $V_{a,max}$ represents ϕ_{max} in Equation 2-7

The Krieger-Dougherty (K-D) equation is one of the most well known equations for fitting relative viscosity data based on effective medium theory arguments (Struble and Sun, 1995). The K-D equation (Equation 2-8) is valid for a broad range of solid volume fractions of a suspension *(ϕ)*; the increase of ϕ increases the viscosity as if small particles were being added to the suspension, which is treated as a homogeneous viscous medium.

$$\frac{\eta}{\eta_0} = (1 - \frac{\phi}{\phi_{\max}})^{-[\eta]\phi_{\max}} \qquad \textbf{Equation 2-8}$$

In this equation, η and η_0 are the viscosities (Pa·s) of the composite and suspending fluid respectively, $[\eta]$ is the intrinsic viscosity parameter, ϕ is the particle volume concentration, and ϕ_{max} is the maximum packing factor of particles. Barrioulet and Legrand (1991) also conducted a study on the semi-empirical modeling for rheology behavior of vibrated fresh concrete, in which it was found that the rheological parameters of concrete depend on all of the parameters including the aggregate concentration, as well as the shape and density of its grains.

Another important model to predict concrete rheological properties from their composition is the compressible packing model (CPM) developed by de Larrard (1999), which was derived from the packing concept. The CPM model uses packing density to characterize the granular skeleton, which takes the packing process, the distribution and the shape of grains and the degree of agglomeration of powders into consideration. According to the CPM model, the rheological properties of composites not only relate to volume fraction of aggregate, but also relate to particle properties including amount, shape, aspect ratio, angularity, and surface texture, which can be reflected by maximum packing density (Chang and Powell, 1994; Geiker et al., 2002b).

Based on the CPM model, Ferraris and de Larrard (1998) found that the relative concentration of solids has a significant effect on the viscosity. As shown in Figure 2-19, the points fall on a single curve, regardless the difference of mixture. An empirical equation for the best fitting curve is:

$$\eta / \eta_0 = \exp\left[26.75\left(\frac{\phi}{\phi_{\max}} - 0.7448\right)\right] \qquad \textbf{Equation 2-9}$$

Where η and η_0 are the viscosities (Pa·s) of the composite and suspending fluid respectively, ϕ is the particle volume concentration, and ϕ_{max} is the maximum packing factor of particles.

However, it was found that the wide range of error exists, which might be caused by the uncertainty of the maximum packing density ϕ_{max}. The error may also be contributed to the fact that tested mixtures under shear are less compacted than the consolidated mixture.

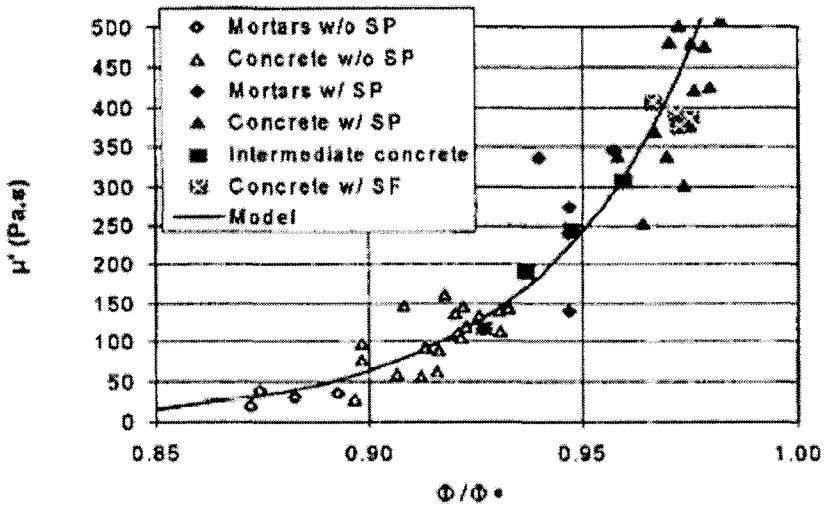

Figure 2-19 Relative viscosity as a function of relative concentration of solids (adopted from Ferraris and de Larrard, 1998)[1]

The same trend as observed from the plastic viscosity can not be obtained when the yield stress is plotted as a function of relative concentration of solids (Figure 2-20). The contributions of the various granular fractions must therefore be considered according to the nature of the materials.

[1] In this figure, μ' referring to relative viscosity, ϕ/ϕ^* referring to ϕ/ϕ_{max} as in Equation 2-9

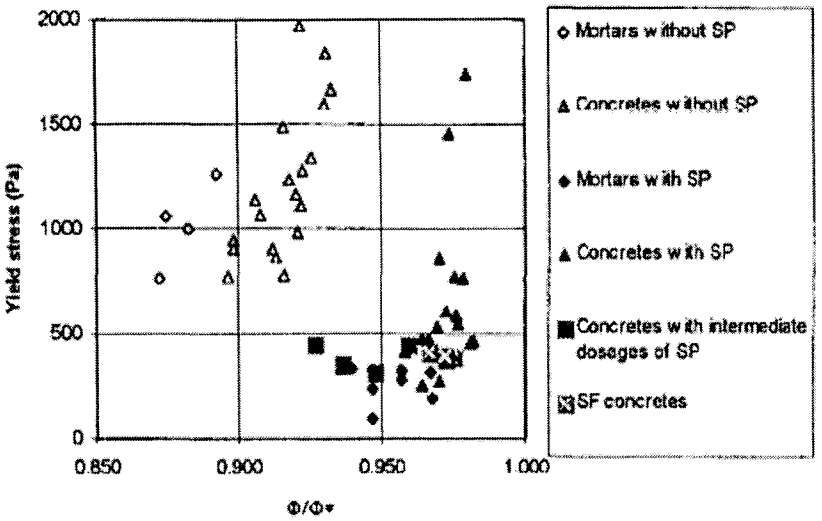

Figure 2-20 Yield stress as a function of relative concentration of solids (adopted from Ferraris and de Larrard, 1998)

According to Ferraris and de Larrard (1998), the yield stress can be calculated by a linear combination of all the components' volume fraction verse close-packing ratios. It appears that different semi-empirical equations can be learned for concrete with and without HRWR as the following equation 2-10 and 2-11 show respectively:

For mixtures without HRWR,

$$\tau_0 = \exp(2.537 + 0.540K_g + 0.854K_s + 1.134K_c) \qquad \textbf{Equation 2-10}$$

For mixtures with 1% HRWR,

$$\tau_0 = \exp(2.537 + 0.540K_g + 0.854K_s + 0.224K_c) \qquad \textbf{Equation 2-11}$$

In this equation τ_0 is the yield stress (Pa) of concrete, and the indices g, s and c refer to gravel, sand and cement, respectively. The compaction indices K_x can be calculated by $(1-\phi_x)/\phi_{x\text{-}max}$.

Various applications had been successfully applied according to CPM or models derived from it. Grunewald (2004) used the CPM approach to study the effect of steel fiber in the rheology of concrete according to the volume fraction and close-packing ratios. However the

major difficulty of the K-D equation and the CPM approach is the determination of the maximum packing factor, which is not a parameter that can be simply measured. A lot of researchers calculated the ϕ_{max} value by fitting the equation provided all the other parameters can be calculated or measured, which actually turns the equation into a semi-empirical equation. Some researchers calculated the ϕ_{max} value by putting individual particles in one by one using computer simulation, which involves a tremendous amount of work. In addition to that, the calculation algorithm and results are still being debated. Different parameters were used in deriving the equations for the rheology model for bimodal suspensions; for example, Mammoli (2002) used the value of ϕ_{max}=0.68 and $[\eta]\phi_{max}=1.8$, while Shikata (2001) used the value of ϕ_{max}=0.63 and $[\eta]\phi_{max}=2$.

(4). Two-phase theory

The previously mentioned Krieger-Dougherty modified model and the CPM treat fresh concrete as solid phase and liquid phase, i.e., aggregate and paste are considered as two phases. However, the range of aggregate size in concrete is so wide, from less than 200μm to up to several inches; it is questionable whether coarse aggregate and fine aggregate can be handled in the same way. Also, there is an advantage to considering coarse aggregate and fine aggregate separately, because practically, fine and coarse aggregate are usually from different sources and proportional independently. Several researchers have attempted to study the workability of concrete by considering it as two-phase composite of coarse aggregate and mortar.

Topcu and Kocataskin (1995) proposed a model to establish basic composition-property relations for fresh concrete, using the two-phase composite materials approach and the law of plastic viscosity. Topcu and Kocataskin found that results from the two most practical tests (slump test and Vebe test) of fresh concrete can be well related to the composition as:

$$S_c = S_m \frac{1 - M \cdot V_a}{1 + k \cdot V_a + k' \cdot V_a^2} \qquad \textbf{Equation 2-12}$$

$$T_c = T_m \frac{1 + k \cdot V_a + k' \cdot V_a^2}{1 - M \cdot V_a}$$ **Equation 2-13**

In this equation S and T are the slump (cm) and Vebe time (s) of concrete, respectively, the indices of *m, a* and *c* refer to mortar, coarse aggregate and concrete, V_a is the volume fraction of coarse aggregate, and the material constants M, k, and k' depend upon the characteristics of the mortar and the coarse aggregate phases. Equations 2-13 and 2-14 show that parameters like slump of concrete are functions of the mortar (one phase) slump, S_m, and volume fraction of coarse aggregate (the other phase), V_a.

Kurokawa et al. (1996) developed a model of concrete rheology based on the two-phase theory approach. They stated that the yield stress of fresh concrete (which was calculated from the slump test) could be expressed by the sum of the yield values of matrix mortar τ_{0m}, and the contribution from the friction of coarse aggregate $\tau_{0(fric)}$ (Equation 2-14). The viscosity (which was calculated from flow time in L-box test) can be expressed by the sum of viscosity of matrix mortar and the contribution from volume fraction and friction of coarse aggregate (Equation 2-15).

$$\tau_{0c} = \tau_{0m} + \tau_{0(fric)}$$ **Equation 2-14**

$$\eta_c = \eta_m + \eta_{(V_g)} + \eta_{(fric)}$$ **Equation 2-15**

In these equations τ_0 and η are the yield stress (Pa) and viscosity (Pa·s) of concrete respectively, the indices of *m, c* refer to mortar and concrete, and the indices of (V_g) and *(fric)* refer to the contribution from volume fraction and by friction of coarse aggregate. The influence of the rheological parameters from the coarse aggregate were also calculated as shown in Figure 2-21. Results demonstrated that with the increase of volume fraction of coarse aggregate, both yield stress and viscosity of concrete increase. Additionally, the yield stress and viscosity of the concrete composite increase with the yield stress and the viscosity of the mortar phase. Nevertheless, the research did not provide specific methods to theoretically calculate the term by friction; on the contrary, $\tau_{0\ (fric)}$ and $\eta_{(fric)}$ are the value

subtracted by the input τ_{0m} and η_m from the test result. Further research is still necessary to develop theoretical methods to calculate the contribution of coarse aggregate friction directly.

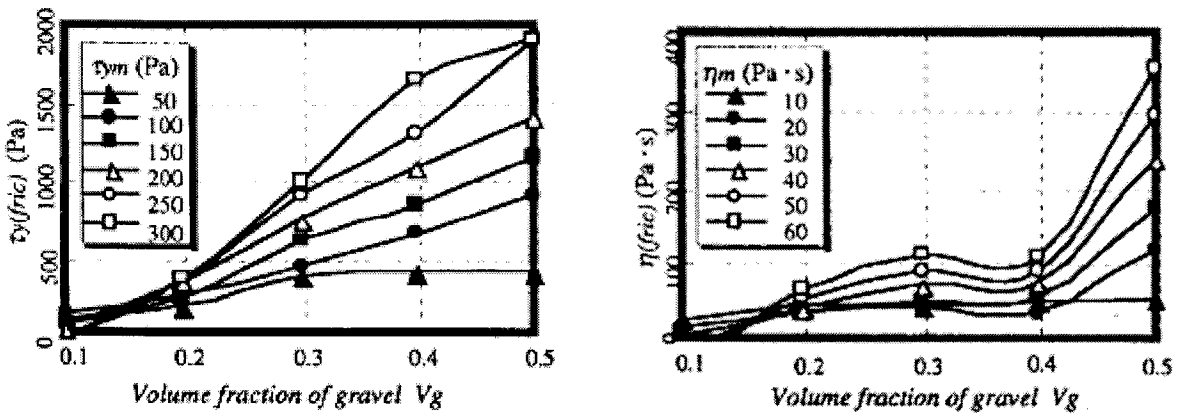

(a) Yield stress **(b) Viscosity**

Figure 2-21 Increase of rheological parameters by friction of coarse aggregate (adopted from Kurokawa et al., 1996)[1]

(5) Gap and aggregate spacing theory

Research shows that by using the concept that a layer of paste surrounds all sand and gravel particles with varying thickness, the influence of aggregate content on workability can be explained (Denis et al. , 2002). The gap existing between the aggregate was used to attempt to link the rheology of the cement paste with that of concrete. Ferraris and Gaidis (1992) used a parallel plate paste rheometer to study the effect of gap distance on the torque acting on the rheometer. Figure 2-22 shows that the torque significantly decreases when the gap increases over the range from a minimum of around 0.05mm up to 0.6mm at a maximum rate of $39s^{-1}$. It is clear that the gap thickness does have significant effect on the applied torque, especially in the range of less than 0.2mm. Based on this fact, they proposed the concept of relating the rheology of cement paste and the gap sbetween particle to the rheology of concrete.

[1] τ_y referring to τ_0 in Equation 2-14 in this figure

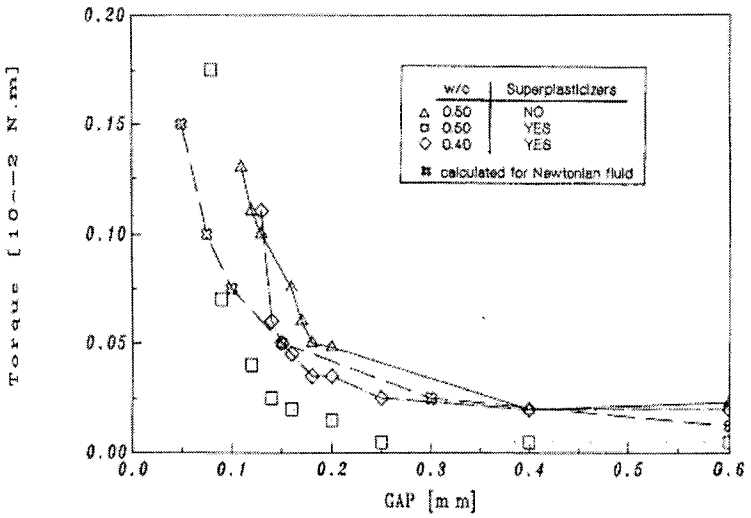

Figure 2-22 Effect of gap (adopted from Ferraris and Gaidis, 1992)

Bui et al. (2002b) presented the idea of a rheological model according to aggregate spacing and average diameter of aggregate. A specific method to calculate aggregate spacing was also proposed based on void-surface area theories.

$$D_{ss} = D_{av}\left(\sqrt[3]{1+\frac{V_p - V_{oid}}{V_c - V_p}} - 1\right) \qquad \textbf{Equation 2-16}$$

In this equation D_{ss} is the average spacing between aggregate particle surfaces (mm), V_p is paste volume (liter) , V_{oid} is the volume of voids between aggregate (liter), V_c is total concrete volume (liter) and D_{av} is the average aggregate diameter (mm).

The gap and spacing approach requires measuring the rheological behavior of paste through independent means, which was not yet done in their study. The rheological models using this approach therefore remain in the qualitative study stage.

(6) Excess paste theory

Kennedy (1940) stated that the rheology of concrete depends on not only the rheology of cement paste, but also the amount of excess paste to fill the voids in between the aggregate. As shown in Figure 2-23, the theory declared that in addition to the paste that fills up the space between aggregate (compacted paste); an excess paste will be require to maintain the

flow. Su et al. (2001) developed a design method for SCC according to this theory. The amount of required aggregates is determined, and then the paste of binders is filled into the voids of aggregates to ensure that the concrete thus obtained its flowability, self-compacting ability and other desired SCC properties.

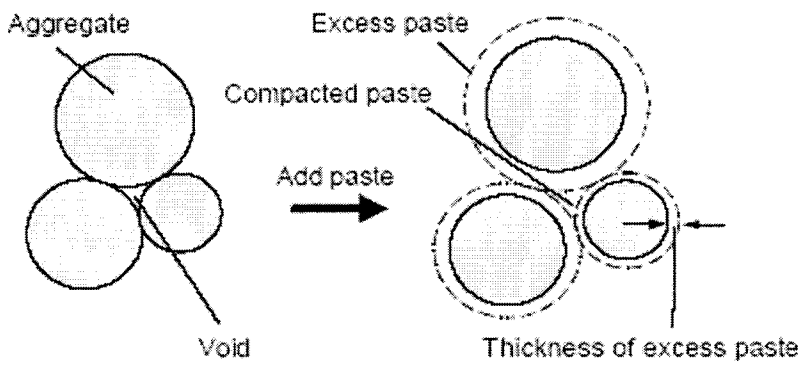

Figure 2-23 Excess paste theory (adopted from Oh et al., 1999)

Oh et al. (1999) found that when the thickness of excess paste increased, both the yield stress and viscosity of concrete decreased. Base on this phenomenon, an excess paste theory was developed by using model concrete with polymer as paste and artificial plastic beads as fine and coarse aggregate. The related excess paste thickness (Γ), which can be defined by the excess paste thickness divided by the average diameter of aggregate, was found to be directly related to the relative viscosity and yield stress of concrete, and the relationship was shown to be independent to the mix proportion of concrete (Figure 2-24). The regression equations are:

$$\tau_{0r} = 0.0525\Gamma^{-2.22} + 1 \qquad \textbf{Equation 2-17}$$

$$\eta_r = 0.0705\Gamma^{-1.69} + 1 \qquad \textbf{Equation 2-18}$$

In these equations τ_{0r} and η_r are the relative yield stress and relative viscosity of model concrete respectively, and Γ is the calculated relative thickness paste thickness.

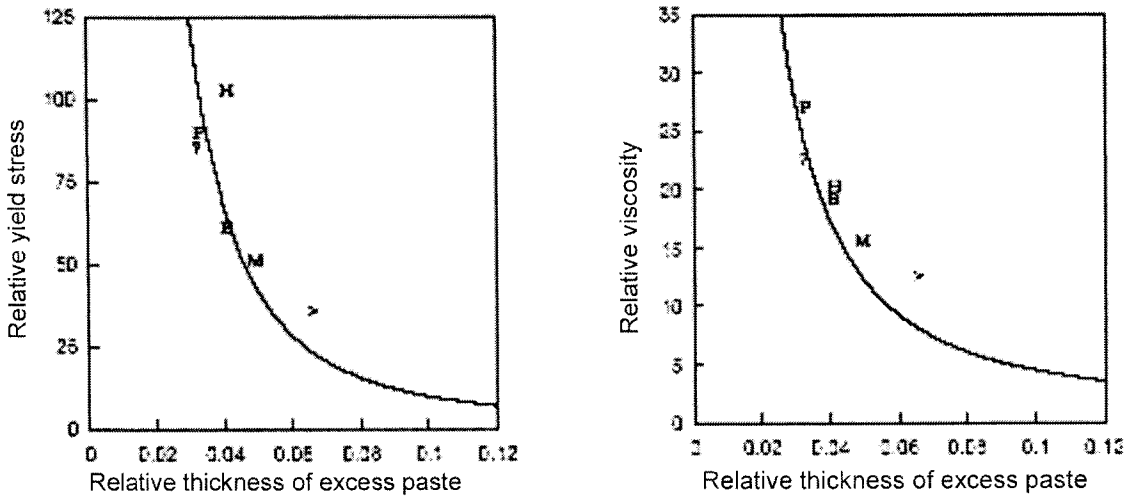

(a) Relative yield stress **(b) Relative viscosity**

Figure 2-24 Relative thickness of excess paste and rheological parameters of concrete (adopted from Oh et al., 1999)

The excess paste thickness theory can be used to explain the benefit of graded aggregate, which can provide larger amounts of excess paste because of the smaller void volume between aggregate particles. Research indicates that there is an optimum aggregate gradation which can produce the most effective w/c and highest strength. The optimum gradation should have the lowest possible surface area and void content per unit weight (Smith and Collis, 2001). Both yield stress and viscosity depend on the amount and grading of the aggregate and the properties of cement paste, which can both reach minimum values at intermediate sand content. This behavior can be expected based on considerations of particle packing (Struble et al., 1998). The relative paste thickness is considered in the modeling within this study, and will be detailed described in Chapter 8.

(7). Others

Finite element methods were adopted as tools to analyze the workability of concrete, especially to simulate the deformation of fresh concrete. Mori and Tanigawa (1992) and Tanigawa and Mori (1989) had successfully used the viscoplastic finite element method (VFEM), viscoplastic suspension element method (VSEM) and viscoplastic divided space element method (VDEM) to simulation the deformation in slump cone test.

The NIST used a computer simulation of the dissipative particle dynamics (DPD) method to simulate the concrete flow between rebars and inside coaxial rheometer (Martys and Ferraris, 2003; Martys, 2005). Flatt et al.'s research (2004) showed very promising results in terms of handling aggregates with a wide distribution of particle sizes and shapes for modeling of concrete rheology. However, he also pointed out that accurate modeling requires reliable input on the interaction of the dispersant with the hydrating cement at the molecular level.

2.7 Summary

Concrete workability is one of the most important properties of concrete because it can not only decide the pumping, spreading, molding and compaction of fresh concrete, but also potentially affects the hardened concrete properties. Concrete rheology, a part of concrete workability, which is the science of deformation and flow of matter, can be used as a tool to quantitatively study the workability of concrete. However, due to the complications of concrete composition and the limitation of measuring equipment, the study of concrete rheology is still very limit.

A variety of test methods can be used to estimate concrete workability. Among all the tests, the slump cone test is the most widely used method; however, it can only be related to yield stress, which is insufficient to fully reflect the rheology of concrete. With the progress of modern techniques, more equipment has been developed for measuring concrete workability. Rotational rheometers are found to be a promising tool to study concrete rheology, which can be used to learn both rheological parameters directly by analyzing the shear stress versus shear rate relation in concrete flow curve.

The Bingham model, with the parameters of yield stress and viscosity, is normally used to describe concrete rheology. These rheological parameters of concrete are decided by different factors, such as mixture components including water, cement, chemical and mineral admixtures, and the mixing and environmental conditions. Among all of these factors, the effects of aggregate are one of the most important, because size, gradation and type of aggregate all have significant effect on concrete workability. However, studying this factor is restricted by the measurement and characterization of aggregate.

A successful rheology model can predict fresh concrete performance from concrete components, and more importantly, can be used to improve concrete mix design. Different models were proposed to study the concrete rheology, from the very simple empirical model considering only aggregate volume fraction to the model considering the gaps between aggregate and excess paste thickness. More systematic and comprehensive models are developed because different factors such as particle properties including amount, shape, aspect ratio, angularity, surface texture and maximum packing density are considered. However, further work is still necessary to develop more practical and widely-used models with more theoretical analysis.

According to the review from previous research, the gap/distance between aggregate particles, void contents and particle friction between aggregate are all important factors that should be considered in the concrete rheology model. A new model using excess mortar thickness will be developed in the present study, which will be based on the excess paste theory and modified by considering concrete as two-phase of mortar and coarse aggregate.

CHAPTER 3. EXPERIMENTAL DESCRIPTION

3.1 Materials Characterization

Type I Portland cement which meets the requirements of ASTM C150 was used throughout the experiment. The chemical composition and physical properties of the cement are listed in Table 3-1. In order to obtain consistent results, only the cement that passed through #200 (0.075mm) sieves was used in paste tests.

Table 3-1 Chemical and physical properties of cement

	CaO	SiO_2	Al_2O_3	Fe_2O_3	MgO	K_2O	Na_2O	(Na_2O) eq.*	SO_3	LOI**
(%)	64.2	20.8	5.55	2.25	1.91	0.50	0.19	0.52	2.96	0.82
Mean size = 23.7μm			Fineness = 399 m^2/Kg					Specific gravity = 3.15		

*(Na_2O) eq. = (Na_2O) + 0.658 (K_2O)

**LOI = loss of ignition

Two different types of fine aggregates-riversand and limestone-were used in mortar tests. The sands were oven dried (OD) and sieved. Five single-sized[1] aggregates retained on sieves of #100, #50, #30, #16 and #8 were used. In order to study the effect of aggregate gradation, some riversand was recombined into three different gradations (G1, G2, and G3) according to the top and low limit specified in ASTM C33 and another middle-point gradation between the limits. Together with one natural graded riversand (G4) and a standard graded sand (ASTM C778); five different sand gradations were studied. The gradation curves of G1 through G4 sands were presented in Figure 3-1. The specific gravity, absorption, uncompacted void content and friction angle of these sands were all measured.

[1] In this dissertation, single-sized aggregate used in the study still have particles size distribution with range from the maximum sieve size aggregate particles retained on to the minimum sieve size aggregate particles passed through. For example, single-sized aggregate of #30 have particles with maximum size of #16 (1.18mm) and minimum size of #30 (0.6mm).

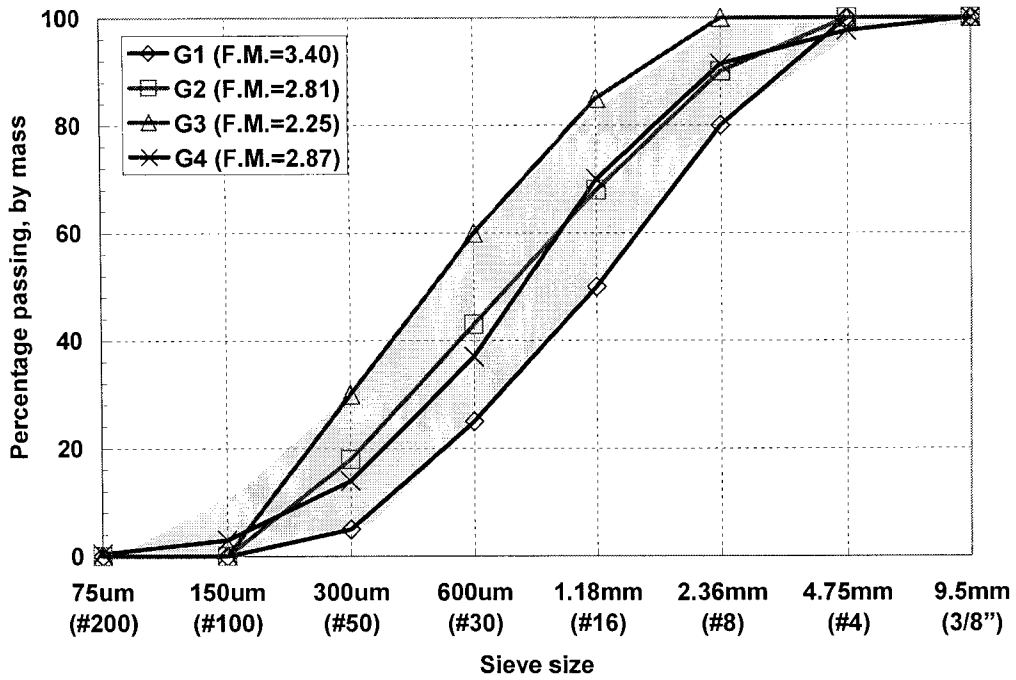

Figure 3-1 Fine aggregate gradation[1,2]

The natural graded riversand used in the concrete study was the same as used in the mortar and has a fineness modulus of 2.92. Four single-sized coarse limestone aggregate (#4, 3/8", 1/2", 3/4") and three designed gradations (G1, G2, and G3) of coarse aggregate were studied in concrete. Graded coarse aggregate were recombined from single-sized aggregate according to the top and low limit specified in ASTM C33 (G1 and G3 respectively) and another middle-point gradation between the limits (G2). The gradation curves of G1 through G3 coarse aggregates are presented in Figure 3-2. Specific gravity, absorption, uncompacted void content and friction angle of different aggregates were measured. In concrete mixing, all coarse aggregates were prepared in saturated surface-dried (SSD) conditions. The aggregates were immersed in water for 24±4 hours, then the surface water was removed according to ASTM C127.

[1] In Figure 3-1, the shaded area indicates grading limits for fine aggregate specified in ASTM C33.
[2] F.M. = Fineness modulus, it is the index of the fineness of an aggregate – the higher the F. M., the coarse the aggregate. According to ASTM C125, the F. M. of either fine or coarse aggregate is calculated by adding the cumulative percentages by mass retained on each of a specified series and dividing the sum by 100.

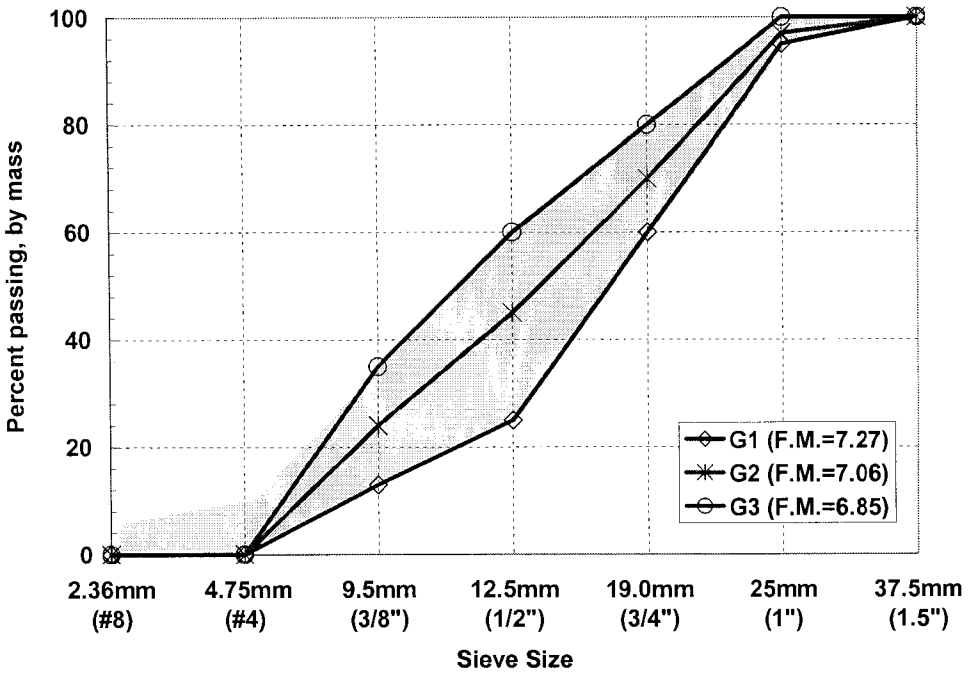

Figure 3-2 Coarse aggregate gradation[1]

Tap water ($73 \pm 3^{o} F$) was used for the mixing of the cement paste, mortar and concrete. The water used for the aggregate specific gravity and absorption measurements meets the requirement of specification ASTM C127. An air-entraining agent (AEA), Daravair 1000, was employed based on cement content in the mix to gain an approximately 6% air content in concrete.

3.2 Mix Proportions

3.2.1 Pastes

The effect of w/c and mixing conditions for cement paste were studied. w/c of 0.30, 0.35, 0.40, 0.50, and 0.60 were selected for the paste tests. The pastes were mixed by either a Hobart mixer or a highshear mixer according to the procedure as described in Section 3.3. Flowability of the cement pastes, with different w/c and different mixing methods, was evaluated by the Brookfield rheometer and the mini-slump cone tests.

[1] In Figure 3-2, the shaded area indicates grading limits for coarse aggregate specified in ASTM C33.

3.2.2 Mortars

In order to study the factors that may affect flow behavior of mortar, a factorial mix design, as shown in Table 3-2, was used. The factors studied include sand-to-cement ratio (s/c), water-to-cement ratio (w/c), fine aggregate size, gradation and type. The s/c in mortars were 1, 2 and 3 by weight. Different w/c were used to ensure the mortars had suitable workability (flowability of mortar can not be measured if the mix is too dry, while too much wetness in the mix will result in segregation). All batches of mortar were mixed according to the specification as described in ASTM C305. oven-dried (OD) sand was used in mortar mixing and the w/c of mortars were calculated saturated surface condition. A total of 136 mixes were studied.

Table 3-2 Mortar mix proportions

	Sand	w/c (s/c = 1)	w/c (s/c = 2)	w/c (s/c = 3)
Riversand	#8	0.30, 0.35, 0.40	0.36, 0.41, 0.46, 0.51	0.41, 0.46, 0.51
	#16	0.35, 0.40, 0.45	0.36, 0.41, 0.46, 0.51	0.46, 0.51, 0.56
	#30	0.35, 0.40, 0.45	0.40, 0.45, 0.50, 0.55	0.46, 0.51, 0.56, 0.61
	#50	0.36, 0.41, 0.46, 0.51	0.41, 0.46, 0.51, 0.56	0.56, 0.61, 0.66
	#100	0.40, 0.45, 0.50	0.46, 0.51, 0.56, 0.61	0.61, 0.66, 0.71
Riversand	#8	0.35, 0.40, , 0.45	0.41, 0.56, 0.51	0.46, 0.51, 0.56
	#16	0.35, 0.40, 0.45	0.46, 0.51, 0.56	0.46, 0.51, 0.56
	#30	0.35, 0.40, 0.45	0.45, 0.50, 0.55	0.56, 0.61, 0.66
	#50	0.36, 0.41, 0.46	0.51, 0.56, 0.61	0.56, 0.61, 0.66
	#100	0.40, 0.45, 0.50	0.50, 0.55, 0.60	0.66, 0.71, 0.78
Graded Sand	G1	0.35, 0.40, 0.45	0.40, 0.45, 0.50	0.45, 0.50, 0.55
	G2	0.35, 0.40, 0.45	0.40, 0.45, 0.50	0.45, 0.50, 0.55
	G3	0.35, 0.40, 0.45	0.40, 0.45, 0.50	0.50, 0.55, 0.60
	G4	0.35, 0.40, 0.45	0.40, 0.45, 0.50	0.45, 0.50, 0.55
	Std	--	0.45, 0.50, 0.55	--

3.2.3 Concretes

The factorial mix design as shown in Table 3-3 was used for the concrete study. The factors include mortar mix design, coarse aggregate content, coarse aggregate size, and gradation. Since concrete is considered as a two-phase material consisting of a mortar phase and a coarse aggregate phase, concrete with three different mortar mix proportions marked as M1, M2 and M3 with different s/c and w/c were used (M1: s/c=1.75, w/c=0.45; M2: s/c=2.21, w/c=0.45; M3: s/c=2.60, w/c=0.50). In mixes Mix7, Mix8, and Mix9, a higher w/c was chosen to provide concrete with acceptable flowability (concrete slump higher than one inch). Limestone, with different sizes and gradations, was used as the coarse aggregate in the concrete.

Table 3-3 Concrete experimental design

Concrete Mix	Mortar	CA Content (%)	CA Size/Gradation
Mix1		37.8	19.0mm, 4.75mm, G1, G2, G3
Mix2	M1	40.8	G2
Mix3		44.0	19.0mm, 4.75mm, G1, G2, G3
Mix4		37.8	G2
Mix5	M2	40.8	G2
Mix6		44.0	19.0mm, 12.5mm, 9.5mm, 4.75mm, G1, G2, G3
Mix7		37.8	G2
Mix8	M3	40.8	G2
Mix9		44.0	G2

Concrete mix design is shown in Table 3-4 (fine aggregate and coarse aggregate were riversand and limestone respectively). A total of 23 concrete mixes, with three different sand contents, three different coarse aggregate contents and seven different coarse aggregate gradations/sizes were prepared. All of the concrete was mixed using the standard "3-3-2" mix procedure as described in Section 3.3.

Table 3-4 Concrete mix proportions

	Cement (pcy)	Water (pcy)	FA (pcy)	CA (pcy)	w/c
Mix1	752	340	1317	1463	0.45
Mix2	716	322	1254	1580	0.45
Mix3	677	306	1185	1705	0.45
Mix4	658	298	1452	1461	0.45
Mix5	627	285	1384	1581	0.45
Mix6	594	266	1310	1707	0.45
Mix7	592	293	1538	1472	0.50
Mix8	562	278	1460	1585	0.50
Mix9	530	263	1380	1707	0.50

3.3 Mixing Procedures

3.3.1 Paste

Two different sets of equipment and procedures were used to study the effect of mixing method on cement paste rheology. The Hobart model N50 mixer as shown in Figure 3-3 was used for standard mixing based on ASTM C305.

The mixing method is described below:

1. Put the water into the mixing bowl on the mixer,
2. Add the cement to the mixing bowl,
3. Wait 30 seconds for the absorption of the water,
4. Mix at a slow mixing speed (140±5r/min) for 30 seconds,
5. Stop the mixer for 15 seconds. During this time scrape down any paste or cement that may have collected on the size of the bowl into the batch, and
6. Mix again at medium speed (285±10r/min) for 60 seconds.

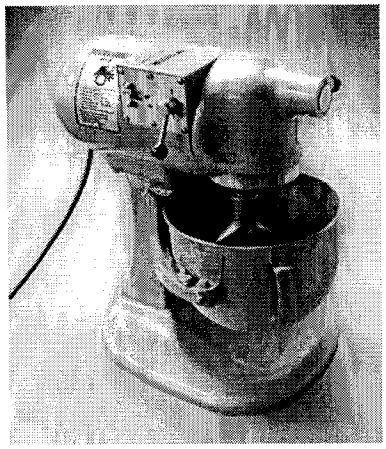

Figure 3-3 Hobart mixer

A high shear mixer was also used for paste mixing in order to compare the pastes from the two different methods. The highshear mixing process was adapted from slurry mixing procedures for oil well cement slurries specified by the American Petroleum Institute (API) Specification 10A (API, 2002). A Chandler Engineering Waring Blender, model 3070, high shear mixer (Figure 3-4) was used.

The mixing method is described below:

1. Put water into the mixing bowl,
2. Add cement into the mixing bowl and allow 30 seconds for the absorption of the water. For low w/c (0.3 and 0.35), cement was added while mixer was running, within 15 seconds,
3. Mix the paste at a mixing speed of 6000r/min for 30 seconds,
4. Stop the mixer for 30 seconds, during this time scrape down any paste or cement that may have collected on the size of the bowl into the batch. For dry mixes, paste inside bowl was also stirred, and
5. Mix again at speed of 6000r/min and mix for 30 seconds.

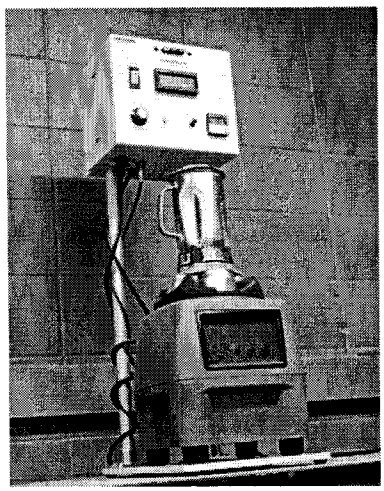

Figure 3-4 Highshear mixer

3.3.2 Mortar

The Hobart mixer was also used in mortar mixing. The mixing procedures as specified in ASTM C305 are described below:

1. Put water into the mixing bowl,
2. Add the cement to the mixing bowl, then start the mixer and mix at slow speed (140±5r/min) for 30 seconds,
3. Add the entire quantity of fine aggregate slowly over a 30 seconds period, while mixing at slow speed,
4. Stop the mixer, change to medium speed (285±10r/min) and mix for 30 seconds,
5. Stop the mixer for 1.5 minute, during first 15 seconds, scrape down into the batch any mortar that may have collected on sides of the bowl,
6. Mix again at medium speed (285±10r/min) for one minute.

3.3.3 Concrete

The Lancaster 30-DH pan concrete mixer (Figure 3-5) was used for concrete mixing. The pan mixers employ a flat cylindrical pan to hold the concrete constituents; the pan is rotating, while the mixing blades (separate from the pan) are also rotating inside of the pan but in the opposite direction as the pan. A separate blade is fixed against the inside edge of the pan and

scrapes the material off the side, moving it towards the center where the mixing blades are rotating.

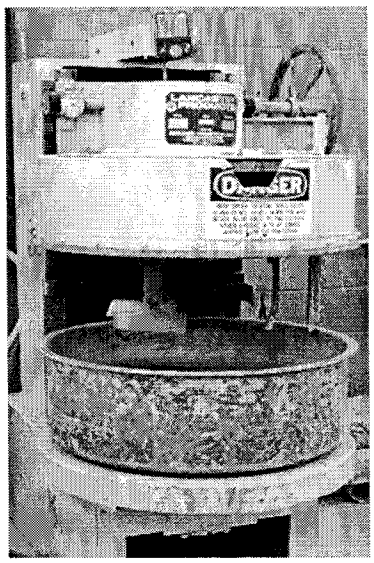

Figure 3-5 Rotating concrete pan mixer

The concrete mixing procedure was based on ASTM C192 lab mixing procedure (multiple-step mixing procedure), and it is described below:

1. Coarse aggregate was mixed with approximate a half of the amount of water, together with air entraining agent (AEA), for about 30 seconds,
2. Sand, cement and the remainder of the water were then added, after which the mixer runs for three minutes,
3. The mixer was in rest for three minutes,
4. The mixer started again for another two minutes.

3.4 Test Methods

Aggregate properties, such as specific gravity, absorption, uncompacted void content, and friction angle, were measured in this research. Paste flowability was measured by the Brookfield rheometer and mini-slump cone. Mortar flowability was measured by the Brookfield rheometer and flow table. Concrete flowability was measured by the portable IBB

rheometer and the slump test. The Unit weight of fresh concrete and the seven day compression strength of concrete were also measured in the experimental study.

3.4.1 Fine Aggregate Property Measurements

The specific gravity and absorption of fine aggregate were measured according to the ASTM C128 specification (See Appendix I for details).

Since no standard test method is available for direct characterization of aggregate particle shape and surface texture, a fine aggregate angularity test was developed based on ASTM C1252. In the test, a given amount of fine aggregate was allowed to fall through a funnel from specified height and fill a nominal 100ml measure. Uncompacted void content is calculated based on three factors: the volume of the cylindrical measure, the dry bulk specific gravity, and the weight of the fine aggregate collected in the measure (Figure 3-6). This method defined fine aggregate angularity as the percentage of air voids present in loosely compacted fine aggregates. Higher void contents generally indicated more fractured faces and more irregular shape, resulting in a more difficult packing of particles.

Figure 3-6 Fine aggregate void content test

In addition to the uncompacted void content of fine aggregate from ASTM C1252, another simple method was developed to estimate the friction angle of the different fine aggregates based on a basic soil mechanics concept. As shown in Figure 3-7, a sample of 1500 to 2000

grams of sand was allowed to flow through a funnel from a height as close to the top of the pile as possible. According to the mechanism of slopes stability, the maximum angle formed by the sand pile (angle of repose) was considered as a constant and correlated to the friction angle of the particles (Lambe, 1969). Three measurements were taken for given sand, and the average value was used as the fine aggregate friction angle.

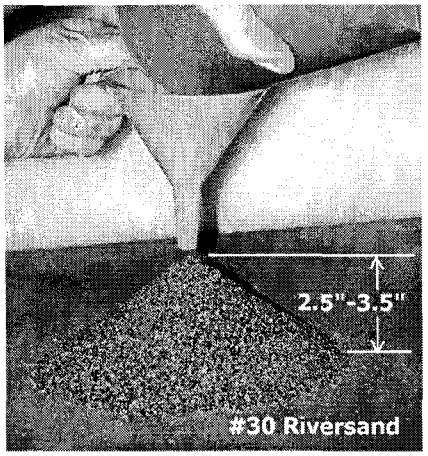

Figure 3-7 Fine aggregate friction angle test

3.4.2 Coarse Aggregate Properties Measurement

The Specific gravity and absorption of coarse aggregate were measured according to the specification of ASTM C127. The void content of coarse aggregate was measured according to ASTM C29.

In a similar manner to measuring the friction angle of the fine aggregate, the coarse aggregate friction angle was measured as shown in Figure 3-8 by forming a pile with the maximum possible angle. A sample of 40 to 80 pounds of aggregate was used to form the pile and a scoop was used to pour aggregate from a height as close to the top of the pile as possible. The maximum angle formed by the limestone pile was considered as a constant and correlated to the friction angle of the particles. Three measurements were taken for a given coarse aggregate, and the average value was used as the coarse aggregate friction angle.

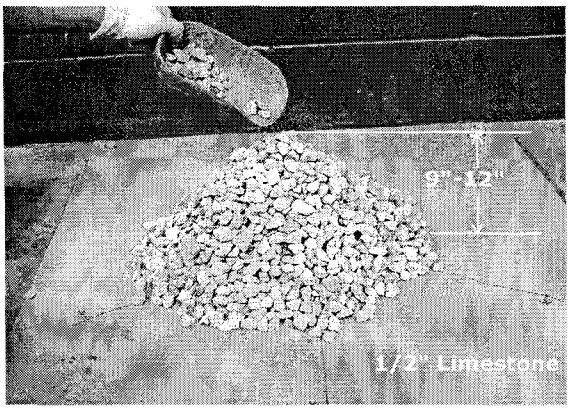

Figure 3-8 Coarse aggregate friction angle test

3.4.3 Paste and Mortar Rheology Measurement

A Brookfield R/S SST2000 rheometer (Figure 3-9) was used to measure the rheology parameters of cement paste and mortar. It is a stress control rheometer controlled by computer program. Shear stress and rate are calculated according to the reading in the load cell and the size of the rotating vane.

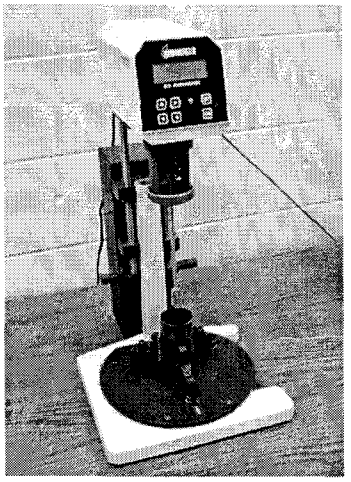

(a) Overview

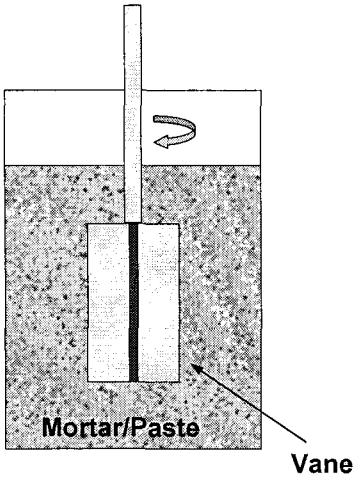

(b) Side view of vane and container

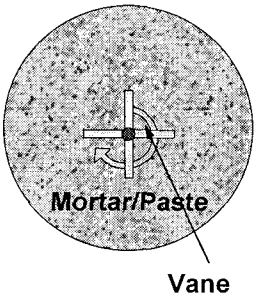

(c) Top view of vane and container

Figure 3-9 Brookfield rheometer

Two different sizes of vanes were used according to the rheology parameters of different materials under test. The physical parameters of the vanes are listed in Table 3-5:

Table 3-5 Vane physical parameters for Brookfield rheometer

	Diameter (m)	Height (m)	Torque range (Pa)	Container
V30-15	0.015	0.030	121-4040	2"x4" Cylinder
V40-20	0.020	0.040	51-1700	3"x6" Cylinder

A rheology measuring procedure as shown in Figure 3-10 was used for paste and mortar rheology measurement. After placing the paste/mortar into the rheometer, the specimens were sheared at a constant rate at relative low level of $15s^{-1}$ (for paste) or $30s^{-1}$ (for mortar) for 60 seconds (referred to as "pre-shear"). In the rheology testing procedure, a pre-shear step is necessary because results showed that if sedimentation occurs in mortar/pastes during viscometric experiments, large errors in the results are possible (Bhatty et al., 1982). Following the pre-shear, the vane will be stopped 60 seconds, within which time the mixing vane was lifted and the sample was gently stirred to mitigate the formation of preferential shear planes due to particle orientation. This stirring was to prevent anomalous low shear stress results during subsequent testing. The sample was then subjected to a controlled rate hysteresis loop where the shear rate was increased from 0 to $50s^{-1}$ (for paste) or $100s^{-1}$ (for mortar) over a 60 seconds period and then immediately decelerated back to $0s^{-1}$ over an additional 60 seconds. For the cement paste measurement, a lower maximum shear rate at $50s^{-1}$ was used determine the linear shear stress - shear rate behavior through the whole measurement process (this will be explained in Appendix II). In order to get an accurate measurement, a zero-calibration was performance for the Brookfield rheometer every day before any tests. The zero-calibration was generally performed by rotating the impeller/vane at several different speeds without applying any torque (without testing materials). The purpose of the operation was to recalibrate the torque sensor to eliminate the friction in the rheometer in the readings.

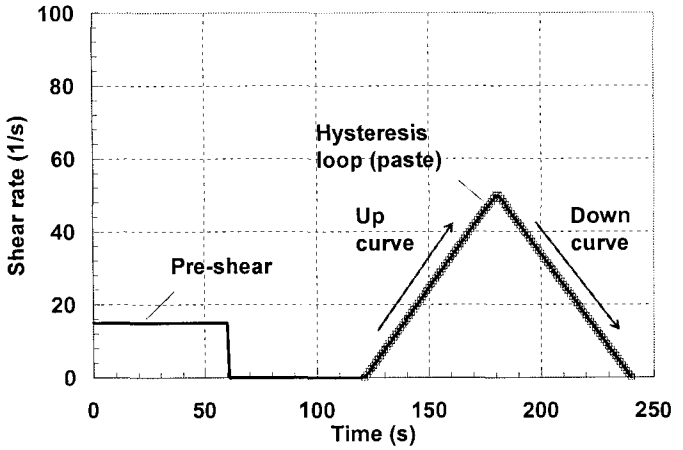

(a) Paste

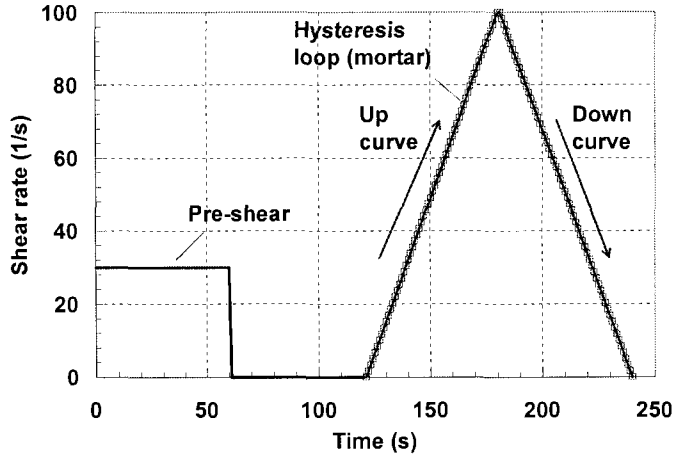

(b) Mortar

Figure 3-10 Paste and mortar rheology testing procedure

A typical test result of mortar rheology measurement is shown in Figure 3-11. The down curve of the rheology measurement, which has the full structure broken down is generally agreed to confirm to the Bingham model and was able to be used to obtain yield stress and viscosity (Banfill, 1994). The yield stress was determined by extending the linear portion of the down curve (shear rate from 100 to $5s^{-1}$) to the y-axis. The yield stress can be defined as the minimum stress required for a material to start flowing/deforming (Schramm, 1994).

The plastic viscosity is defined as the ability of a material to resist flow, which can be obtained from the slope of the linear portion of the down curve for Bingham material. High

plastic viscosity is normally characteristic of a less flowable suspension than low plastic viscosity suspension.

The hysteresis loop is the area between the up and down curves of the shear stress- shear rate diagram. The loop is created from a phenomenon called thixotropy, where there is a shear thinning or shear thickening behavior of the material. This is caused by a decreasing or increasing in the viscosity as a stress is applied followed by recovery as the stress is removed (Mindess et al., 2003). The area of the hysteresis loop has units of energy and is related to the energy required to break down interparticle attractions and weak bonds in the material.

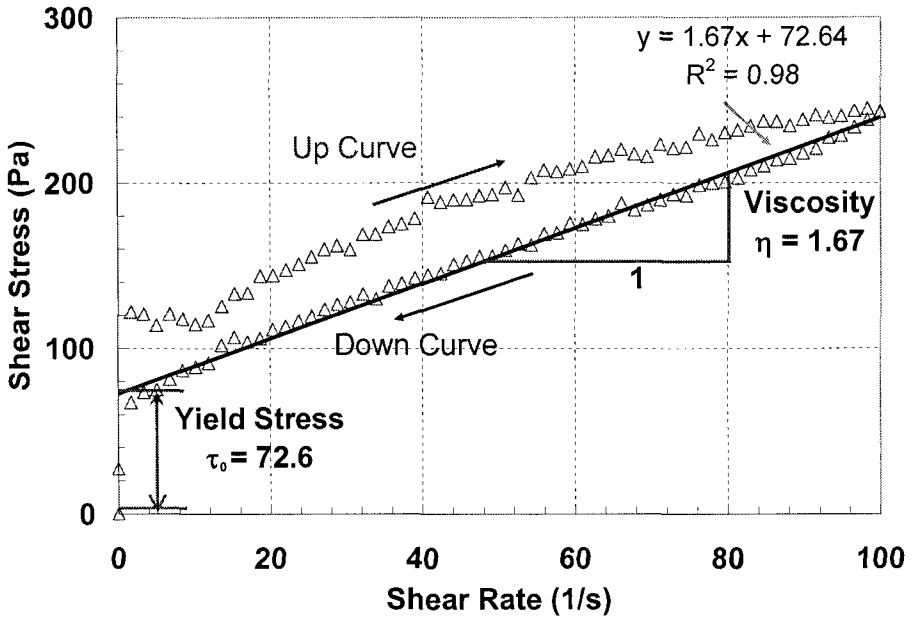

Figure 3-11 Typical flow curve of mortar (#30 riversand, s/c=2, w/c=0.50)

In addition to the rheometer tests, two other methods were also used to estimate the flowability in order to compare the rheology test with standard test results: (1) a mini-slump cone was used to estimate the flow of cement paste (Appendix III), (2) a flow table (ASTM C230) was used to estimate the flowability of mortar. The flow table test estimates the flowability of mortar based on the spread of a mortar cone using fewer than 25 drops of the flow table (Figure 3-12). Generally the higher flow percentage represents higher flowability of mortar. A flow table test for mortar was performed according to the procedure described in

ASTM C1437. For mortar with higher flowability, the flow percentage will be very high, which will result in a flow larger than the measurable range at 25 drops. In those cases, a modified flow table test considering the drop times was applied. It was found that the drop times have good correlation with spread diameter in logarithm scale, which is described in Appendix IV. A transfer equation of the calculated flow percentage from different number of drops to the standard 25 drops was also derived from experiment data.

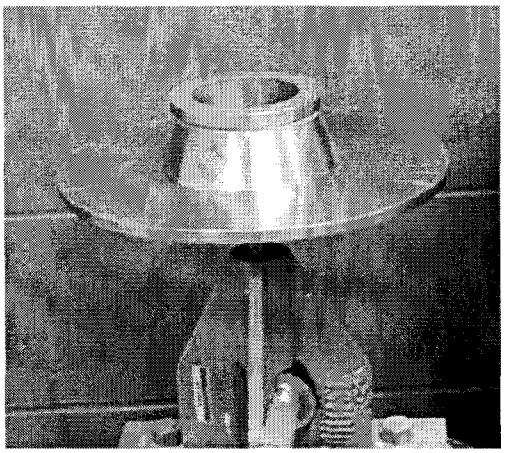

Figure 3-12 Flow table for mortar

3.4.4 Concrete Rheology Measurement

A portable IBB rheometer as shown in Figure 3-13 was used for concrete flowability measurements. The rheometer is a modification of the Tattersall two-point device (Tattersall, 1991) which has been successfully used on a wide range of concretes, from concrete with a slump of 1 inch to self-compacting concretes (Ferraris and Brower, 2004; 2001). The IBB rheometer has a rotating impeller inserted into fresh concrete placed in a cylindrical container. A computer controlled DC motor turns an H-shape impeller capable of rotating in a planetary motion. For low-workability concretes it should be necessary to introduce planetary motion of the impeller because a relative loose portion may be formed if the impeller keeps passing through original orbit (Tattersall, 1991). The sample size of concrete is around $0.8ft^3$, while the cross sectional area of the impeller is 6.20 in^2.

A load cell in the IBB rheometer measures the reaction torque from the impeller while a tachometer measures the impeller's rotation speed. Similar to the Tattersall's two-point device for material following the Bingham model, the linear relationship between torque and speed is defined by the slope H and the zero speed intercept G, which can be related to plastic viscosity and yield stress, respectively (Tattersall and Banfill, 1983; Tattersall, 1976).

The portable IBB, as shown in Figure 3-13 is constructed on an aluminum frame and includes wheels for easy transport. It is designed to be portable or transportable and can be used at a construction site.

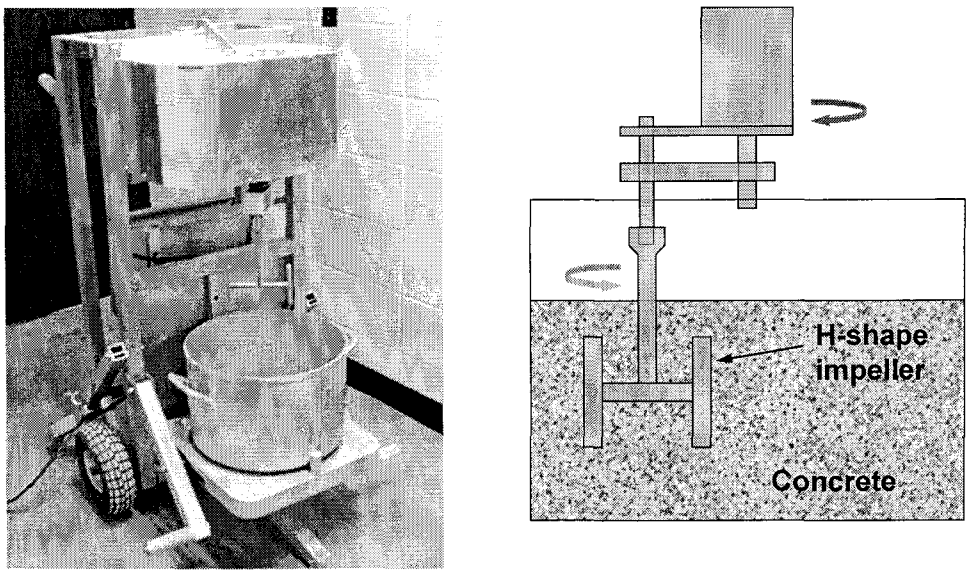

(a) Overview **(b) Side view of impeller and container**

Figure 3-13 IBB portable concrete rheometer

A computer program was used to control the rotation speed of the impeller during the test. Figure 3-14 shows the test sequences used in the present research. Similar to the paste/mortar rheology test, the specimen was pre-sheared after placing the concrete into the container at a low constant rate, approximate 0.2 (rev/s), for 30 seconds. Following the pre-shear, the impeller stopped for 30 seconds, and a mallet was used to gently strike around the side of the container for 10 times, thus preventing the formation of preferential shear planes due to particle orientation. The sample was then subjected to a controlled rate hysteresis loop where the shear rate was increased from 0 to 1 (rev/s) over a 100 seconds period and then

immediately decelerated back to 0 (rev/s) over an additional 100 seconds. In order to get an accurate measurement, a zero-calibration was performed for the portable IBB rheometer every day before any tests.

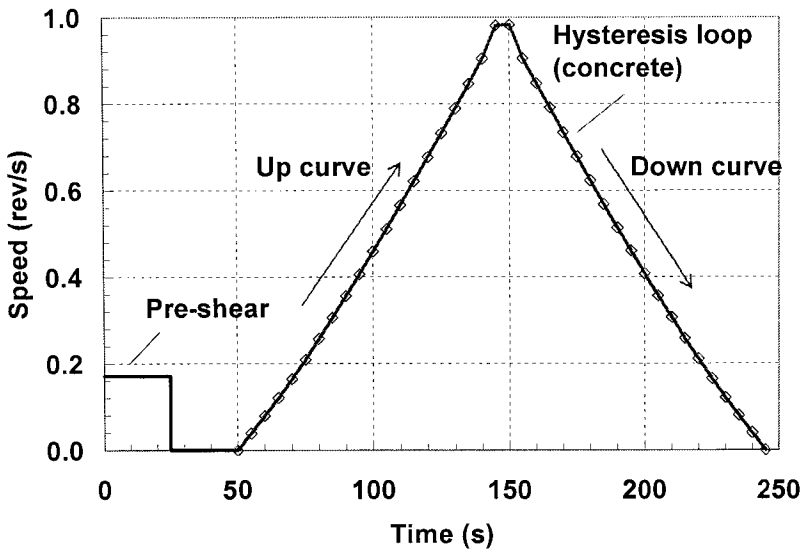

Figure 3-14 Concrete rheology testing procedure

When the impeller is rotating at different speed according to the testing procedure as shown in Figure 3-14, the resistance acted on the impeller was measured by the load cell. A typical result from IBB concrete rheology measure is shown in Figure 3-15, in which the measured data of the impeller speed and the measured torque are used to calculated *G* and *H*. Similar to the paste/mortar rheology measurement, the down curve of the rheology measurement, which confirmed to the Bingham model was used to obtain the term related to yield stress and viscosity. The yield term *G* (Nm) is determined by extending the linear portion of the down curve (1 to $0.04s^{-1}$) to the y-axis, which can represent the minimum stress required for a material to start flowing/deforming; hence, it can be related to concrete yield stress. The viscosity term *H* (Nm·s) is found from the slope of the linear portion of the down curve, which can represent the plastic viscosity as defined as the ability of a material to resist flow. Results showed that hysteresis loops were also observed for most of the concrete rheology measurements, which indicated that certain degree of structural breakdown still existed in the concrete rheology measurement. It was also observed that the rheological curve looks rough

compared to the curves observed in mortar or paste as shown in Figure 3-11. The contact of individual piece of aggregate with rheometer paddle significantly affected the reading of the force applied on the paddle.

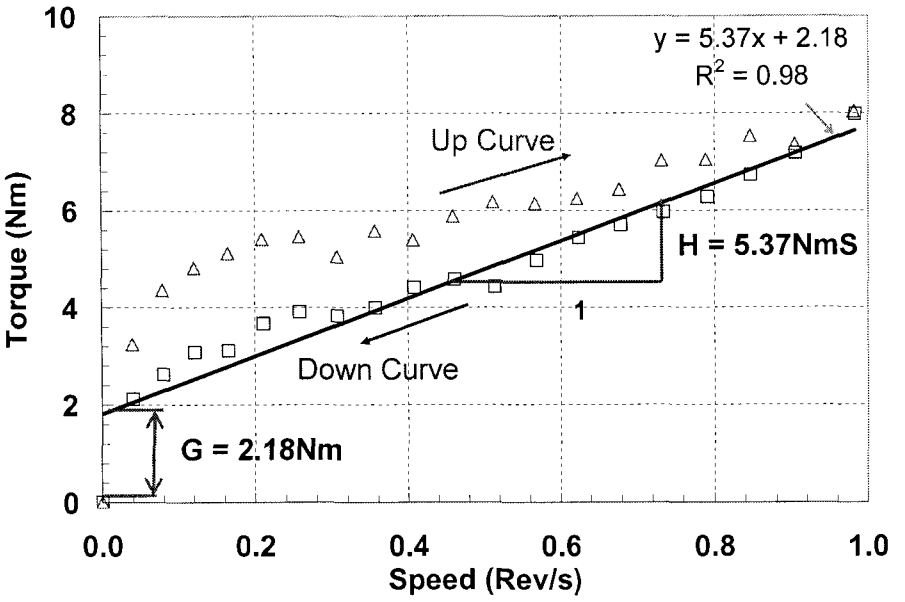

Figure 3-15 Typical flow curve of concrete (Mix1-G2)

In addition to the rheology measurement, concrete slump and unit weight were measured right after a batch mixing according to ASTM C143 and ASTM C138 respectively.

Three 4 inch by 8 inch cylinders were cast for each mix, and the cylinders samples were prepared and stored in a curing room according to ASTM C192. The Seven day compressive strength of the cylinders was measured according to ASTM C39. Three cylinders were measured for each batch of concrete, and the average value was used as the compression strength.

CHAPTER 4. AGGREGATE TEST RESULTS

In order to quantitatively study the effect of aggregates on the rheology performance of mortar and concrete, it is important to characterize the differences between the aggregates. The properties of fine and coarse aggregates, such as absorption, specific gravity, bulk density, uncompacted void content, and friction angle are presented in this chapter.

4.1 Fine Aggregate Properties

4.1.1 Specific Gravity and Absorption

The specific gravity and absorption of the fine aggregates are presented in Table 4-1.

Table 4-1 Specific gravity of riversand and limestone

	Riversand	Limestone	Standard Sand
OD	2.59	2.42	2.66
SSD	2.63	2.53	2.66

As mentioned in the previous chapter, all of the fine aggregates used in this study were in an OD condition because it is practically very difficult to have all fine aggregates prepared in the SSD condition. Since dry aggregate absorbs water right after contact with water, the w/c of the mortar will change from the original mix design based on the OD condition fine aggregate. Two kinds of absorption from different fine aggregates were measured according to the modified testing method for fine aggregate specific gravity and absorption (Appendix I). The actual absorption within the test period, $Abs_{Act}\%$ (first ten minutes after aggregate contacted with water) and the total absorption, $Abs_{Tot}\%$ (absorption capacity) of different fine aggregates were shown in Figure 4-1. The results indicated that riversand absorbs less water than limestone. The absorption of riversand increased with the size of aggregate, which might be caused by the larger amount of porosity contained inside larger aggregate particles, but this tendency was not clearly observed in limestone. The absorption of graded riversand used in the present research lay between the absorption of #30 and #16 riversand (which is the range of average size of these graded aggregate). The standard sand was found to have a

very low absorption capacity. This is likely due to the natural properties of silica sand, which has a very dense structure and is composed almost entirely of naturally-rounded grains of nearly pure quartz.

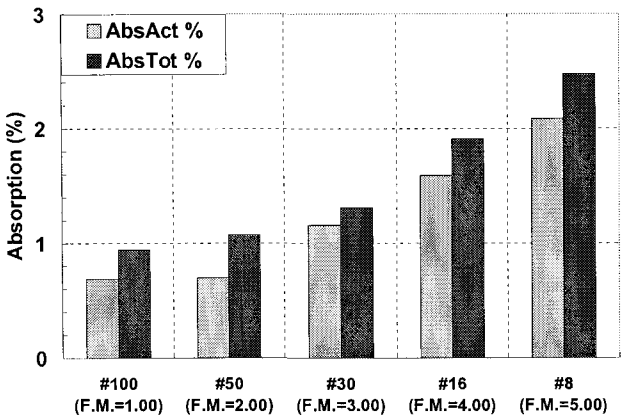

(a) Single-sized riversand

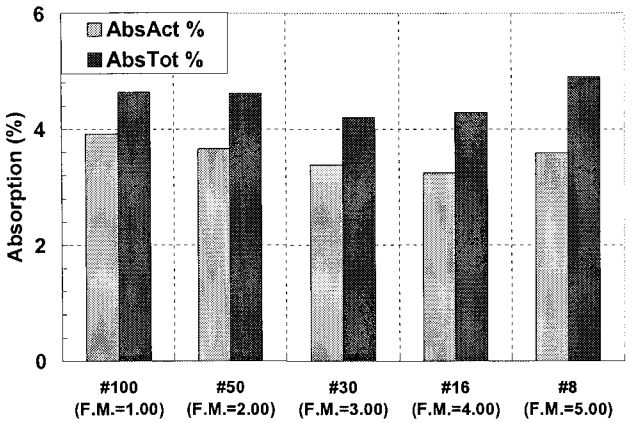

(b) Single-sized limestone

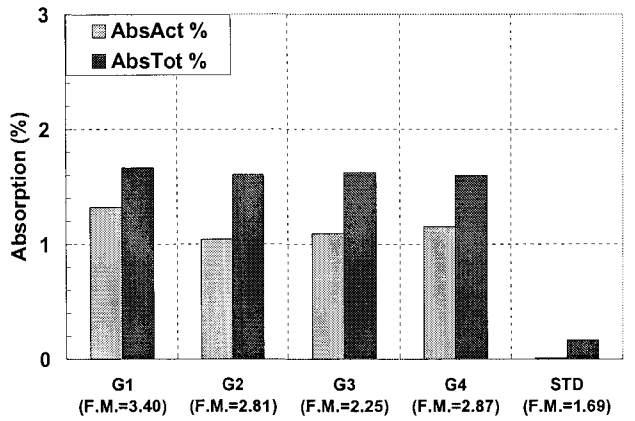

(c) Graded riversand and standard sand

Figure 4-1 Absorption of fine aggregate

4.1.2 Void Content

In order to estimate the void content of fine aggregate, a fine aggregate angularity test was employed. Based on procedure from ASTM C1252, the fine aggregate angularity was defined as the air voids present in loosely compacted fine aggregates. Higher void contents generally indicate more fractured faces and more irregular shapes, which result in a more difficult packing of particles.

In the fine aggregate angularity test, a sample of fine aggregate was poured into a cylinder with known volume by flowing through a standard funnel. The uncompacted voids percent can then be calculated based on the difference between the cylinder volume and fine aggregate volume collected in the cylinder. The calculation of this uncompacted void content of fine aggregate can be shown as the following equation:

$$V_{n-FA} = \frac{V_{FA} - W_{FA} / \gamma_{FA}}{V_{FA}} \times 100\% \qquad \textbf{Equation 4 - 1}$$

In this equation, $V_{n\text{-}FA}$ is the uncompacted voids (%), V_{FA} is the volume of cylinder (mm^3), W_{FA} is the weight of aggregate in cylinder (g), and γ_{FA} is the density of fine aggregate (g/mm^3), which can be calculated according to the specific gravity of sand at OD condition from section 4.1.1 ($\gamma_{FA} = G_{sb\text{-}FA} x 10^{-3} g/mm^3$).

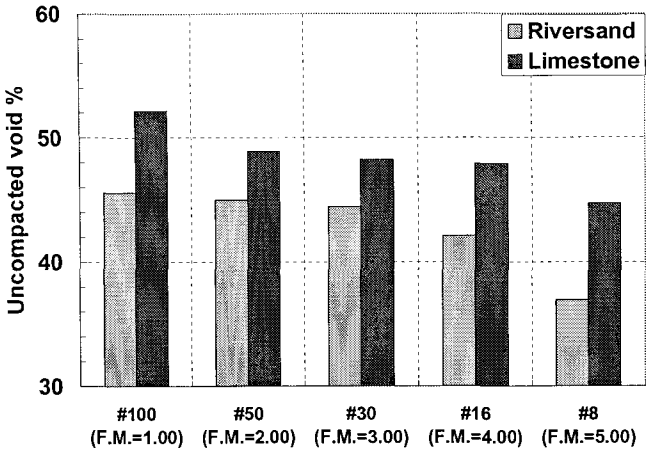

(a) Single-sized aggregate

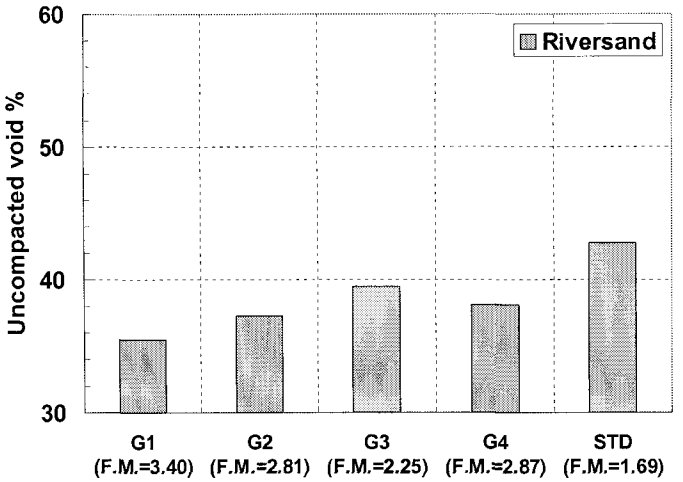

(b) Graded aggregate

Figure 4-2 Void content of sand

Figure 4-2 (a) indicated that limestone had higher uncompacted void percentages than riversand, which is because of the irregular shape of the particle. The smaller aggregate showed higher uncompacted void content. This phenomenon may caused by the fact that the effect of self weight in bigger size of aggregate is not negligible on particle compaction which might result in a denser packing comparing to smaller size of aggregate. Results as shown in Figure 4-2 (b) indicate that graded aggregate has lower void content than aggregate with just one single size, because smaller particles can fill up the space between bigger particles, in which case the space between aggregate particles significantly decreases.

4.1.3 Friction Angle

In order to study the effect of aggregate friction on the flow performance of mortar and concrete, another test was used to estimate the aggregate friction angle based on the maximum angle formed by the sand pile (slope repose). The friction angles of different sands are presented in Figure 4-3.

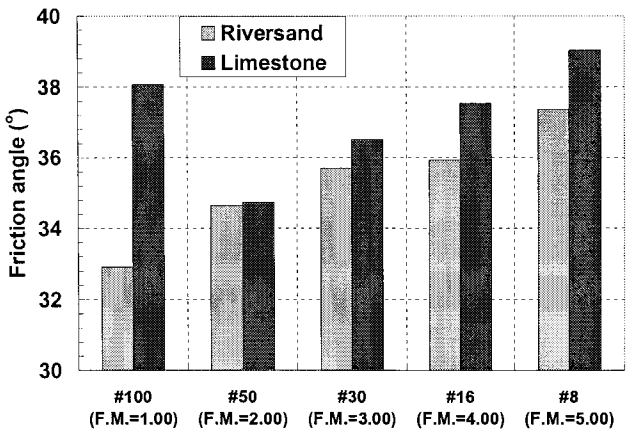

(a) Single-sized aggregate

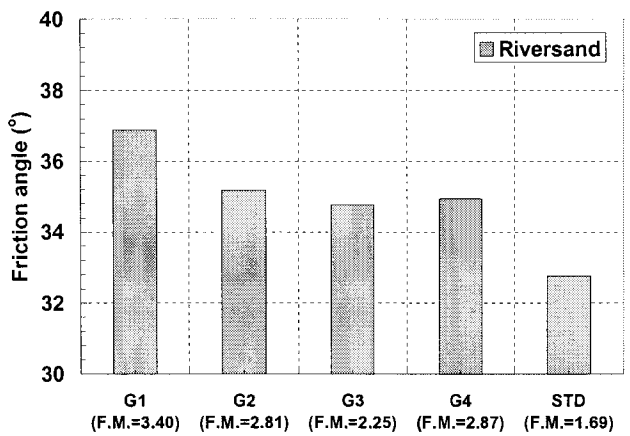

(b) Graded aggregate

Figure 4-3 Friction angle of sand

Results showed that the measured friction angle of fine aggregate used in present research lay between 32° to 39°, which is consistent with previous research which stated that the angle of friction for sands usually ranges from 26° to 45° (Das, 1995). The friction angle test showed

that larger aggregate had higher friction because of the higher degree of internal friction and interlock from the higher percentage of rough and irregular shape particles. The #100 limestone was found to have a much higher friction than #50 sand, this phenomena was caused by the relatively large amount of fines on aggregate particles which result in cohesion between aggregates. This result indicated that the test method may not be able to reflect the actual fraction angle of very fine sand.

It is expected that angular particles will have a higher degree of interlocking than rounded particles, and hence that sands composed of higher percentage of angular particles would have the larger friction angle. The data of friction angles of riversand and limestone presented in Figure 4-3 (a) confirm this prediction. Riversand has lower friction angles when compared to limestone because of the relative round shape and smooth surface. No obvious difference of the friction angle between single-sized and graded sand was found in the test. The friction angles of the graded riversand used in present study lay between friction angle of #30 and #16 riversand, and the standard sand has a comparable friction angle with #100 riversand because of the similar size and nature of its particles.

4.2 Coarse Aggregate Properties

The properties of the coarse aggregate used in the concrete study are presented in this section. The limestone aggregates studied had single sizes of #4, 3/8", 1/2", and 3/4". Three recombined limestone with designed different gradations (G1, G2, and G3) were also studied.

4.2.1 Specific Gravity and Absorption

The specific gravity and absorption of the coarse aggregate used in this study were measured according to ASTM C127. The measured specific gravity of limestone was 2.53 and 2.45 under the SSD and OD condition, respectively. Absorptions of different coarse aggregate are listed in Table 4-2.

Results indicated that the absorption capacity of an aggregate declined with increased size, which is in consistent with fine aggregate results. The absorptions of graded coarse aggregate used in this study were close to the absorption capacities of 3/8" and 1/2" aggregate.

Table 4-2 Coarse aggregate absorption

	Single-sized				Graded		
	#4	3/8"	1/2"	3/4"	G1	G2	G3
Absorption (%)	3.77	3.22	3.15	2.76	3.07	3.14	3.26

4.2.2 Void Content

According to ASTM C29, the uncompacted void content of different coarse aggregate were measured by fill up the measuring container by shoveling aggregate inside with minimum compaction. The following equation can be used to calculate uncompacted void content of fine aggregate:

$$V_{n-CA} = \frac{V_{CA} - W_{CA}/\gamma_{CA}}{V_{CA}} \times 100\% \qquad \textbf{Equation 4 - 2}$$

In this equation $V_{n\text{-}CA}$ is the uncompacted voids (%), V_{CA} is the volume of cylinder (mm^3), W_{CA} is the weight of coarse aggregate in cylinder (g), and γ_{CA} is the density of the aggregate (g/mm^3), which can be calculated according to the specific gravity at OD condition from section 4.2.1 ($\gamma_{CA} = G_{sb\text{-}CA} \times 10^{-3} g/mm^3$).

Figure 4-4 presented the void content of different coarse aggregate; results showed that smaller aggregates have lower uncompacted void content because of the smaller degree of particle interlocking. Results also indicated that an aggregate with gradation has lower void content than an aggregate with just one single size particles. The smaller particles can fill up the space between bigger particles in graded aggregate, and thus the space between aggregate particles will significantly decrease.

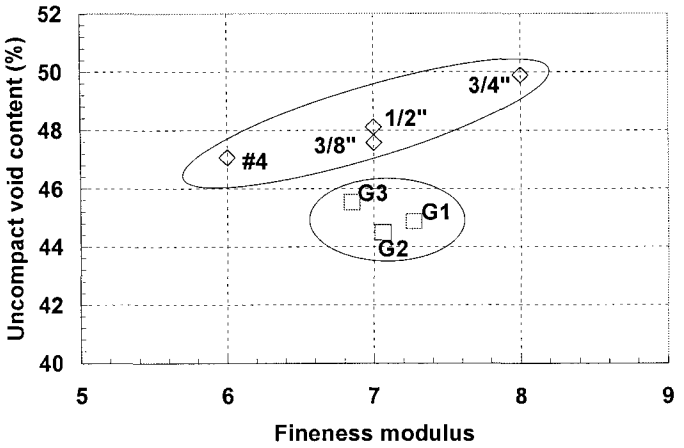

Figure 4-4 Void content of coarse aggregate

4.2.3 Friction Angle

Coarse aggregate friction tests were also performed to study the friction angle of different coarse aggregates based on the maximum angle formed by the aggregate pile. The friction angles of coarse aggregates are shown in Figure 4-5.

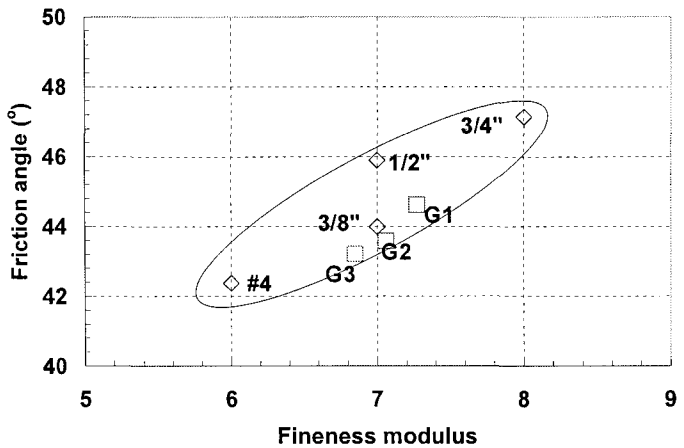

Figure 4-5 Friction angle of coarse aggregate

Similar to the aggregate uncompacted void test, the friction angle test demonstrated that larger aggregates have higher friction because of the internal friction and interlock from the higher percentage of irregular shape particles, which also resulted in larger void content. No obvious difference of the friction angle between single size and graded coarse aggregate was

found in the test. The friction angles of the graded limestone used in the present study lay between the friction angle of 3/8" and 1/2" coarse aggregates.

The comparison of the coarse aggregate friction angle and void contents showed that with the increase of size of coarse aggregate, both friction angle and void contents increase. This is because the increase of particles size results in a higher degree of interlocking from the irregular shape particles, which not only increases the friction angle, but also results in a lower degree of compaction.

CHAPTER 5. PASTE RHEOLOGY TEST RESULTS

In this chapter, the rheological performances of cement pastes were studied using the Brookfield rheometer. The effects of different w/c (0.30, 0.35, 0.40, 0.50, and 0.60) and different mixing methods (the Hobart versus the highshear mixer) were studied. Statistical analyses were performed to quantitatively study the effect of w/c on different rheology parameters. This can be used to discover the paste rheological properties for using in the concrete modeling study.

The results showed that the rheology of cement paste from low to high w/c is significantly different, and that the relationship between rheology parameters and w/c can be expressed by an exponential equation. Previous studies examined the effects of using different mixers, which showed that cement paste mixed through the higher energy technique provided paste with better flowability (Yang and Jennings, 1995; Ferraris et al., 2001). Also, the effect of the mixer is different under different mixing procedure. In the present chapter, the rheological performance of cement paste mixed through Hobart and highshear mixers were studied, results were consistent with previous researches. The rheological parameters of cement paste mixed by highshear mixer will be used in the mortar and concrete rheology modeling study described in Chapter 8.

5.1 Effect of w/c

Water content is well known to have the most significant effect on the rheological performance of cementitious materials including cement paste, mortar and concrete rheology (Tattersall, 1991). The plasticity of cement paste can be attributed to a combination force between cement particles and the lubricating action of the water between them. The increase of water content causes the paste to become softer because it results in a greater dispersion of cement particles. The freedom of individual particles thus increases. Liberation becomes greater, and the mobility of the paste increases, which further causes the decrease of yield stress and viscosity (Popovics, 1982).

In the present research, cement pastes were mixed according to the procedure as described in Chapter 3. The rheometer tests were performance based on the procedure with a preshear period and testing loop with maximum shear rate of $50s^{-1}$ as shown in Figure 3-10 (a). The flowabilities of cement paste at different w/c (from 0.30 to 0.60) were compared.

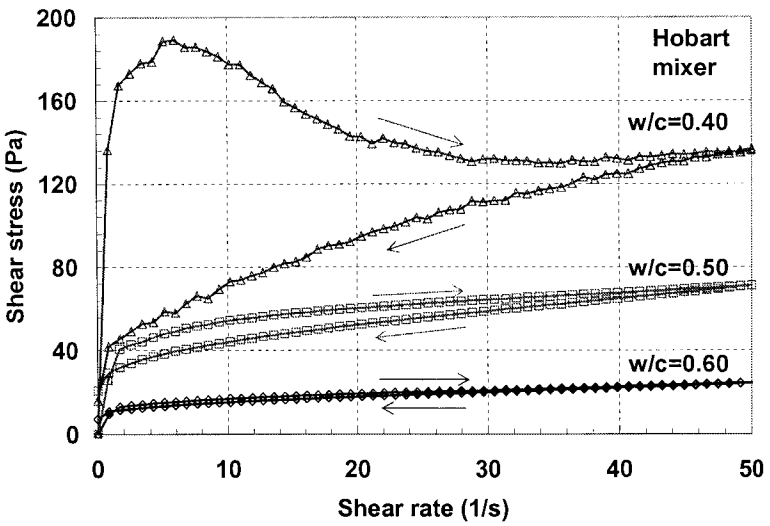

Figure 5-1 Effect of w/c on paste rheology

As shown in Figure 5-1, the shapes of the flow curve for cement paste at different w/c were significantly different. It was found that down curves were generally observed to be below up curves, which indicated that less shear stress was required to maintain the same shear rate. This indicated structural breakdowns in the cement paste and the hysteresis phenomenon were obtained. The extent of thixotrophy behavior (hysteresis areas between the up and down curves) increased when w/c declined. Results showed that a significant thixotrophy property was observed at low w/c (0.4), which indicates that higher energy was required to break down the structure inside the cement particle, while at high w/c (0.6), thixotrophy was hardly observed. It was also found that, regardless the shape of up curves, the down curves generally performance linearly. The Bingham parameters of the broken down material were calculated from the down curves in the present study as shown in Figure 3-11. Results demonstrated that decreased w/c increased both yield stress (interception) and viscosity (slope) significantly. This indicates that more force will be required to initiate the flow and more force will be necessary to maintain a higher flow rate because of stronger inter-particle forces

acting of cement particles. These results agreed with the results from other researchers (Tattersall and Banfill, 1983).

5.2 Effect of Mixing Method

Previous research stated that low-shear mixing produces cement pastes which behave as two-phase systems, in which case suspensions of cement stay in water. While high-shear mixing produces cement paste of a different nature, the paste tends to behave as a single-phase material (Bartos, 1992).

A comparison of cement paste mixing from different mixers (a Hobart mixer and a highshear mixer) was also made in present research. Results showed that in cement pastes using a Hobart mixer, a higher and leaner curve is observed and the hysteresis loops are bigger than cement pastes mixed by a high shear mixer (Figure 5-2). These results agree with previous research by Williams et al. (1999), which stated that because of the higher mixing speed and stronger mixing energy during mixing process, the highshear mixer would break down more cement paste inter-particle force and the paste can be mixed better. Also, the yield stress and viscosity of cement paste from the Hobart mixer is higher than from the highshear mixer because of the lower amount of mixing energy.

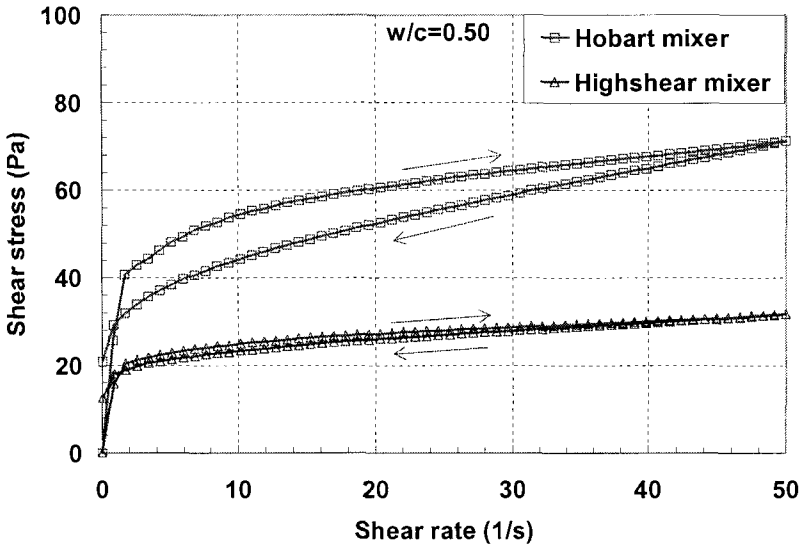

Figure 5-2 Effect of mixer on paste rheology

5.3 Results and Discussion

The Bingham model rheology parameters of cement paste at different w/c and from different mixer are summarized in Figure 5-3. Results show that when the w/c of the paste increased from 0.30 to 0.60, the viscosity fell from around 7 to 0.1 PaS, while yield stress decreased from around 200 to 10 Pa. The thixotrophy dropped dramatically from over 10000 Pa/s to almost zero. The same tendencies were observed with paste mixed through either the Hobart mixer or the high shear mixer. Cement pastes mixed by the Hobart mixer tended to have larger value of yield stress, viscosity and thixotrophy comparing to pastes mixed through the highshear mixer. Test results were consistent with previous research on cement pastes made by different mixing procedures, which showed that a change from the least severe to the most severe mixing procedure caused both the yield stress and plastic viscosity to decrease by about 60% and the width of the hysteresis loop decreased at the same time (Roy and Asaga, 1979).

At low w/c (0.30 and 0.40), pastes mixed with the highshear mixer had larger yield stress values compared to pastes mixed through the Hobart mixer. This was probably caused by the fact that when cement pastes were relatively dry, they can not be mixed thoroughly by a Hobart mixer and did not perform with liquid-like behavior. However, the viscosity and thixotrophy of paste mixed with the Hobart mixer still showed much higher values compared to cement paste mixed by the highshear mixer.

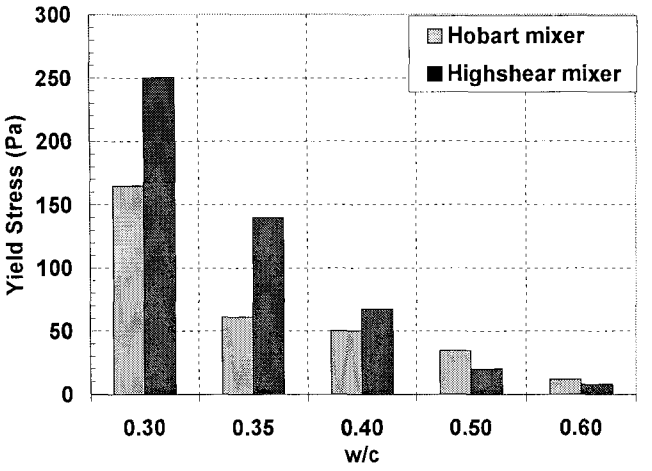

(a) Yield stress

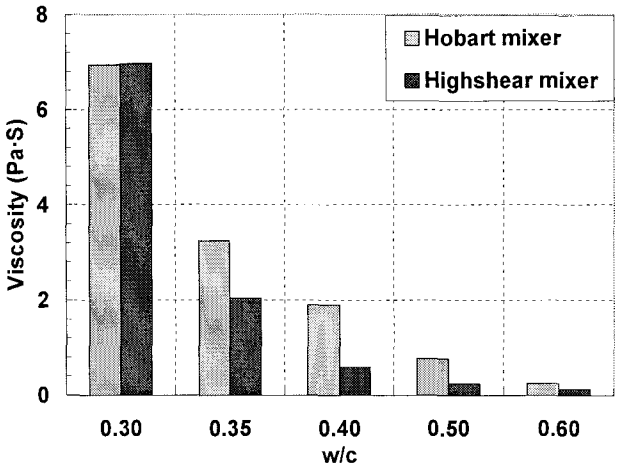

(b) Viscosity

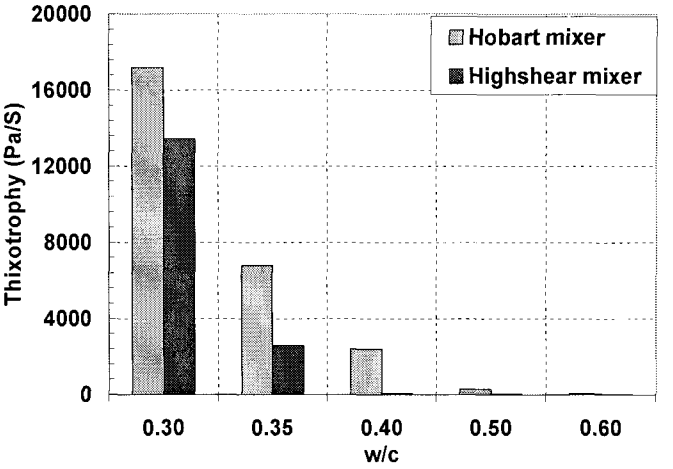

(c) Thixotrophy

Figure 5-3 Rheological parameters from different paste mixes

In order to develop the mathematical equations for further modeling studies in predicting mortar and concrete rheology, statistical analyses were performed to quantitatively study the effect of w/c on paste rheology. Exponential relations were chosen according to previous research (Tattersall 1991; Wallevik and Wallevik, 1998). It was found that both yield stress and viscosity decrease exponentially as w/c increases. Best regression curves and equations used in fitting the viscosity and yield stress from different w/c were shown in Figure 3-5.

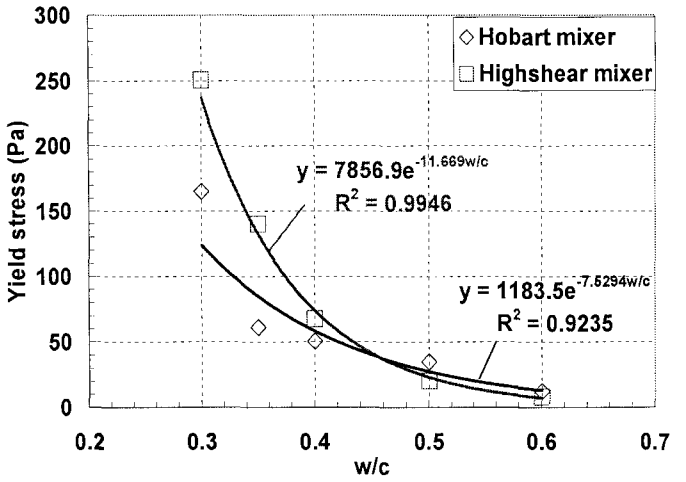

(a) Yield stress

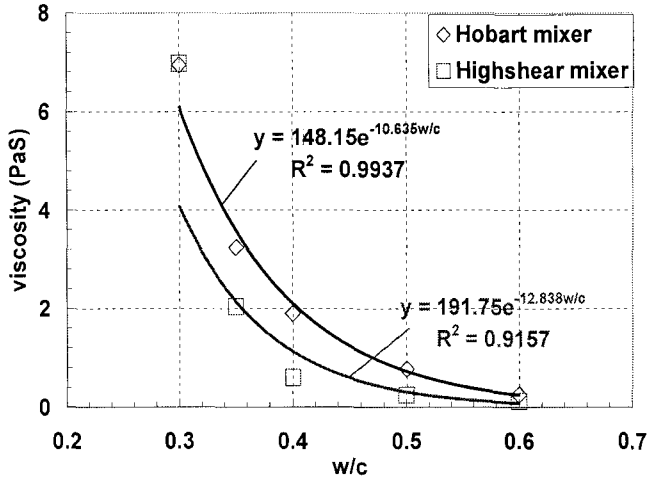

(b) Viscosity

Figure 5-4 Rheological parameters with different w/c

According to Williams et al. (1999), comparing to standard mixing procedure follow ASTM C305 using Hobart mixer, cement paste experiences more shear energy and structure

breakdown in mortar and concrete mixing due to the interaction with aggregate. Cement paste mixed by highshear mixer at moderate speed was found to be similar to paste from concrete. The statistical equations (Equation 5-1, and 5-2) for rheological parameters of cement paste mixed by highshear mixer will hence be used in future mortar and concrete rheology modeling study in Chapter 8.

$$\tau_{0p} = 7856.9e^{-11.669w/c} \qquad \textbf{Equation 5 - 1}$$

$$\eta_p = 191.75e^{-12.838w/c} \qquad \textbf{Equation 5 - 2}$$

In these equations τ_{0p} and η_p are the yield stress (Pa) and viscosity (Pa·s) of cement paste.

Preliminary research has been done to study the testing procedure of rheometer (Appendix II). Two different maximum shear rates of $50s^{-1}$ and $100s^{-1}$ were used in the rheology measurement. Results showed that in cement pastes with high w/c (0.5 to 0.6), down curves at high shear rates (larger than $70s^{-1}$) did not follow the Bingham model any more, although the lower portions of down curves were still linear and can be used to calculate the Bingham parameters. This phenomenon was different from that observed during the low maximum shear rate test because of the different degree of structural breakdown throughout the testing period. Another reason may be the current interference in the measurement container when the mixing vane was rotating at very high speeds. The effect of the testing procedure is not further discussed because it is out of the scope of this research. In the present study, only results from the testing procedure with a maximum shear rate of $50s^{-1}$ were considered.

Additional research has also been performed to study flowability using mini-slump cone tests for paste with different w/c and different mixing methods. Results showed that the flow percentage of different cement paste can also be used to reflect the rheology behavior of the cement paste. A good correlation between flow percentage from the mini-slump cone test and the yield stress of various pastes was found. This trend is consistent with previous research (Roussel et al., 2005). The comparison of the rheometer test results and the mini-slump cone test results are summarized in Appendix III.

CHAPTER 6. MORTAR RHEOLOGY TEST RESULTS

In this chapter, the effects of fine aggregate characteristics on the rheology of mortar are investigated. Different sand content (s/c=1, 2, and 3), w/c (from 0.2 to 0.62), type (riversand and limestone), size (#100, #50, #30, #16, and #8) and gradations of fine aggregate (G1, G2, G3, G4, and graded standard sand) were considered.

Mortars were mixed according to the procedure as described in section 3.3.2. The Brookfield rheometer was used to measure the mortar rheological parameters of different mortars according to the procedure as shown in Figure 3-10 (b), with a preshear period and a testing loop. The flow percentages of mortars were also measured by a flow table test as specified in ASTM C1437. The results were compared with the measured rheological parameters.

6.1 Effect of w/c

Three to five w/c ranging from 0.20 to 0.62 were used for each type of sand. These ratios were chosen in order to make mortar with proper flowability and measurable rheological parameters. Neither too low nor too high w/c were desired, because they can cause low consistency or segregation, which are inappropriate for rheology measurement.

Figure 6-1 (a) demonstrated typical flow curves of mortar samples made with different w/c. For each flow curve, there is a thixotrophy loop, formed with the up-curve due to the increased shear rate and the down-curve due to the reduced shear rate. The thixotrophy loop area indicated the degree of test material interconnected structure broken down during testing process. Generally, the thixotrophy phenomenon becomes more significant as the mortar becomes dryer (decreased w/c). The test results showed that the down curves are generally a straight line, which can be described with the Bingham model. Therefore, in the present study, the yield stress and viscosity of a tested material are calculated from the down curves. The thixotrophy is not considered in the models within this study.

Figure 6-1 (b) shows the down parts of the flow curves of mortars with different w/c. Similar to cement paste, both the yield stress and viscosity of the mortars increased when the w/c

decreased. This means that a larger force is required to initiate the flow and to maintain a high flow rate because of the stronger interparticle forces acting between cement particles.

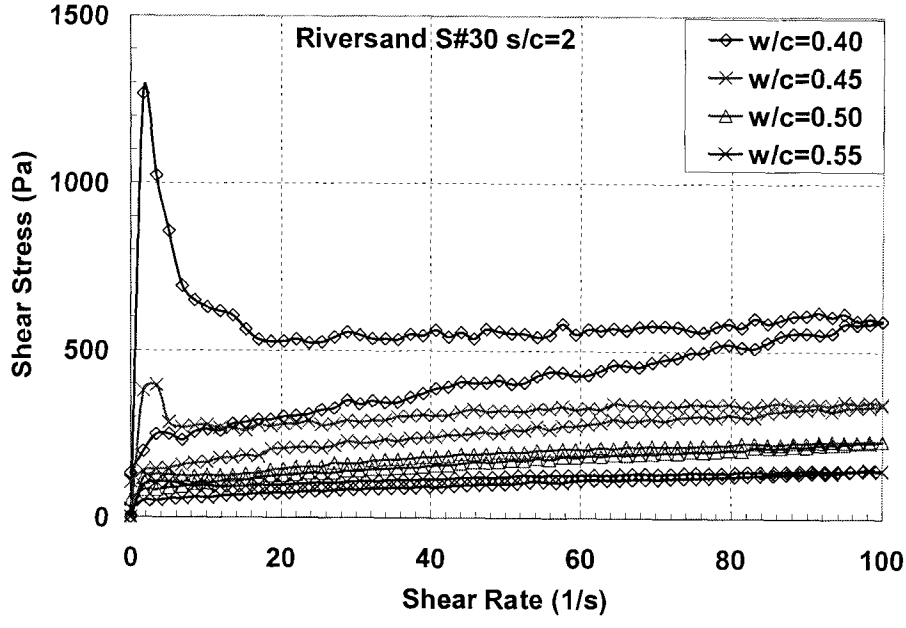

(a) Complete flow curves

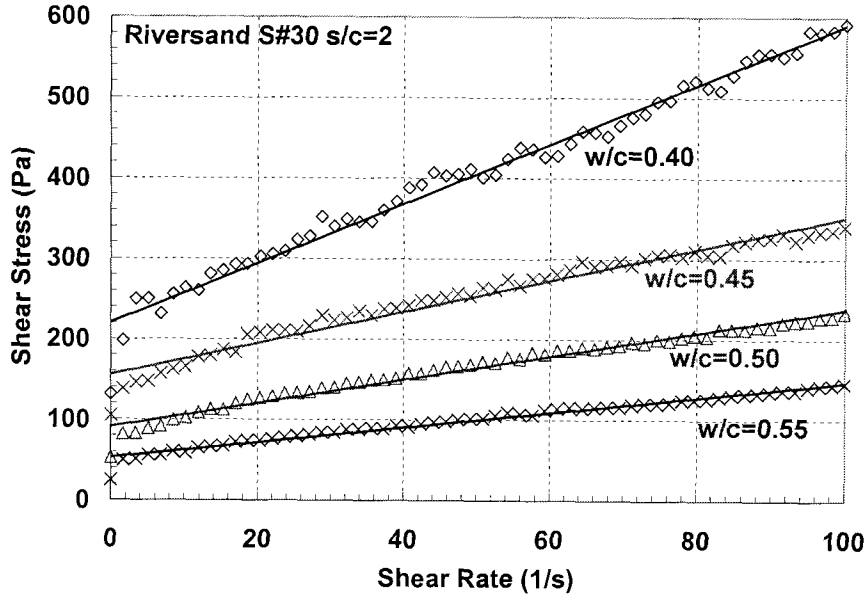

(b) Down curves

Figure 6-1 Effect of w/c on mortar rheology

6.2 Effect of Sand Type

As summarized in Chapter 2, the shape and texture of the aggregate particles also affects mortar/concrete workability. Spherical particles generally result in more workable mortar. In order to study the effect of shape on mortar rheology, two types of aggregate - riversand and crushed limestone fine aggregate (simplified as limestone) were chosen for this study.

As shown in Figure 6-2, the flow curves of mortar with limestone as aggregate (dash lines) generally lie above flow curves of mortar with riversand for a given aggregate content, which indicates that limestone provides mortar with lower flowability than riversand.

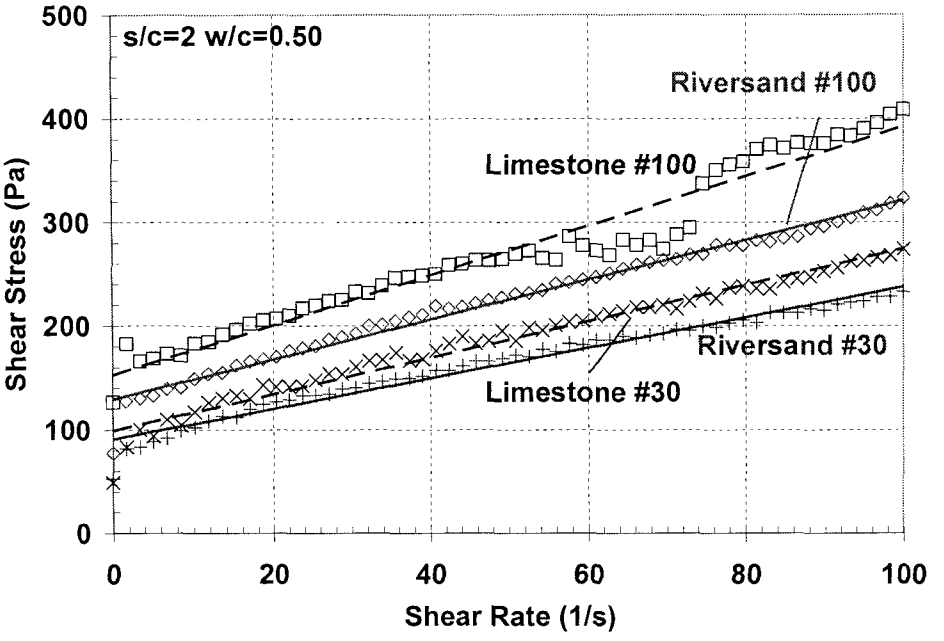

Figure 6-2 Effect of sand type on mortar rheology

Examples of the calculated viscosity and yield stress of mortar with different fine aggregate are shown in Figure 6-3. For a given mix proportion and a given size of aggregate, limestone provides the mortar with higher yield stress and viscosity. This result is expected because the uncompacted voids in limestone are larger, which requires more cement paste to fill up the space between aggregate particles. As a result, less cement paste was available to coat the aggregate particles, thus reducing mortar flow. In addition, the spherical particles of

riversand could act as "ball bearings", while angular particles provided mortar with more mechanical interlock or higher internal friction, thus requiring more energy for initiating and processing flow (Mindess et. al., 2003).

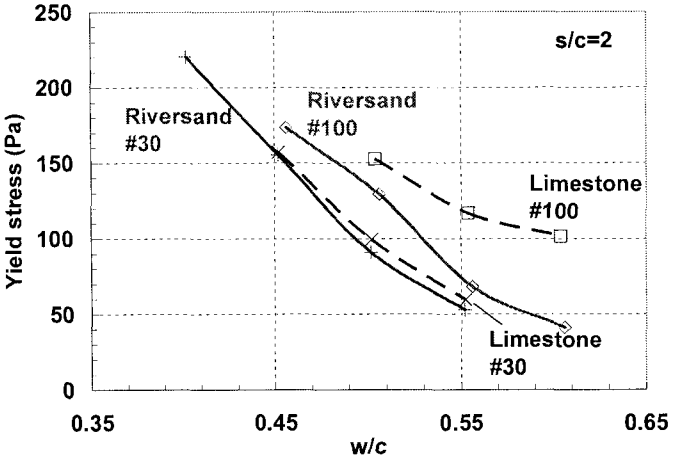

(a) Effect on yield stress

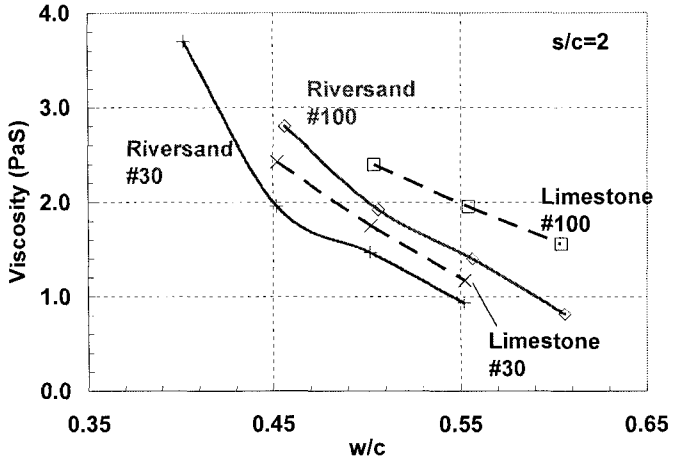

(b) Effect on viscosity

Figure 6-3 Rheological parameters of mortar with different type of sand

6.3 Effect of Sand Content

In the present study, three different s/c were chosen to study the effect of aggregate content on mortar rheology. As shown in Figure 6-4, the flow curves of mortars with different fine aggregate contents were significantly different. It was observed that when the fine aggregate content increased, both the yield stress and viscosity of the mortar increased. This was caused

by the higher degree of friction and interlock of solid particles, which reduced mortar flowability. Figure 6-4 also showed that when the s/c increased from 1 to 3, the flow curve become rough because test errors were caused by the direct contact of individual fine aggregate particles with the rheometer paddle.

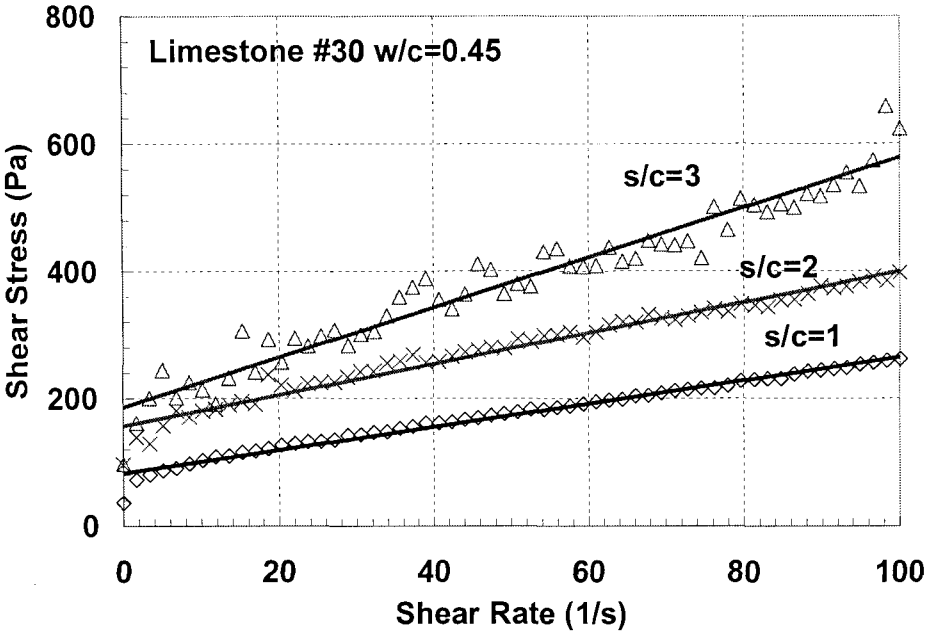

Figure 6-4 Effect of s/c on mortar rheology

Examples of the calculated Bingham parameters for different mortars were summarized in Figure 6-5. It can be observed that for mixtures with a low s/c (Figure 6-5 (a-1) and (a-2)) the difference in mortar rheology resulting from different sizes of aggregate was insignificant. However, this difference became obvious when the s/c increased (Figure 6-5 (b-1) and (b-2)) due to the increasing of volume concentration of aggregate. The changes in the yield stress are more significant than the viscosity changes.

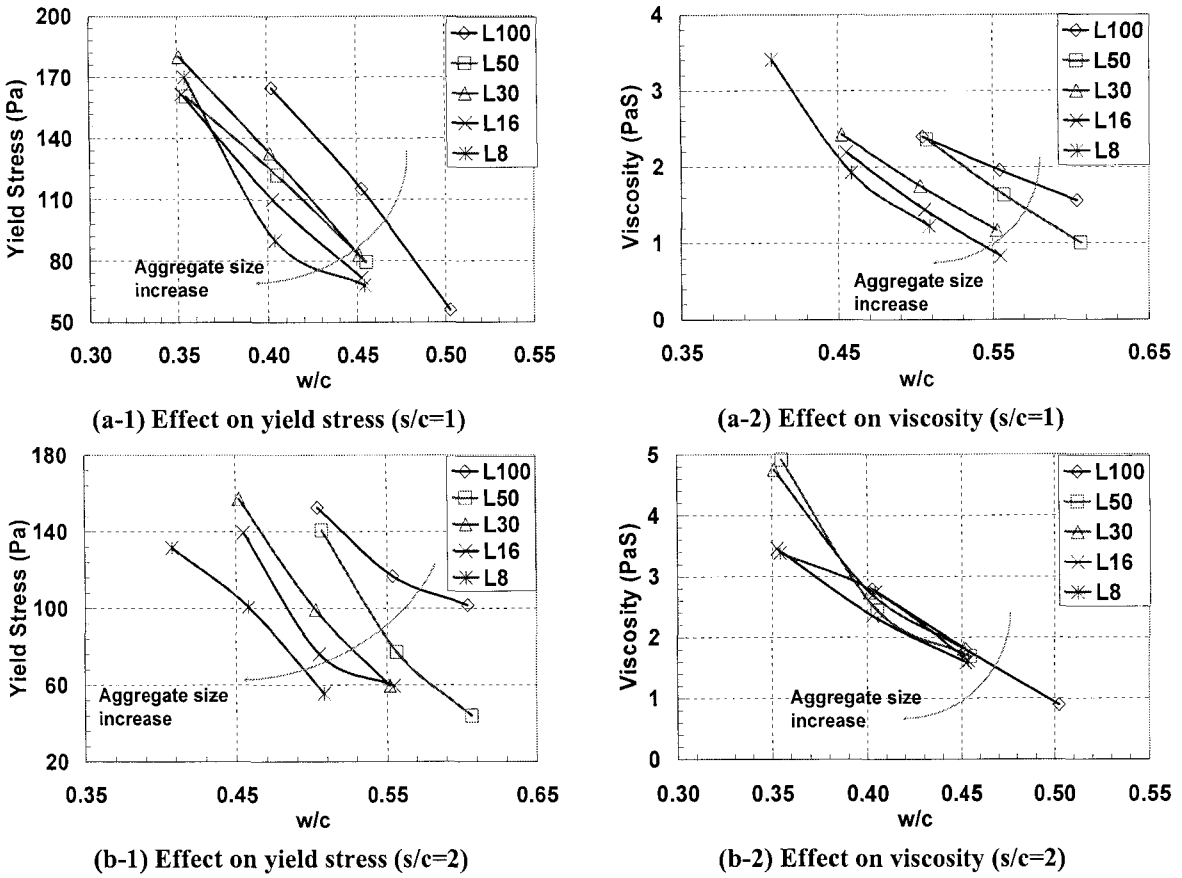

(a-1) Effect on yield stress (s/c=1)

(a-2) Effect on viscosity (s/c=1)

(b-1) Effect on yield stress (s/c=2)

(b-2) Effect on viscosity (s/c=2)

Figure 6-5 Effect of sand and w/c on mortar rheological parameters

6.4 Effect of Sand Size

Typical rheology test results of mortars made with different size of aggregate sizes are shown in Figure 6-6. For a given w/c and amount of fine aggregate, the mortar made with larger sand had a higher flowability. It was observed that when the size of aggregate increased from #100 (0.15mm) to #8 (2.36mm), the flow curve became rougher. This could be attributed to the test error caused by the direct contact of aggregate particle with the rheometer paddle. The error might become more significant when the ratio of the aggregate size to the diameter of the rheometer vane (15mm) becomes high.

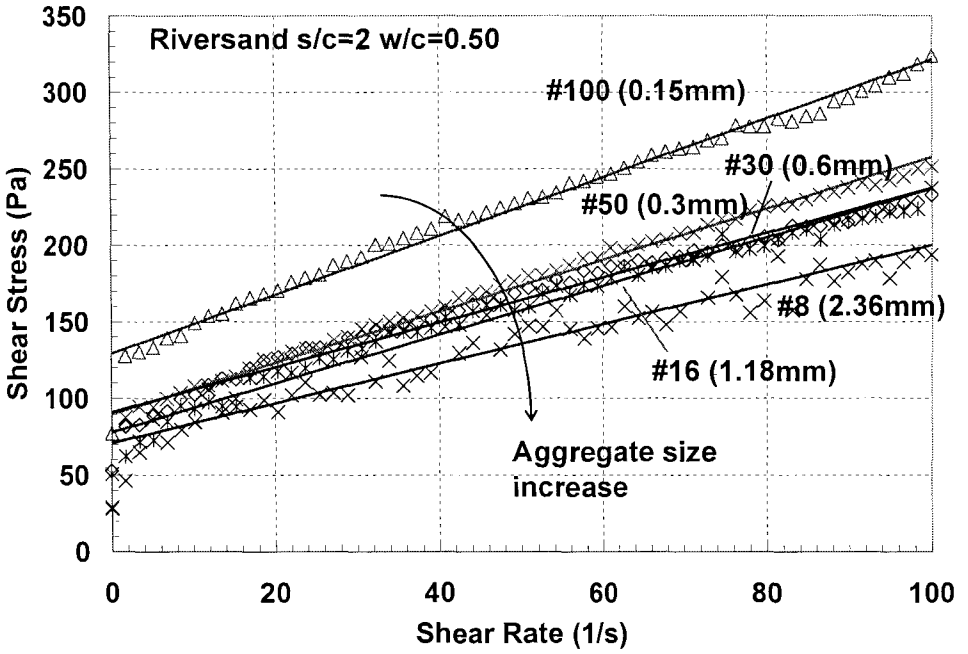

Figure 6-6 Effect of sand size on mortar rheology

The rheological parameters of mortar with different size of sand were also calculated. As shown in Figure 6-7, a smaller aggregate generally results in mortar with higher yield stress and viscosity. The much higher surface area results in a smaller excess paste thickness to coat the aggregate and provide flow. This result agrees with previous findings that the decreasing of maximum particle size generally increases the water demand (Mehta and Monteiro, 1993).

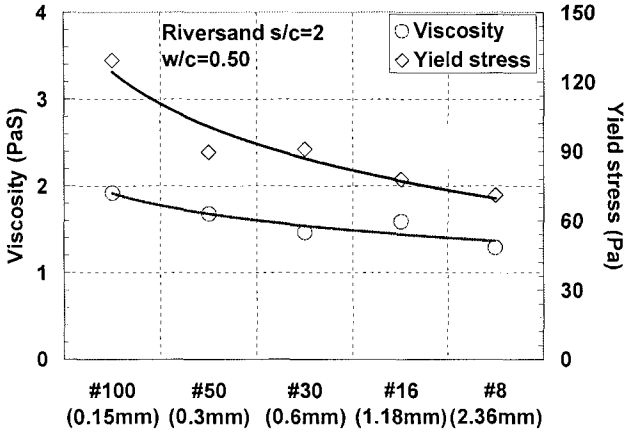

Figure 6-7 Rheological parameters of mortar with different size of sand

6.5 Effect of Sand Gradation

In order to provide the mortar with enough workability, a sufficient amount of cement paste is needed to fill up the space between aggregate particles. For a given paste content in mortar, less space (void) between aggregate particles requires less paste to fill it up, thus leaving more paste to coat the aggregate particles and to provide the mortar with improved flowability. Graded aggregate can improve the filling condition of the space between particles, hence resulting in a higher degree of packing. Figure 6-8 shows that flow curves of mortar with graded aggregate lay below those of mortar with single-sized aggregate. This confirms the fact that graded aggregate significantly improves the workability of mortar compared to single-sized aggregate.

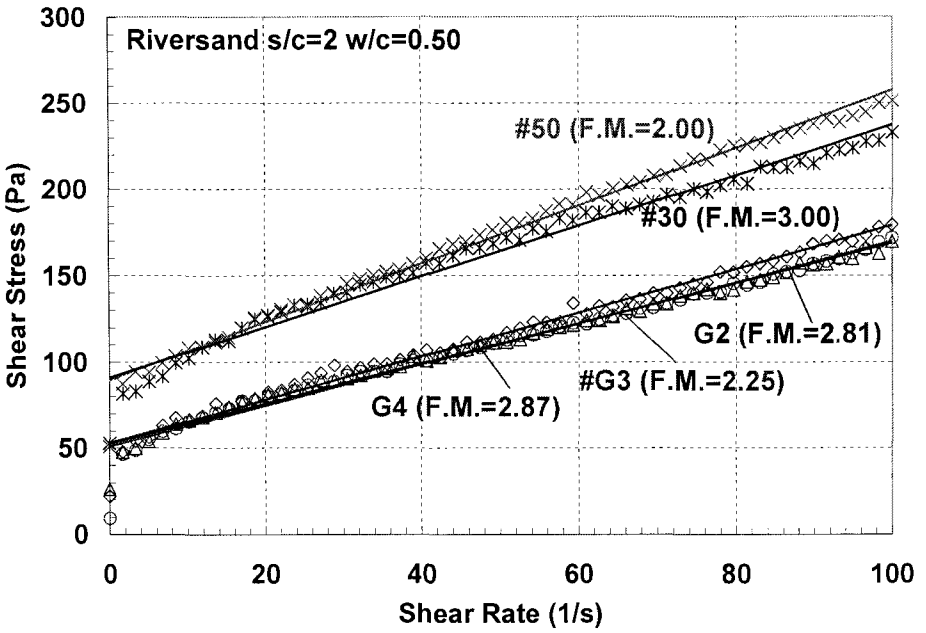

Figure 6-8 Effect of sand gradation on mortar rheology

According to the relationship between the fineness modulus of aggregate with the calculated rheological parameters as shown in Figure 6-9, graded aggregate provides the mortar with a lower yield stress and viscosity than single-sized aggregate at a similar fineness modulus. Graded aggregate had a lower amount of uncompacted void content and hence requires less cement paste to provide the same flow.

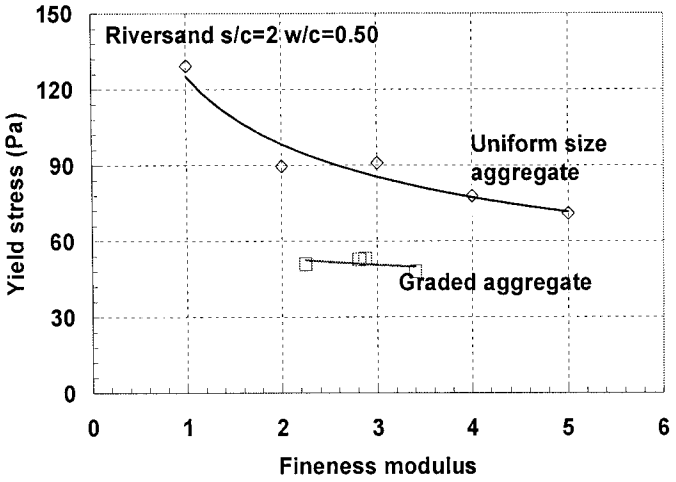

(a) Yield stress

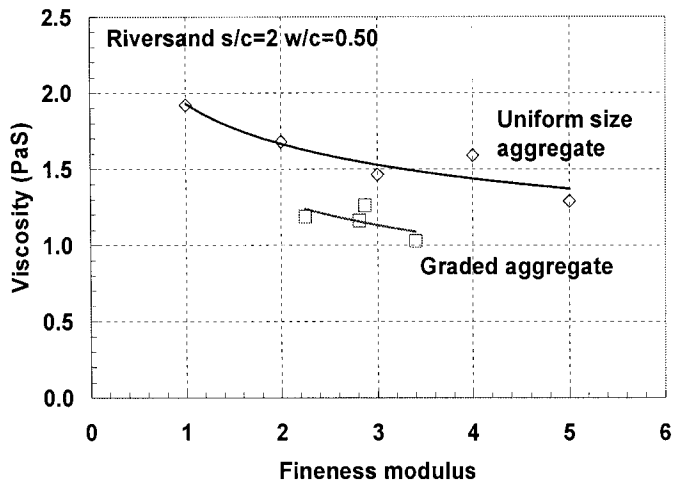

(b) Viscosity

Figure 6-9 Rheological parameters of mortar with different graded or single-sized sand

6.6 Flow Table Test and Rheological Parameters

A modified flow table test based on ASTM C1437 (as shown in Appendix IV) was performed to further verify the trends observed from the mortar rheology tests. These comparison of flow table results and rheology test results (as shown in Appendix V) are presented in Figure 6-10.

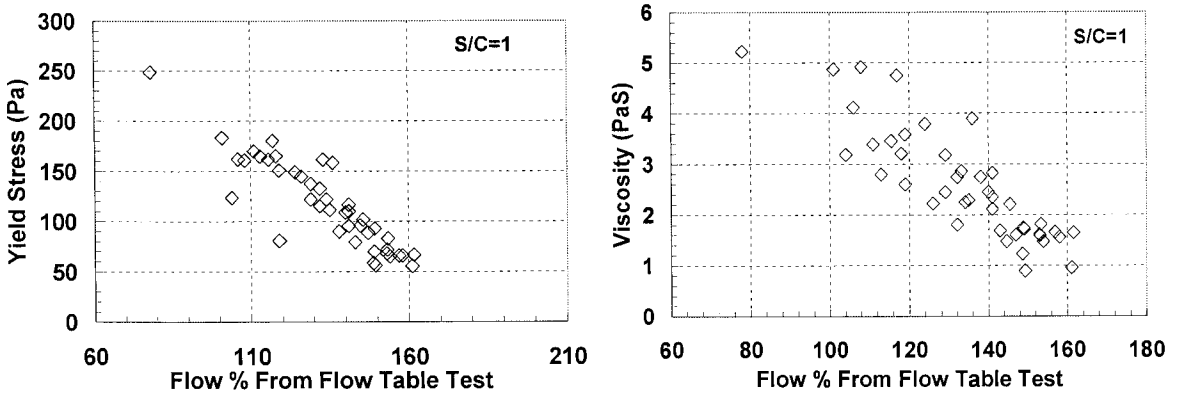

(a-1) Yield stress, s/c = 1 (a-2) Viscosity, s/c = 1

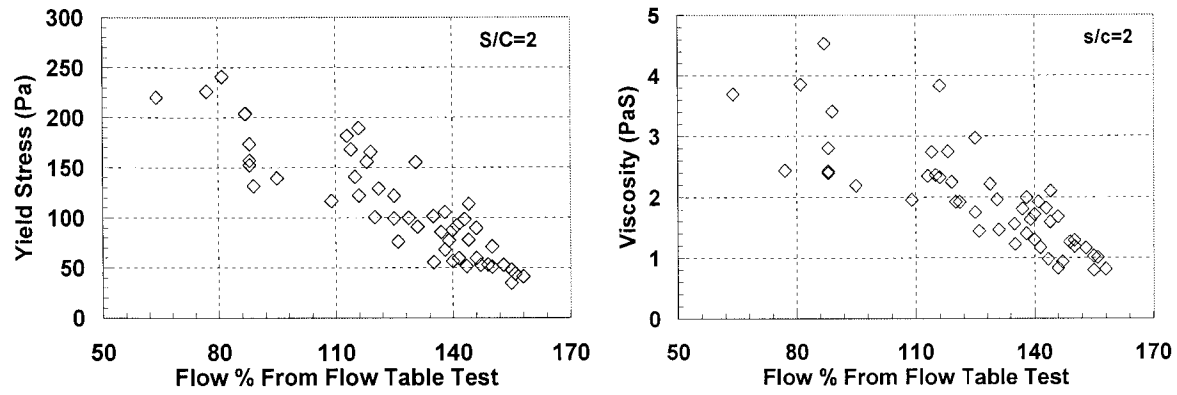

(b-1) Yield stress, s/c = 2 (b-2) Viscosity, s/c = 2

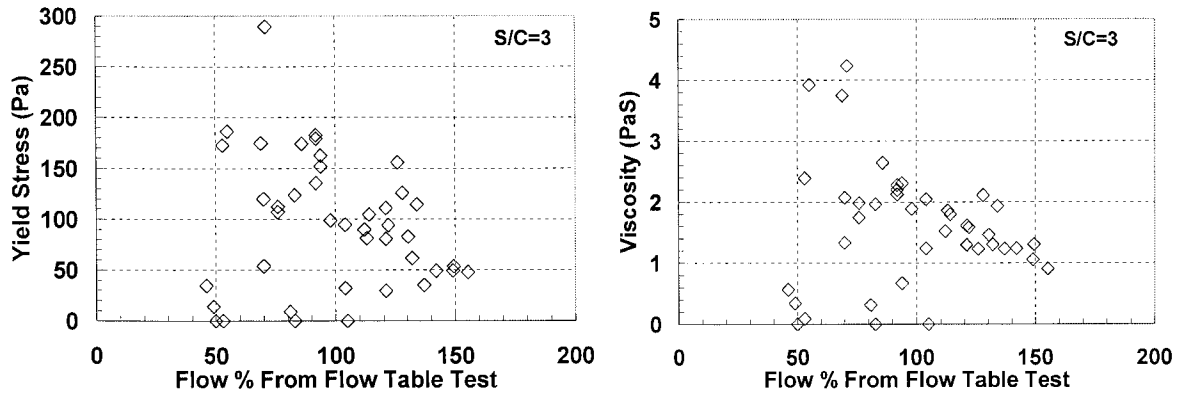

(c-1) Yield stress, s/c = 3 (c-2) Viscosity, s/c = 3

Figure 6-10 Comparison of flow table test results with rheological parameters

The relationship between the flow table test and the rheometer parameters showed that the flow percentage from the flow table test has a strong correlation with yield stress and viscosity at relatively low aggregate contents whereas material can perform in liquid like

behavior. Figure 6-10 also showed that at relatively low aggregate content (s/c=1 and 2), a high flow percentage correlated with lower yield stress and viscosity. When the aggregate content is high (s/c = 3), there are no clear tends. High aggregate content levels means that there was not enough paste to fill up the space between aggregate. Aggregate was observed to be not able to be fully coated in most of the cases, which resulted in the non-liquid like performance of the mortar, and thus the rheological parameters of Bingham liquid are inappropriate. Some data sets with zero viscosity and yield stress value were observed. In this case, the rheometer test is not appropriate.

6.7 Discussion

The results showed that the effect of w/c on mortar rheology is very substantial and larger w/c generally result in lower viscosity and yield stress due to the more workable matrix (paste). In addition to the w/c, aggregate size, gradation, and volume fraction significantly influence mortar rheology. Particle size distribution and aggregate gradation are important characteristics because they can determine the paste requirement for a workable mortar. Finer aggregate normally provides mortar with lower workability because of the increase of surface area and thus the need for more paste to coat the aggregate particle. On the other hand, graded aggregate can considerably improve the workability of mortar because the optimized packing of aggregate particles results in fewer voids that need to be filled by cement paste to provide same flow.

The study of different types of aggregate also illustrated that rounded and smooth surface aggregate (riversand) can be used to improve mortar workability. With the increase of aggregate volume content, the flowability of mortar decreases, which is caused by the higher degree of friction and interlock of aggregate particles. For mortar with low aggregate volume content, the effect of aggregate size/gradation/shape on the mortar rheology may not be significant, but the effect will become significant as the volume of aggregate increases.

CHAPTER 7. CONCRETE RHEOLOGY TEST RESULTS

In this chapter, the rheological performances of various concretes were studied using a portable IBB rheometer. The effects of coarse aggregate content (CA% = 37.8, 40.8, and 44.0), sand-to-cement ratios (s/c = 1.75, 2.21, and 2.60) and coarse aggregate gradations (single-sized coarse aggregate at #4, 3/8", 1/2", and 3/4"and three graded coarse aggregate G1, G2, and G3) were studied.

Concretes were mixed according to the "3-3-2" procedure as described in section 3.3.3 and rheometer tests were performed based on the procedure (complete with a preshear period and testing loop) as shown in Figure 3-14. The rheology measurement results were compared with the standard slump cone test. The unit weight and seven-day compression strength from each batch of concrete were also measured.

7.1 Effect of Coarse Aggregate Content

The flow curves in Figure 7-1 showed that the torque applied on the paddle increases with the rotation speed. The relationship was almost linear, which indicated that a yield term and viscosity term related to the Bingham rheology model can be obtained. As it was expected, the flow curves are not as smooth as observed in cement paste or mortar, due to the error cause by the direct contact of coarse aggregate with the rheometer paddle. Generally, as the fresh concrete became stiffer, the correlation coefficient to the Bingham model was slightly reduced, probably because the laminar flow assumption was no longer quite correct as the volume content of solid proportion increase (Nehdi and Mindess, 1996). It was also appeared that, similar to cement paste and mortar, the flow curve of concrete mixes demonstrated thixotrophy loops (i.e., up curves above down curves) which indicate that a certain degree of structural breakdown also occurred in the concrete throughout the testing process.

Groups of concrete were designed to have the same mortar properties (same s/c and w/c for mortar) but different coarse aggregate proportions (CA%). As shown in Figure 7-1, the flow curves of concretes with the same mortar properties but different coarse aggregate content

were significantly different. The greater portion of coarse aggregates in concrete provides larger surface area and requires a higher quantity of cement paste or mortar to coat all of the coarse aggregate particles and to fill the interstitial spaces between particles. As a result, when the coarse aggregate content increases, the yield stress and the viscosity of concrete both increase.

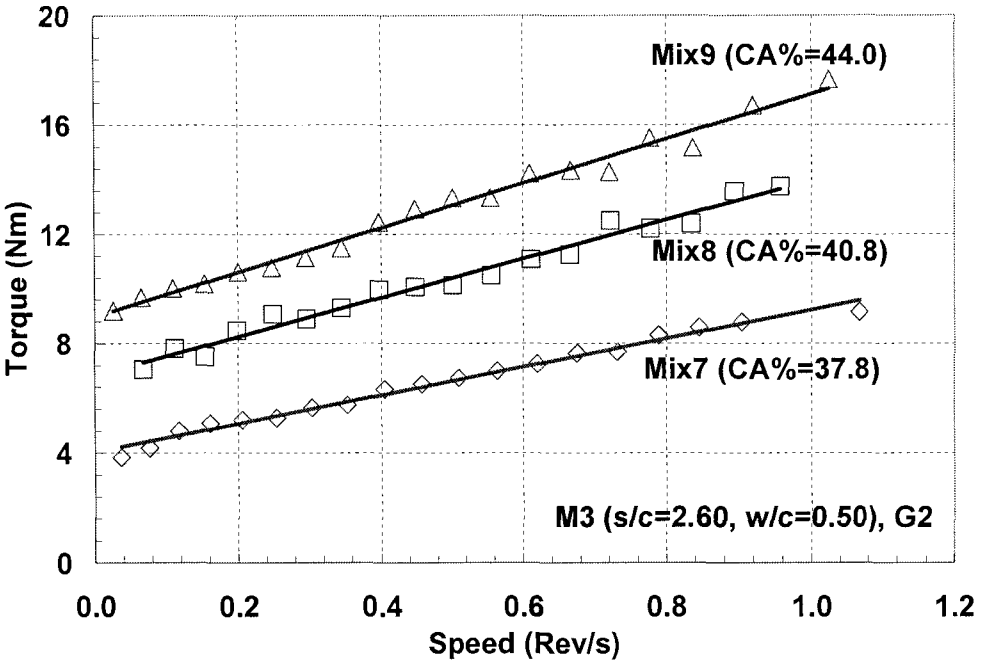

Figure 7-1 Effect of coarse aggregate content on concrete rheology [1]

7.2 Effect of Fine Aggregate Content

When fresh concrete is considered as a two-phase material consisting of mortar and coarse aggregate, the rheological properties of the matrix (mortar) can significantly affect the rheological properties of the composite (concrete). According to the results as shown in Chapter 6, the fine aggregate content, i.e. s/c, strongly influenced the rheology of mortar. The influence of mortar's rheology properties on concrete is examined in this chapter. The

[1] In order to clearly show the effect of and the coarse aggregates on flow curves, only the down curves and the best fitting lines for linear regression of down curves will be shown from this figure and later on within this chapter. In this figure, Mix7, Mix8, and Mix9 referred to concrete mix design identification as shown in Table 3-4 (Mix1 through Mix9), M3 referred to mortar design, G2 referred to size or gradation of coarse aggregate used in concrete (single-sized aggregate #4, 3/8",1/2", 3/4", or graded aggregate G1, G2, and G3).

factorial mix design method considers mortar rheology effect was employed with the concrete mixes, the concretes were designed to have same coarse aggregate content but with different properties of mortar inside.

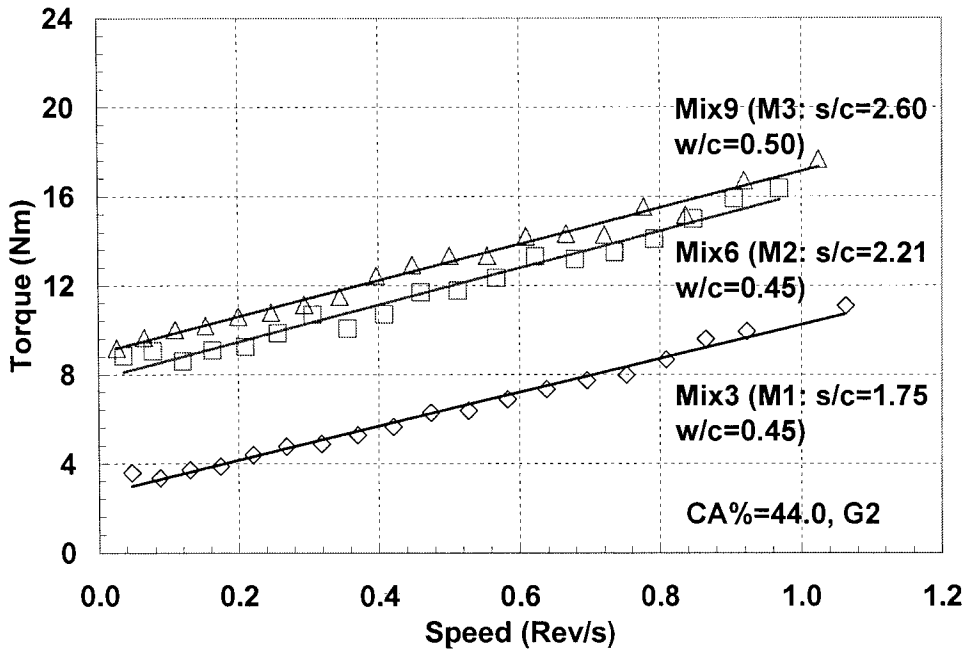

Figure 7-2 Effect of fine aggregate content on concrete rheology

A comparison can be made between concretes with same coarse aggregate content (CA%) but different mortar properties, resulting from different s/c and w/c. The results shown in Figure 7-2 indicated that higher s/c resulted in flow curves above concrete with lower s/c. The results showed that when the fine aggregate content increases, the yield stress and viscosity of concrete both increase, even though the Mix9 mix has a higher w/c (0.50) than mix Mix3 and Mix6 (0.45). This phenomenon can be attributed to the fact that the yield stress and the viscosity of mortar increase as the s/c of mortar increases. Results also showed that comparing to viscosity, yield stress showed more difference through different mortar design, which is consistent with the rheological parameters difference for different mortar as presented in Table A-4.

7.3 Effect of Coarse Aggregate Size and Gradation

The particle size distribution (or grading) of a coarse aggregate supply is an important characteristic because it determines the paste requirements for a workable concrete. In order to study the effect of coarse aggregate gradation and size, four different single-sized coarse aggregate (#4, 3/8", 1/2" and 3/4") and three graded coarse aggregates (G1, G2, and G3) were chosen for the selected mix design, and the rheology of different concrete mixes was examined.

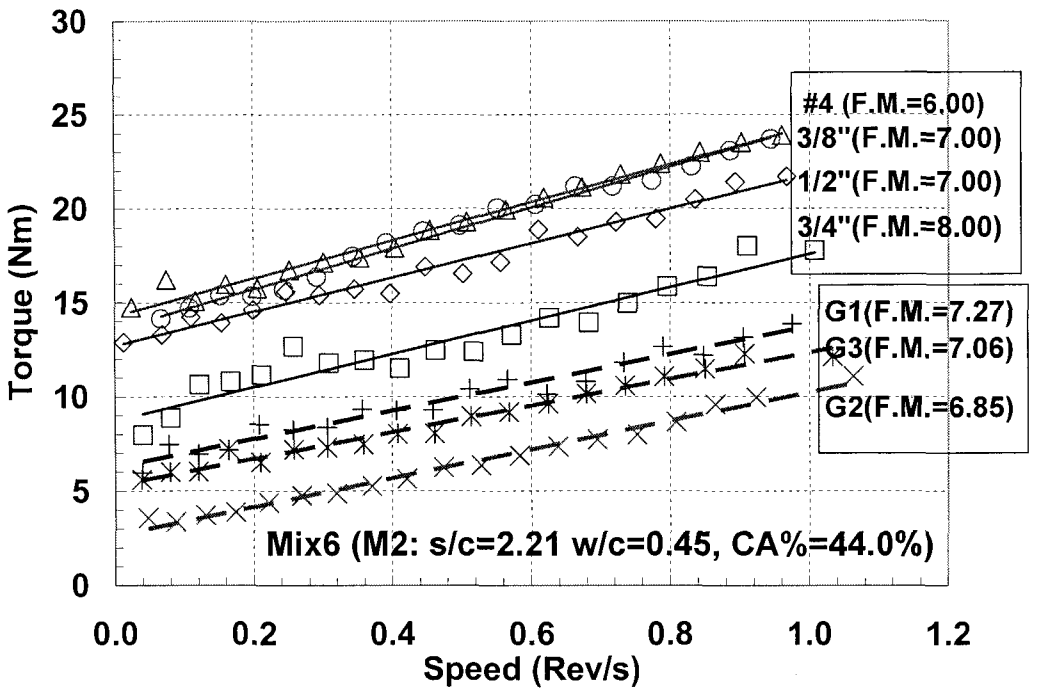

Figure 7-3 Effect of coarse aggregate grading on concrete rheology

As shown in Figure 7-3, the difference between graded and single size coarse aggregates was obvious. Provided same mix design, the down curves of the three concrete mixtures with graded coarse aggregate lay below concrete mixtures with uniform size coarse aggregate, which indicates that aggregates with gradation provide concrete with better flowability, this phenomenon is in agreement with previous researchers (Mindess et. al., 2003). When aggregate with a range of different sizes is used, the smaller particles can fill up the spaces between the larger particles, thereby decreasing the void space and lowering the amount of paste or mortar required for filling the spaces. Thus, excess amount of paste or mortar can

coat the aggregate surface and improve concrete workability. Results also showed that in this chosen concrete mix design (Mix6), a higher flow curves were observed with the smaller size of aggregate, which indicated that the flowability of concrete decrease with the decrease of single size coarse aggregate used.

The parameters related to Bingham rheology parameters from different concrete mixes can be calculated based on the down curve from the thixotrophy loops using the best-fitting linear equation. The calculated yield stress related parameter (interception (G)) and viscosity related parameter (slope (H)) from concrete with the same mix design but different sizes of coarse aggregate were summarized in Figure 7-4. Results showed that both the slope and interception decreased with increased aggregate size. This is consistent with the general knowledge that a bigger size of aggregate will result in higher flowability because of the lower surface area that needs to be coated. However, the trend in slope is not as clear as in interception, which might be caused by the fact that the effect of this coating thickness will counteract the interaction between aggregate. A larger size aggregate may cause a higher degree of friction and interlocking between particles; thus, the effect of the size of coarse aggregate on concrete rheology sometimes can not be clearly observed. Concrete with graded coarse aggregate had lower rheological parameter values than concrete with single-sized aggregate. Graded aggregate can pack better, which requires a lower amount of paste to fill the spaces and therefore provides concrete with better workability.

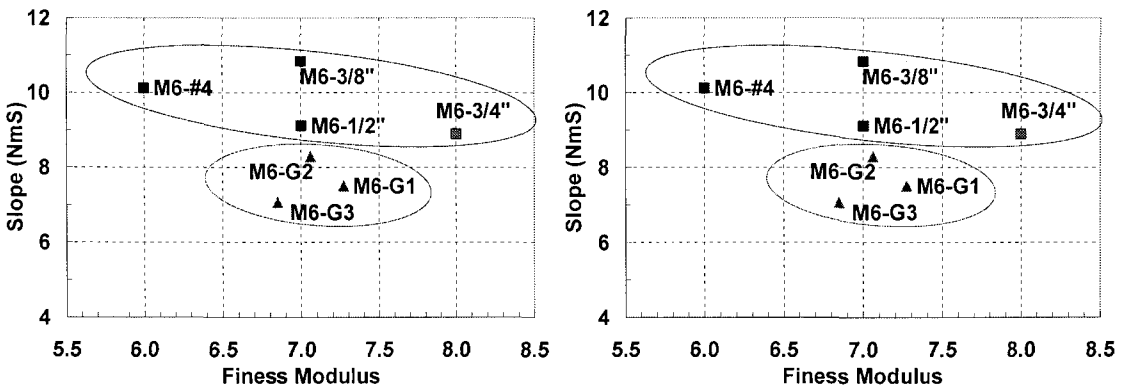

(a) Yield parameter **(b) Viscosity parameter**

Figure 7-4 Rheological parameters of concrete with different graded or uniform size coarse aggregate

7.4 Results and Discussion

The properties of 23 concrete mixtures are shown in Table 7-1:

Table 7-1 Concrete tests results

Symbol	Slump (in.)	G (Nm)	H (NmS)	R^2	Unit weight (pcf)	$f_{c,7}$' (psi)
Mix1-3/4"	6.50	2.57	6.06	0.955	143.8	5383
Mix1-G1	7.75	2.13	4.81	0.985	144.2	5623
Mix1-G2	8.50	2.18	5.37	0.979	142.2	5408
Mix1-G3	8.25	1.99	5.06	0.998	142.4	5197
Mix1-#4	6.50	3.34	5.72	0.995	140.0	5792
Mix2-G2	7.50	2.60	5.73	0.985	140.0	5351
Mix3-3/4"	4.75	4.99	8.02	0.938	144.6	5291
Mix3-G1	6.75	3.45	6.42	0.987	144.6	5322
Mix3-G2	7.00	3.18	7.24	0.985	144.4	5273
Mix3-G3	7.50	3.22	7.49	0.986	142.4	5267
Mix3-#4	4.00	4.41	7.98	0.989	141.8	5731
Mix4-G2	5.50	4.59	5.78	0.988	138.2	4990
Mix5-G2	4.00	5.70	6.30	0.950	140.6	4918
Mix6-3/4"	2.50	8.71	8.90	0.926	144.0	5332
Mix6-G1	4.00	6.25	7.50	0.962	143.8	5290
Mix6-G2	3.00	7.82	8.29	0.972	144.8	5308
Mix6-G3	4.50	5.29	7.07	0.978	144.0	5358
Mix6-1/2"	1.75	12.69	9.12	0.975	145.0	5343
Mix6-3/8"	1.25	13.55	10.84	0.986	143.8	5985
Mix6-#4	1.50	14.27	10.12	0.984	143.8	5456
Mix7-G2	5.00	4.03	5.19	0.986	139.6	5239
Mix8-G2	2.00	6.83	7.14	0.981	143.8	5880
Mix9-G2	1.50	8.98	8.15	0.982	143.2	5576

Notes: *G* is the interception, *H* is the slope, and R^2 is the coefficient of correlation of linear regression.

The calculated interception and slope values from concretes with same gradation (G2) but different mix designs are summarized in Figure 7-5. As shown in this figure, a clear trend was observed that generally the yield term (interception G) and viscosity term (slope H) both increased with the sand content (s/c) or coarse aggregate content (CA%). These phenomena demonstrated that within a certain range of aggregate proportion, an increase of aggregate content (which can be either coarse aggregate or fine aggregate) will result in lower flowability of concrete, provided the other portions of the concrete mix design remain fixed. Results indicated that when considering the effect of aggregates on workability, two factors are important: the amount of total aggregate and the relative proportions of fine to coarse aggregate.

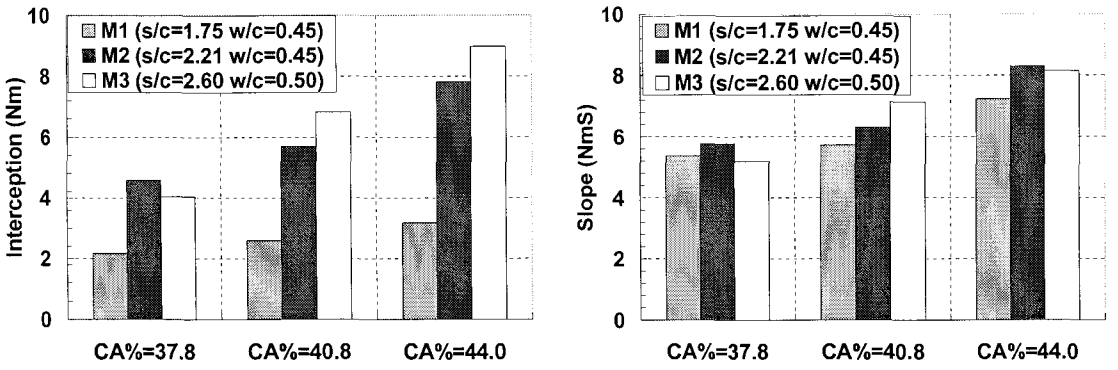

(a) Yield parameter **(b) Viscosity parameter**

Figure 7-5 Rheological parameters of concrete with different aggregate proportion

The effects of aggregate gradation on concrete with the same mix designs are summarized in Figure 7-6. Results showed that regardless of the concrete mix design, concrete with graded coarse aggregate provides concrete with better flowability, i.e., lower interception and slope values. As shown in the figure, the calculated yield and viscosity parameter from concretes with different size and gradation of coarse aggregates indicated that graded aggregate provides concrete with better flowability comparing to single size aggregate. As shown in the figure, concrete with graded coarse aggregate had lower rheological parameter values than concrete with uniform size aggregate. Graded aggregate generally have better packing, which requires a lower amount of paste to fill the spaces and therefore provides concrete with better workability.

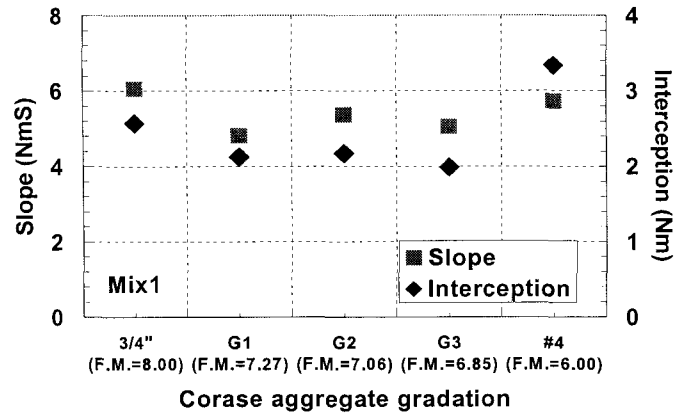

(a) Mix 1 (M1: s/c=1.75, w/c=0.45; CA%=37.8)

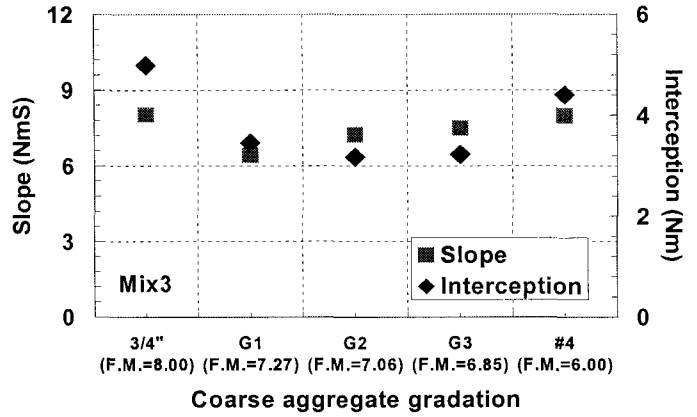

(b) Mix 3 (M1: s/c=1.75, w/c=0.45; CA%=44.0)

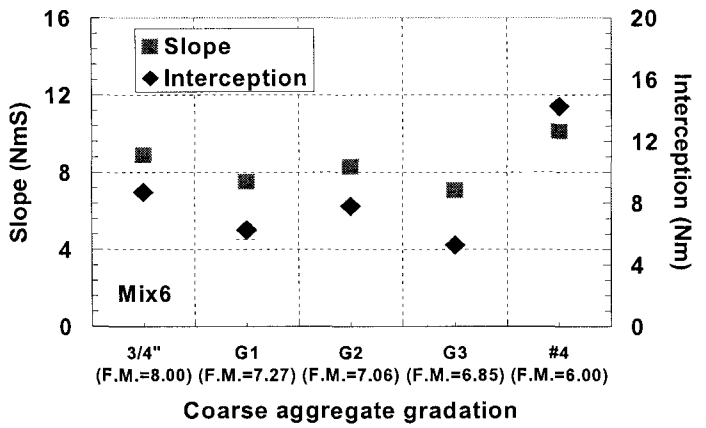

(c) Mix 6 (M2: s/c=2.21, w/c=0.45; CA%=44.0)

Figure 7-6 Rheological parameters of concrete with different graded or single-sized coarse aggregate

The effect of size on concrete rheology, however, was not clearly observed in all mixes in present research. Concrete with the same mix design but smaller sizes of coarse aggregate generally increase yield stress and viscosity because of the increase of the aggregate surface area. However, the effect of coarse aggregate friction might counteract with the effect of coating thickness on aggregate. An increase of size of aggregate used in present study generally resulted in higher friction angle. As a result, the friction of aggregate inside concrete might be stronger because of the increase of aggregate size. Results in Figure 7-6 showed that the concrete rheological performance might not have significant difference because of the using of different size of coarse aggregate.

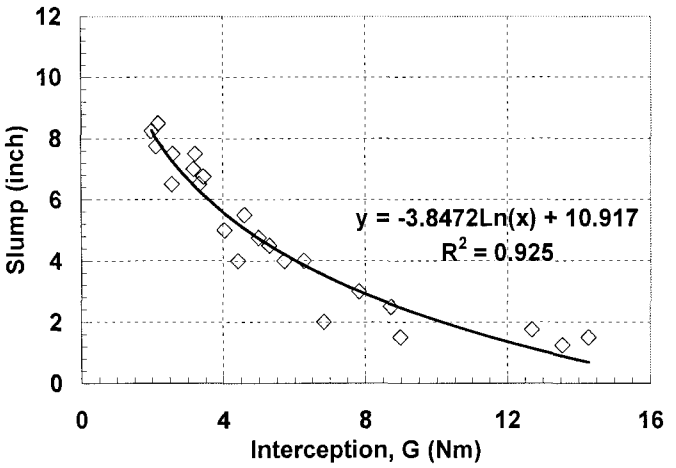

(a) Slump vs. yield parameter

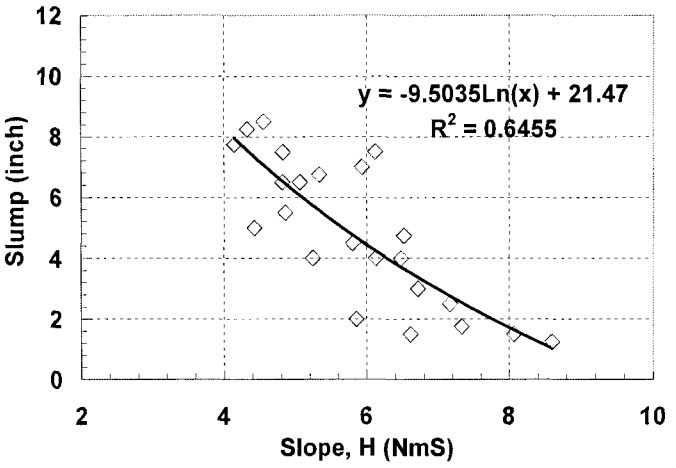

(b) Slump vs. viscosity parameter

Figure 7-7 Comparison of slump test results with rheological parameters

Based on the measured results (Table 7-1), the relation between slump value and rheology related parameters were examined. As shown in Figure 7-7, the slump value was found to have a strong correlation with the interception (with a very high R^2 value of 0.93), while the relation between slope and slump value was not significant. This is consistent with previous research, which indicated that the slump value can be strongly correlated with yield stress of fresh concrete; however, it can not pickup the change on viscosity (Murata and Kikukawa, 1992; Tattersall, 1991). These results support the need to use the rheometer test fully reflect the concrete flowabilities.

The unit weight of fresh concrete and seven-day compression strength of concrete was measured on each batch of concrete. The results as shown in Table 7-1 indicate that no clear pattern of effect of aggregate or mix design of concrete on these two parameters was observed within the selected concrete mixtures.

CHAPTER 8. MODELING OF MORTAR AND CONCRETE RHEOLOGICAL BEHAVIOR

The degree of importance of effects from various factors on mortar and concrete rheology was evaluated. Theoretical parameters relate to the rheological properties of mortar and concrete were developed. Statistical analyses were used to evaluate the significance of different parameters and to finalize the rheology model. This chapter contains four sections.

- In the first section, an artificial neural network (ANN) method was used to evaluate the relative degree of importance of the factors that may affect the rheology of mortar and concrete. Results of this study can also be used to predict rheological properties of mortar and concrete.
- The second section discusses how and why the properties and thickness of suspension (paste or mortar), aggregate friction and volume fraction affect the rheology of composite materials (mortar and concrete). The parameters that relate to mortar and concrete rheology were developed, the approach to modeling mortar and concrete rheology is also presented.
- In the third section, the rheology of mortar is studied; the excess paste thickness for mortar was calculated according to the excess paste theory. A statistical analysis was conducted to predict the rheology of mortar from the nominal excess paste thickness and paste rheological parameters.
- In the last section, according to the excess paste theory and two-phase theory (concrete was considered as two phases of mortar and coarse aggregate), the excess mortar thickness for was calculated. A model was developed to predict the rheology of concrete using the rheological parameters of mortar, nominal thickness of excess mortar and the friction of coarse aggregate.

Models developed from this chapter can not only be used for concrete rheology prediction, but also have the potential to be used to design concrete with desirable rheology parameters.

8.1 Study of Major Factors Affecting Concrete Rheological Behavior

As shown in previous chapters, the mix component, especially aggregate, significantly affects mortar and concrete rheology. Increasing the amount of aggregate content results in an increase in yield stress and the viscosity of mortar and concrete because of the decrease of the paste or mortar thickness coating on the aggregate to provide flow. Aggregate with lower uncompacted void content generally reduces concrete yield stress and viscosity. Graded aggregate can considerably reduce yield stress and viscosity of mortar and concrete because it packs together better, resulting in fewer voids and thus requires less paste or mortar to provide same flow. Irregular shape and rough surface aggregates have higher uncompacted void content and higher friction angles than round and smooth aggregates. Increasing the w/c results in paste with low yield stress and viscosity, this will further reduce the rheological parameters of the concrete composite.

A statistical analysis was performed to examine the importance of effects from different factors which affect the rheology of mortar and concrete. Since materials like mortar and concrete are composite materials, different parameters from their compositions might be related to each other. For example, aggregate with higher angularity will not only require a larger amount of paste because of the increase of uncompacted voids, but will also increase the friction force between the aggregate. These kinds of different but interrelated factors make it difficult to decide upon the analysis parameters. The ANN analysis method was therefore used to select the parameters used in the modeling analysis later in this section.

8.1.1 Effects on Mortar Rheology

The neural network model is inspired by the biological structure of neurons and the internal operation of the human brain, which consists of multiple layers of interconnected linear or nonlinear processing units operating in parallel fashion. ANN had already been used in concrete studies such as SCC mix design (Nehdi et al., 2001) because of its advantages in handling multi-parameter situations. A brief description of ANN and some of the results from the ANN analysis were shown in appendix VII.

ANN typically consists of many simple processing units, which are wired together in a complex communication network. In the modeling for mortar rheology, five different parameters were selected as the input layer, which covered the mix design of mortar and the properties of the aggregate used. The five parameters used are s/c, w/c, the fineness modulus, the friction angle and the uncompacted void content of fine aggregate. Several network architectures were tried (using a trial-and-error approach). The final network as shown in Figure 8-1 was used for the present study.

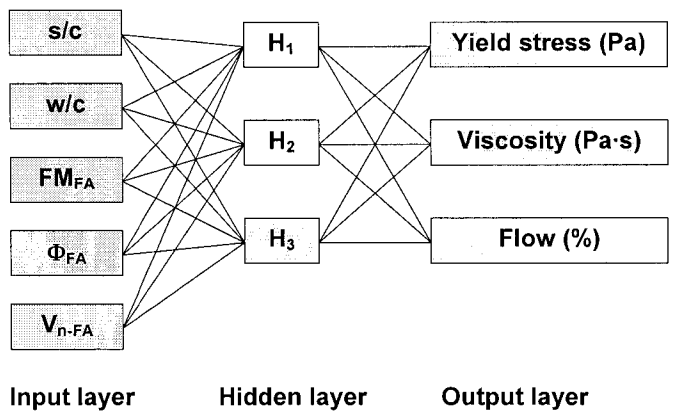

Figure 8-1 Architecture of neural network model of mortar rheology

The actual versus predicted values of mortar rheology parameters (as shown in Appendix VII) demonstrated that this model can capture the relationship between the input and output parameters, and the model can be used successfully to predict the rheology of mortar from original mix design and aggregate properties. A relatively high R^2 value (around 0.90) was found through the model.

The effect of five parameters (the *s/c*, *w/c*, the fineness modulus (FM_{FA}), friction angle (Φ_{FA}) and uncompacted void content of fine aggregate ($V_{n\text{-}FA}$)) is shown in Figure 8-2. Results indicated that, as expected, the w/c and the aggregate uncompacted void have the most significant effects on the rheology parameters. These two parameters directly affect the excess paste thickness and the paste rheological properties. However, the effect of the friction angle of the fine aggregate did not show any significant difference, which indicates that within the range of sand used in this research, the fine aggregate friction angle either did

not have a significant effect on the rheology of mortar or the effect was concealed by the other parameters used in the model.

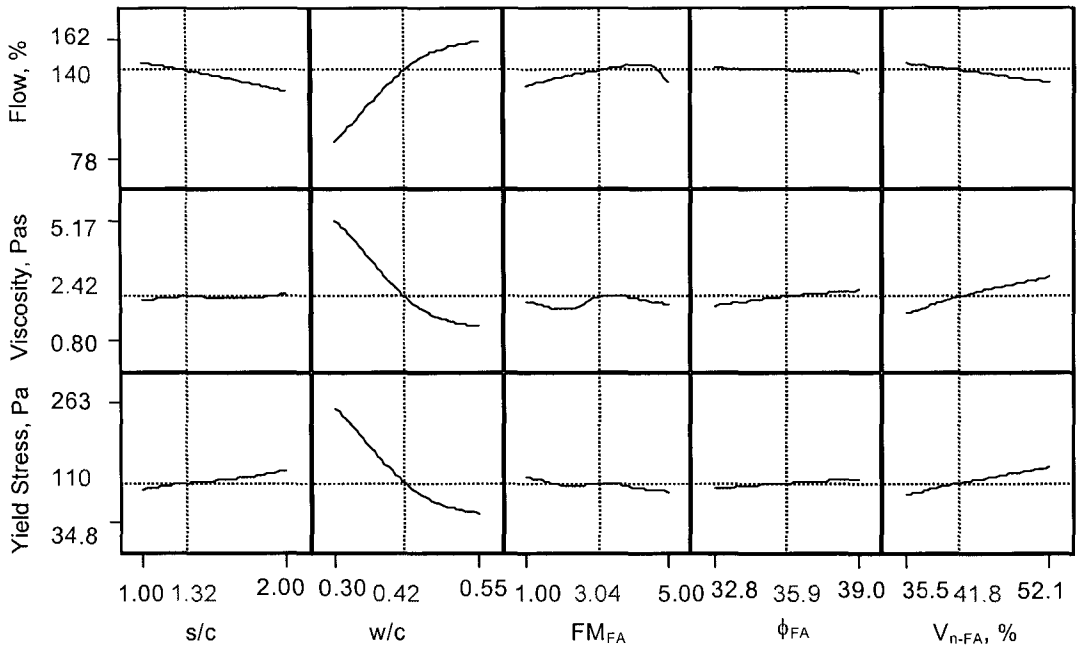

Figure 8-2 Effects of different parameters on mortar rheology

According to the analysis from this study, the rheological parameters of cement paste and the excess paste thickness might have significant influence on mortar rheology, which shall be considered in the model for predicting the rheology of mortar.

8.1.2 Effects on Concrete Rheology

Similar to the mortar study, six parameters were selected as the input layer for the concrete studies. These parameters covered the mix design of concrete and the properties of the aggregate used, and they are coarse aggregate content (*CA%*), fine aggregate content (*s/c*), water content (*w/c*), the fineness modulus (FM_{CA}), the friction angle (Φ_{CA})and the uncompacted void content ($V_{n\text{-}CA}$) of coarse aggregate. After several network architectures had been attempted according to the trial-and-error approach, the network as shown in Figure 8-3 was used for the present study.

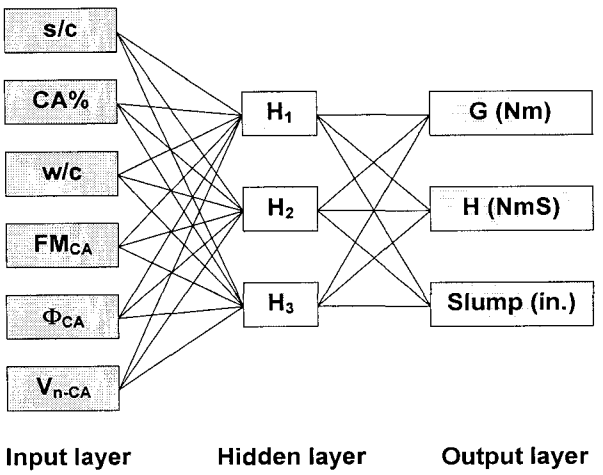

Figure 8-3 Architecture of neural network model of concrete rheology

The actual versus predicted value of the concrete rheology parameters (Appendix VII) demonstrated that this model can capture the relationship between input and output parameters. The model can be used successfully to predict the rheology of concrete from the original mix design and aggregate properties. A relatively high R^2 value (higher than 0.90) was found through the model.

The effect of parameters including CA%, aggregate friction angle and the fineness modulus of aggregate was shown in the Figure 8-4. Results indicate that the coarse aggregate content has a significant effect on the rheology parameters, because it directly determines the mortar thickness. The size of the aggregate also influences the rheology of concrete because of the decrease or increase of the excess paste thickness. The aggregate friction angle affects the rheology of concrete, at least among the coarse aggregates used in this research. Its effect is very significant, because an increasing aggregate friction angle increases the force of friction between aggregates. The s/c and w/c also showed different affects on concrete rheological parameters because they decided the rheological performance of the matrix of the composite - mortar.

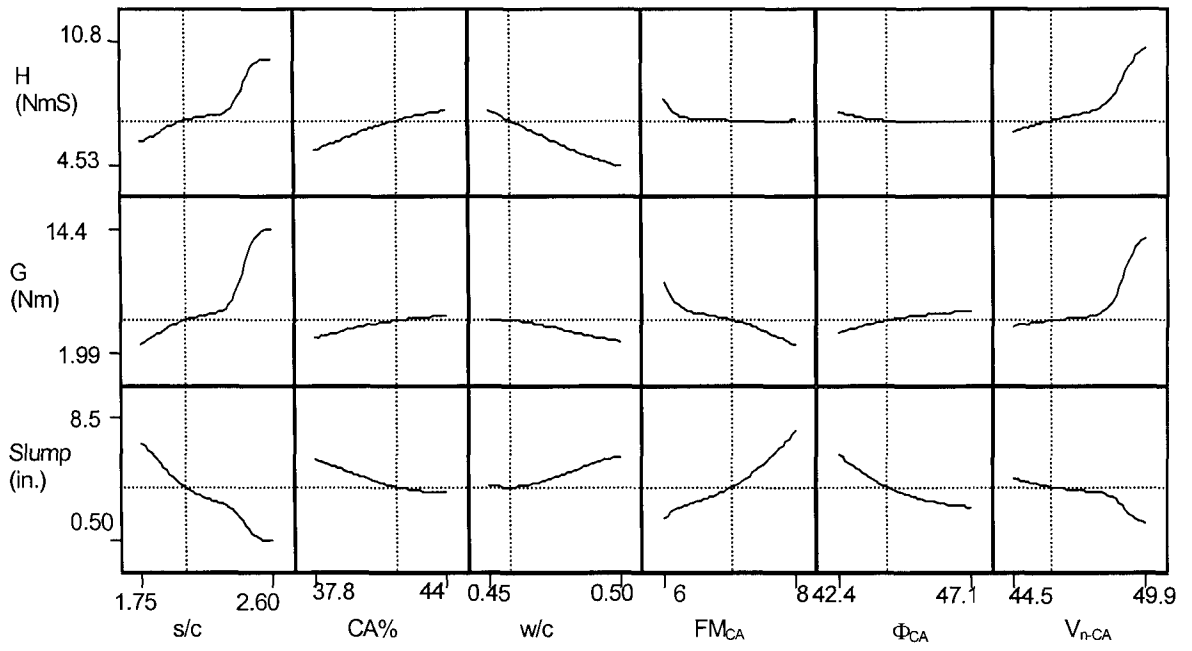

Figure 8-4 Effects of different parameters on concrete rheology

The analysis in this section indicated that the ANN model can provide us information concerning how the mortar thickness, mortar rheology and coarse aggregate friction angle factors might have significant effects on the rheology of concrete, which should be considered in further modeling studies.

The analysis in the present section provided a useful guide in the modeling of mortar or concrete rheology, especially in choosing the parameters for the theoretical study. Results also showed that the ANN model can be successfully used to predict the rheology of concrete and mortar from their original mix design and aggregate properties. The model developed in this section also have very good potential for practical use as a tool to design concrete according to desired rheology parameters.

8.2 Approach to Predict Mortar and Concrete Rheology

8.2.1 Mortar and Concrete Rheology Model

The research in last section indicated that the rheology of a suspension - such as a cement paste or mortar - can determine the rheology properties of the whole composite (mortar or

concrete). The volume concentration of a suspended material (aggregate) can significantly influence the rheology of the composite. Meanwhile, aggregate properties, including size, gradation, uncompacted void content and friction angle aggregate also proved to have important effects on mortar and concrete rheology. However, models with efficient parameters needed to be found and applied in a successful rheology model.

As mentioned in Chapter 2, many researchers have studied the rheological performance of composite materials including concrete. Different models have been proposed to predict concrete rheology. Previous research illustrated that the rheology of concrete or mortar will be significantly affected by the "gap" between aggregate (Ferraris and de Larrard, 1992). According to Kurokawa et al. (1996), the rheology parameters of concrete are related to the aggregate concentration inside the concrete, the friction between the aggregate inside mixture and the volume fraction of aggregate. When the concrete mixture is moving, the pieces of aggregate have the chance to contact each other because of the deformation of the suspension. The force between contacted particles is therefore related to the friction between aggregate particles and the volume fraction of the aggregate, which provides the chance that the aggregate particles in contact with each other. Topcu and Kocataskin (1995) found that concrete rheology depended upon the characteristics of the mortar and the coarse aggregate phases. In other words, when considering concrete rheological performance, mortar can be considered as one whole phase while coarse aggregate considered as another phase. Thus, the rheology of concrete is affected by both the thickness of the layer coating the aggregate particles and the friction between the aggregate particles. In the consideration of paste or mortar thickness and the friction between aggregate particles, a model, shown in Figure 8-5, is proposed.

According to two-phase theory (Topcu and Kocataskin, 1995), fresh concrete (or mortar) can be considered as a composite material composed with different size and shape of coarse aggregate (or fine aggregate) coated with mortar (or paste), similar approach can hence be used in mortar and concrete rheology model development. Assume all coarse (or fine) aggregate particles are evenly dispersed in the mixture and separated from each other, a fresh concrete (or mortar) (case (I) as in Figure 8-5) can be simplified as irregular shape particles

each coated with layer of mortar (or paste) which were uniformly dispersed in the whole material as shown in Figure 8-5 (II). Case (II) can be further simplified as contribution from sphere particles coated with same thickness of mortar (or paste) and contribution from coarse (or fine) aggregate friction because of the irregular shape of particles according to Kurokawa et al. (1996) as shown in case (III-a) and (III-b). In case (III-a), coarse (or fine) aggregate was assumed to be coated by same thickness of mortar (or paste); aggregate particles was in spherical shape and with smooth surface, which means there is no friction between aggregate particles. In case (III-b), a material with just aggregate particles was studied, friction caused by the irregular shape and unsmooth surface was the only factor considered. In this model, concrete and mortar rheology can be considered as a result of two parts: (a) the rheology contributed by spherical coarse aggregate particles coated with a uniform mortar (or paste) layer and (b) the rheology contributed by the friction between coarse (or fine) aggregate particles.

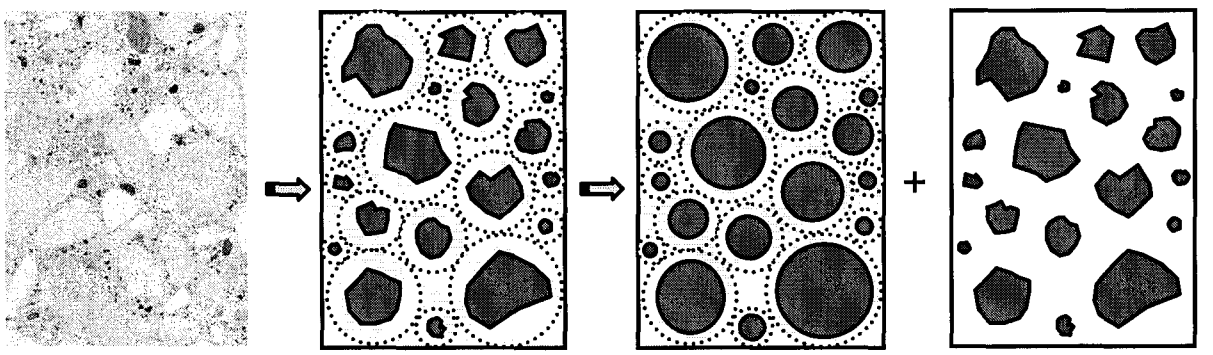

Figure 8-5 Simplification of the modeling

According to the proposed model, the rheology of the concrete or mortar can be decided by both from spacing and from friction as shown in the following two equations:

$$\tau_0 = f(\tau_0{}^o, \tau_0{}^\Delta) \qquad \textbf{Equation 8-1}$$

$$\eta = f(\eta^o, \eta^\Delta) \qquad \textbf{Equation 8-2}$$

Where, τ_0^o and η^o are the yield stress and viscosity contributed by the mortar or paste coated on spherical particles; τ_0^Δ and η^Δ are the yield stress and viscosity contributed from the direct friction of coarse or fine aggregate particles.

Approach of the concrete (or mortar) rheology modeling study in this research was summarized in the following Figure 8-6. Theoretical parameters relating to mortar (or paste) coating thickness and mortar (or paste) rheological properties were obtained according to concrete microstructure and rheology theory. The thickness of the mortar (or paste) coating on aggregate can be calculated from the mix design and aggregate properties and used to obtain the relationship between thickness and rheology. Contribution from aggregate friction was also study based on mechanics equation, the friction angle of coarse (or fine) aggregate were measure and the relationship between friction and concrete (or mortar) rheology was obtained accordingly. With the information of the measured mortar and concrete rheology properties, models for the prediction of mortar and concrete rheological properties using these theoretical parameters were finalized by statistical analysis. The degree of significance level of the developed parameters that influence the mortar and concrete rheological behavior were evaluate as well.

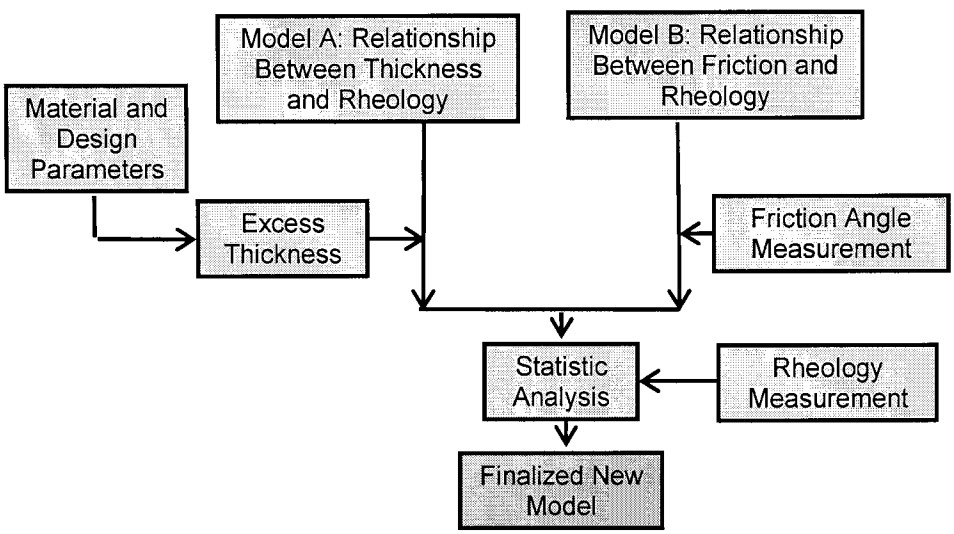

Figure 8-6 Flowchart for concrete and mortar rheology prediction process

8.2.2 Rheology by Paste and Mortar Layer Thickness

According to the proposed modeling as specified in Figure 8-5, the contribution from mortar coating (III-a) is studied first. The rheology of a material can be analyzed through deformation of the material under a shear stress. For a cubic particle with height of Y and top surface area of A, it has a deformation of δ under a shear stress when a shear force of F is applied (Figure 8-7). The following equations 8-3 to 8-6 can be used to describe the material rheological behavior (obtained from Tattersall and Banfill, 1983):

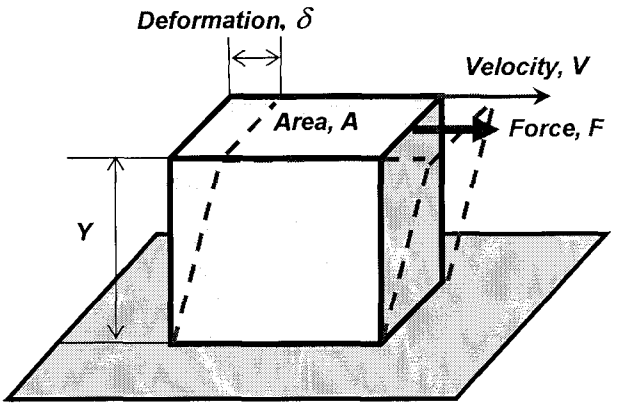

Figure 8-7 Definition of rheological parameters

The shear stress τ (Pa) is defined as the shear force (F, N) divided by the area of the force applied on (A, m^2):

$$\tau = F / A \qquad \textbf{Equation 8-3}$$

The shear strain γ is the deformation (δ, m) divided by the height of the particle (Y, m):

$$\gamma = \delta / Y \qquad \textbf{Equation 8-4}$$

Shear strain rate $\dot{\gamma}$ (s^{-1}) is the differentiation of shear strain over time (or viscosity over height), which is normally just simply called the shear rate:

$$\dot{\gamma} = d\gamma / dt = dV / dY \qquad \textbf{Equation 8-5}$$

Plastic viscosity η (Pa·s) is defined as the rate of shear stress over shear rate:

$\eta = \tau / \dot{\gamma}$ **Equation 8-6**

With the relation of shear stress and shear rate of material, the rheological behavior of fresh concrete can be studied. In order to study the effect of aggregate size and mortar (or paste) coating thickness on concrete rheological performance, the following study is performed. Assume the mortar (or paste) and aggregate solid particles are uniformly deformed under shear force and all relative position of aggregate particle remain the same in concrete (or mortar), two aggregate particle at same size and coated with same thickness of mortar (or paste) were isolated and considered as study object studied. The two spherical particle coated with mortar (or paste) was assumed to be able to represent the whole material as shown in case (III-a) in Figure 8-5. When force is applied on concrete (or mortar) composites, if the aggregate diameter (r_{agg}) is much bigger comparing to the coating thickness (t_s), the objects in the boxes with dash lines was assumed to be able to simplified as two pieces of aggregate with a layer of mortar (or paste) inside, as shown in Figure 8-8.

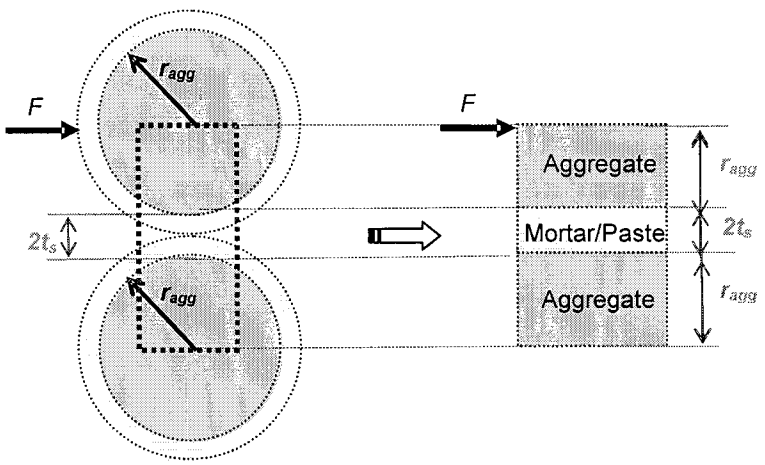

Figure 8-8 Spherical aggregate coated with mortar/paste

Based on the simplification as described in Figure 8-8, in order to study the rheological performance of composite with same material but different mix design, two objects, A and B, with different thickness of mortar (or paste) placed between two aggregate particles as shown in Figure 8-9 were analyzed:

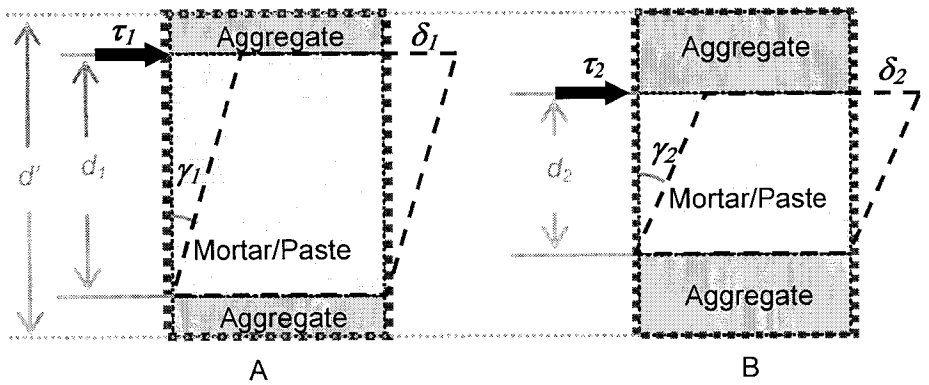

Figure 8-9 Apparent rheological parameters of composite with different thickness

As it was shown in Figure 8-9, object A has the mortar (or paste) thickness of d_1 between two solid plates, while object B has thickness of d_2. When objects were under shear stress (τ_1 and τ_2 respectively), material had deformation of δ_1 and δ_2. In a small range of deformation, the material can be assumed to behave elastically and the relationship between the shear stress and shear strain can be expressed based on Hooke's law as:

$$\tau = G\gamma \qquad \textbf{Equation 8-7}$$

where G is the shear modulus of mortar (or paste) (GPa) and γ is the shear strain, which equals to the deformation divided by the thickness (δ/d).

The shear stresses of objects A and B are:

$$\tau_1 = G_1 \frac{\delta_1}{d_1} \qquad \textbf{Equation 8-8}$$

$$\tau_2 = G_2 \frac{\delta_2}{d_2} \qquad \textbf{Equation 8-9}$$

Therefore, the relationship between τ_1 and τ_2 are:

$$\tau_1 / \tau_2 = \frac{G_1(\delta_1 / d_1)}{G_2(\delta_2 / d_2)} \qquad \textbf{Equation 8-10}$$

In order to consider effect of coating thickness on concrete (or mortar) rheological behavior, the same volume of the selected parts from mix A and mix B (as shown in Figure 8-9 inside the rectangular boxes in dash lines) were studied (the apparent distance *d'* was considered as same in these two boxes). Given same deformation ($\delta_1 = \delta_2$), and assumed that forces act on top or bottom of the plates do not perform differently in small range of deformation. As it was previously summarized in section 2.2.3, since aggregate particles have negligible deformation comparing to mortar, all the deformations in the concrete composite are assumed to be on mortar part. Based on the assumption that the internal layer mortars (or paste) are same, the material properties shear moduli are equal ($G_1 = G_2$). Therefore, for given same deformations ($\delta_1 = \delta_2$), Equation 8-10 can be rewritten as:

$$\tau_1 / \tau_2 = d_2 / d_1 \qquad \textbf{Equation 8-11}$$

Hence, the yield stress, which is the shear stress on material when movement is initiated, of two composite objects have the following relationship as:

$$\tau_{01} / \tau_{02} = d_2 / d_1 \qquad \textbf{Equation 8-12}$$

Based on the definition from Equation 8-4 to 8-6, the apparent viscosity of these two objects can be calculated:

$$\eta_1 / \eta_2 = \frac{\tau_1 / \dot{\gamma}_1}{\tau_2 / \dot{\gamma}_2} = \frac{\tau_1 / [d(\delta_1 / d') / dt]}{\tau_2 / [d(\delta_2 / d') / dt]} \qquad \textbf{Equation 8-13}$$

Since the deformation were assumed to be equal ($\delta_1 = \delta_2$), following relation between apparent viscosity can be found:

$$\eta_1 / \eta_2 = d_2 / d_1 \qquad \textbf{Equation 8-14}$$

Equation 8-12 and 8-14 indicated that for concrete (or mortar) composite with same mortar (or paste), the yield stress and viscosity are both in direct proportion to reciprocal of distance between aggregate particles.

In order to obtain concrete (or mortar) rheology properties from the rheology properties of the different two phases, the matrix (mortar or paste) and composite (concrete or mortar) rheological performance with the aggregate particles inside are studied. Two simplified cases as described were considered: the first is a solid sphere with a radius of r_{agg} and each particle is coated with suspension (mortar or paste) of thickness of t_s. In order to compare with object in same condition, a second object with only a suspension with the same volume as the first case was considered, which means the radius of this uniform material is $r = r_{agg}+t_s$. According to the simplification as in Figure 8-8, these two study objects can be simplified as in Figure 8-10. If a force is applied on the two hypothetical aggregate particles in the case with just suspension inside, the inner layer thickness as d_1 or d_2 is then changed.

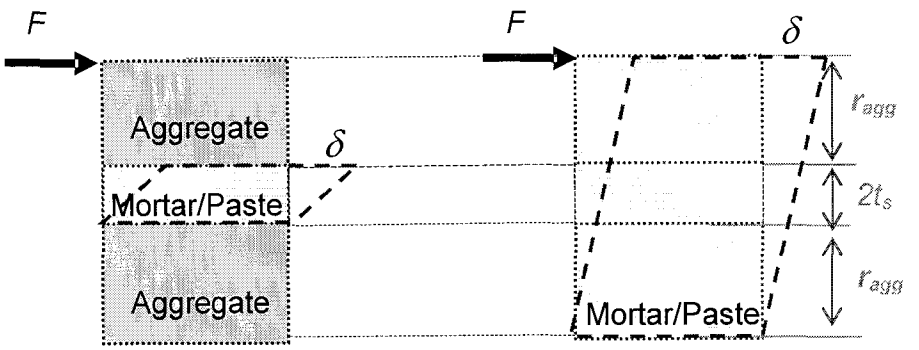

(a) Concrete **(b) Mortar**

Figure 8-10 Effect of coating thickness and aggregate radius on rheological parameters

In the case with spherical aggregates coated with mortar, the distance between solid particles is:

$$D_1 = 2t_s \qquad \textbf{Equation 8-15}$$

In the suspension-only case, i.e., with only mortar phase, the spheres in first case will be replaced with same size of mortar; hence, the distance will then change to:

$$D_2 = 2r_{agg} + 2t_s \qquad \textbf{Equation 8-16}$$

According to the derived equations 8-12 and 8-14, the yield stress and viscosity of composite is proportional to the distance between the solid particles, the relationship between the yield stress and viscosity of the composite as shown in Figure 8-10 can be calculated as:

$$\tau_0^{\,o} / \tau_{0s} = D_2 / D_1 = (r_{agg} + t_s) / t_s \qquad \textbf{Equation 8-17}$$

$$\eta^o / \eta_s = D_2 / D_1 = (r_{agg} + t_s) / t_s \qquad \textbf{Equation 8-18}$$

Results showed that the rheology of the composite can be directly affected by the thickness of the coating of paste and mortar. Equation 8-17 can 8-18 can be used to calculated τ_0^o and η^o in Equation 8-1 and Equation 8-2 respectively.

8.2.3 Rheology by Friction

In order to study the contribution from aggregate friction as described in Figure 8-5 (III-b), the performance aggregate friction under shear force is studied first. The calculation of the rheology caused by friction is shown in Figure 8-11. Assume there is an object composed of aggregates particles in a column packed together and there is a negligible amount of confined pressure applied on the sample in order to hold the shape of the column. According to basic idea of soil mechanics (Das, 1995), when this object is under a normal force and lateral force and material be treated as a uniform material, the tensile stress (τ, Pa) equals to the normal stress (σ, Pa) applied to the material times tangent of friction angle ($tan\phi$) plus the cohesion (c, Pa):

$$\tau = \sigma \tan\phi + c \qquad \textbf{Equation 8-19}$$

In cohesionless soil, such as dry aggregate with neglectable amount of fines, the cohesion c = *0* (Rao et al., 2002); hence, the tensile stress equals to the normal stress (σ) times the tangent of the friction angle of the material ($tan\phi$).

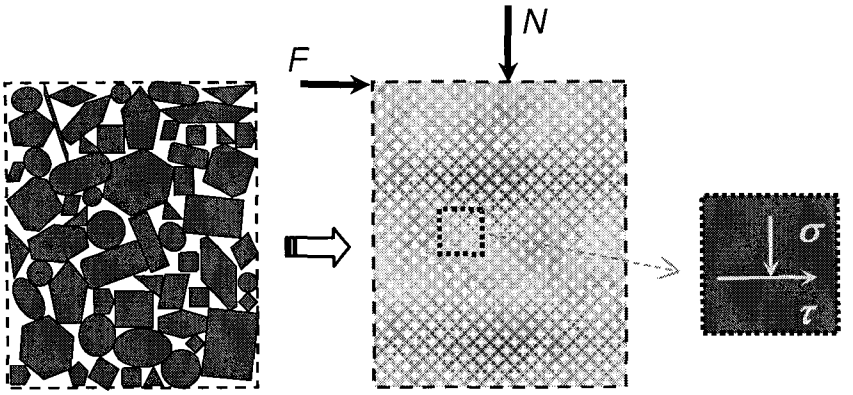

Figure 8-11 Shear stress from direct contact of aggregate

According to the definition of yield stress (shear stress when the movement is initiated) and viscosity (rate of shear stress over shear rate) in Equation 8-6, it is can be proposed that the effect of friction from the aggregate particles on concrete or mortar rheological property is proportional to the friction angle of aggregate. However, it was also found that when fresh concrete (or mortar) is under movement, the volume fraction of aggregate in concrete (or mortar) also affects the rheological performance because it is related to the probability that aggregate particles are in contact with each other (Kurokawa and Tanigawa, 1996).

When paste or mortar was added into the aggregate, the aggregate particles were pushed apart by the mortar (or paste) and were not in contact with each other. Consequently, after the flow of concrete or mortar was initiated, the higher the volume concentration the aggregate, the higher the possibility that the aggregate will be in contact with each other and hence the friction will be higher. The yield stress from aggregate friction τ_0^{Δ} can be related to the friction angle of aggregate as shown in Equation 8-20, while the viscosity from aggregate friction can hence be to be related to both friction angle and volume fraction of aggregate by Equation 8-21:

$$\tau_0^{\Delta} = f(\tan\phi_a) \qquad \textbf{Equation 8-20}$$

$$\eta^{\Delta} = f(\tan\phi_a, V_a\%) \qquad \textbf{Equation 8-21}$$

Where $tan\Phi_a$ is the friction angle of aggregate, $V_a\%$ is the volume fraction of aggregate.

Previous research on lateral pressure from SCC found out that the lateral pressure from SCC decrease with the increase of aggregate volume and/or the increase of the maximum size of aggregate (Assaad and Khayat, 2005). This fact was considered to be contributed from higher degree of aggregate friction inside concrete, which is consistent with the derivation in this section. It is necessary to point out that although aggregate friction will affect concrete and mortar rheology performance, the contribution may not be as significant as contribution from paste and mortar rheology and coating thickness. This is due to the fact that the shear stress is also decided by the normal stress applied on aggregate (σ as in Equation 8-19), which is relative low because of the small difference between paste, mortar and aggregate specific gravity values.

The rheology from aggregate friction in concrete and mortar is difficult to be calculated directly because of the complicated flow pattern of aggregate and suspension inside composite like fresh concrete. The relationship will be examined using statistical analysis that compares the calculated and measured rheological parameters, which will be specified later in this chapter.

8.3 Mortar Rheology Model

8.3.1 Excess Paste Thickness

As it was stated in Figure 8-5, in order to calculate the contribution of aggregate coating, it is important to calculating the coating thickness on coarse aggregate. Concrete and mortar are composite of solid phase and liquid phase (mortar or paste), in which only the liquid phase provides flowability. However, it was found that only part of the paste is able to provide flow, the rest is used to fill up the space between solid particles (Kennedy, 1940). Even for well-graded aggregates, there are still some spaces between aggregate particles, which mean a certain amount of paste is required to fill up these spaces. The additional amount of paste coating the aggregate particles can be therefore used to minimize the friction between them and hence attain high workability on mortar and concrete. According to Oh et al. (1999), the total volume of cement paste can be divided into two portions. One part is the paste in the

voids among aggregates, while the other part is the excess paste which coats the aggregate and separates them. It is the amount of excess paste, instead of the whole paste, that decides the rheology of mortar.

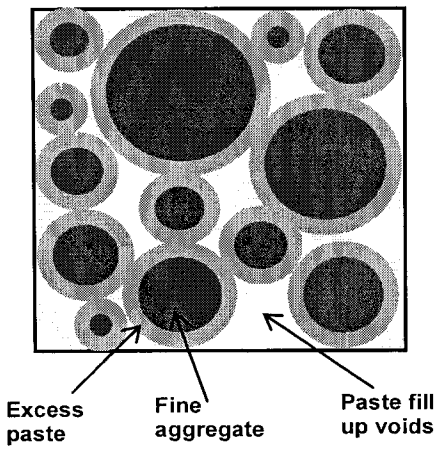

Figure 8-12 Definition of excess paste thickness (after Oh et al., 1999)

According to Oh et al. (1999), an approach as described in Figure 8-13 was used to calculate the excess paste volume. The total volume of paste is divided into two portions, in which one part is the paste in between voids among fine aggregates and the rest part is the excess paste, which covers the fine aggregate particles and separates them from contact with each other.

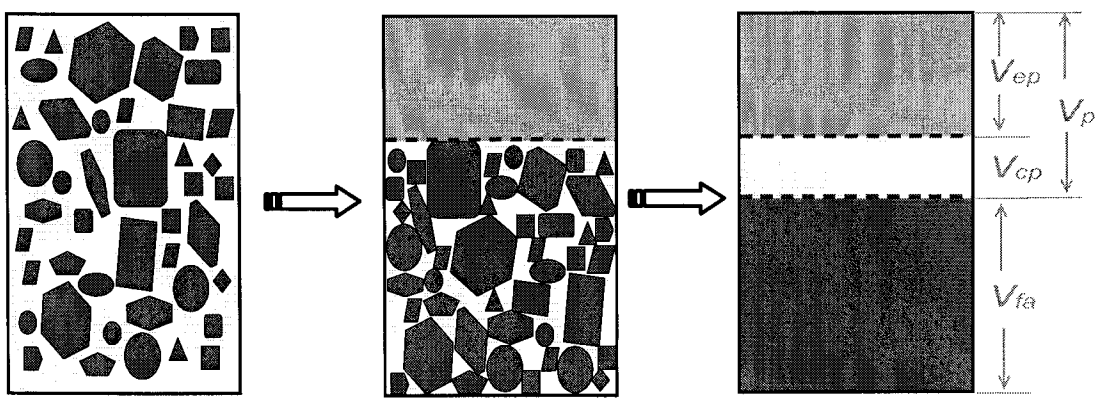

Figure 8-13 Calculation of excess paste volume (after Oh et al., 1999)

The volume of the excess paste can therefore be calculated as:

$$V_{ep} = V_p - V_{cp} \qquad \textbf{Equation 8-22}$$

In this equation V_{ep} is the whole volume of the excess paste (mm^3), V_{cp} is the volume of paste that fill up the voids (mm^3), and V_p is total volume of paste (mm^3).

The volume of paste can be calculated according to the mix design of mortar based on:

$$V_p = (W_w + W_c)/\gamma_p \qquad \textbf{Equation 8-23}$$

In this equation W_w is the weight of water (g), W_c is the weight of cement (g) and γ_p is the density of the cement paste (g/mm^3) (normally it can be assumed to be $2.6x10^{-3}g/mm^3$ (Mindess et al., 2003)). Assuming the weight of the cement is defined (use a value of one gram), the weight of the water and fine aggregate (W_{FA}) can then be calculated according to the mix design by one times the w/c or s/c. According to the definition, the uncompacted void $V_{n\text{-}FA}$ can be expressed as:

$$V_{n-FA} = \frac{V_{v-FA}}{V_{v-FA} + W_{FA}/\gamma_{FA}} \qquad \textbf{Equation 8-24}$$

In this equation, W_{FA} is the weight of fine aggregate (g), $V_{v\text{-}FA}$ is the volume of void between fine aggregate particles (mm^3), and γ_{FA} is the density of fine aggregate (g/mm^3), which can be calculated according to the specific gravity of fine aggregate at SSD condition from section 4.1.1 ($\gamma_{FA} = G_{sb\text{-}FA}x10^{-3}g/mm^3$). Equation 8-24 can be rewritten as following:

$$V_{v-FA} = \frac{V_{n-FA}W_{FA}/\gamma_{FA}}{1 - V_{n-FA}} \qquad \textbf{Equation 8-25}$$

When the space between fine aggregate is filled up with cement paste, the $V_{v\text{-}FA}$ will be the same as V_{cp} in Equation 8-22.

Different from the standard method of determine the surface area of the aggregate by multiplying the percentages of material passing a given set of sieves by a set of surface area factors and adding the products (Asphalt Institute, 1989), an approach similar to Heitzman's index model of calculating asphalt film thickness was applied (Heitzman, 2005). In present research, the surface area of the coarse aggregates was calculated by the number of aggregate

at specific size times the surface area of the individual aggregate, a procedure based on volume of aggregate instead of weight of aggregate was employed. Assuming the aggregate particles are all in spherical shape, according to the density of aggregate, γ_{FA}, the number of aggregates at different size can be calculated as:

$$N_{FA} = \frac{W_{FA} / \gamma_{FA}}{\frac{4\pi}{3} r_{FA}^{3}} \qquad \textbf{Equation 8-26}$$

In this equation N_{FA} is the number of fine aggregate at individual size, r_{FA} is the average radius of aggregate on individual sieve (mm), which can be calculated according to the average of the sieve size where aggregate particles in between:

$$r_{FA} = \frac{D_{\min} + D_{\max}}{4} \qquad \textbf{Equation 8-27}$$

In this equation, D_{min} is the maximum sieve size (mm) the aggregate can not pass through and D_{max} is the maximum sieve size (mm) aggregate can pass through. For example, the average size of aggregate retained on a #100 sieve can be calculated according to the size of #100 sieve (D_{min} = 0.15mm) and #50 sieve (D_{max} = 0.3mm), which will be 0.1125mm.

For graded fine aggregate, the average radius of the particles can be calculated according to the number of particles at different size as:

$$r_{G-FA} = \frac{\sum N_{i-FA} r_{i-FA}}{\sum N_{i-FA}} \qquad \textbf{Equation 8-28}$$

By the assumption that all the aggregate particles are spherical, the surface area of the aggregates can be calculated by the number of particles within the aggregate times the area of the individual aggregate surface included as:

$$S_{FA} = N_{FA} \times 4\pi r_{FA}^{2} \qquad \textbf{Equation 8-29}$$

In this equation S_{FA} is the surface area of aggregate (mm^2). For graded fine aggregate with several different sizes, the surface area can be calculated by summing up the surface area at different aggregate sizes:

$$S_{G-FA} = \sum N_{i-FA} \times 4\pi r_{i-FA}^{2} \qquad \textbf{Equation 8-30}$$

In this equation, N_{i-FA} is the number of aggregate in certain size and r_{i-FA} is the average radius of aggregate in certain size (mm).

According to the assumption that each particle will be covered with same thickness of paste, the excess paste thickness can be calculated by dividing the volume of excess paste by the surface area as (adopted from Oh et al., 1999):

$$t_p = \frac{V_{ep}}{S_{FA}} \qquad \textbf{Equation 8-31}$$

Figure 8-14 shows the calculated results of excess paste thickness of mortar in the same mix design but different size and type of aggregate. The calculated results are in agreement with the results from Ferraris and Gaidis (1992), which stated that the average gap between aggregates was computed to be around 0.2mm. It was found from the results that with the increase of the dimension of the aggregate, the excess paste thickness will be significantly increased because of the decreasing surface area, which requires less cement paste to cover the surface of aggregate. Figure 8-14 also shown that riversand and limestone resulted in different excess paste thickness, where the thickness of paste by using limestone and is lower because of the higher angularity and hence there is a larger uncompacted void percentage within the aggregate, meaning more cement paste is necessary to fill up the space in between aggregate particles. Results in Figure 8-14 (a) and (b) did not show obvious difference of the calculated excess paste thickness between graded and single-sized riversand, the calculated excess paste thickness by using graded riversand lay between the thickness resulted from #50 to #16 riversand.

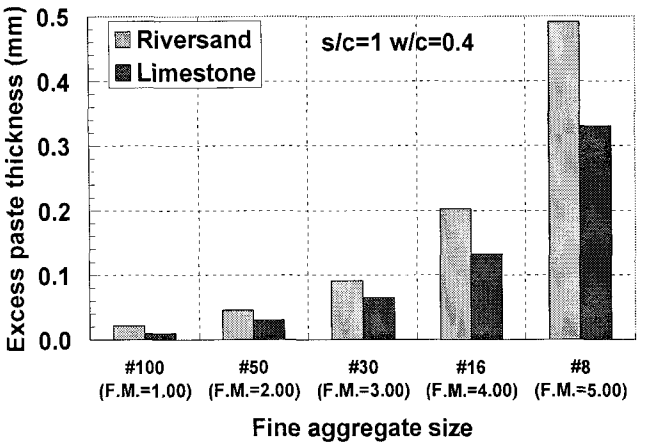

(a) Single-sized sand

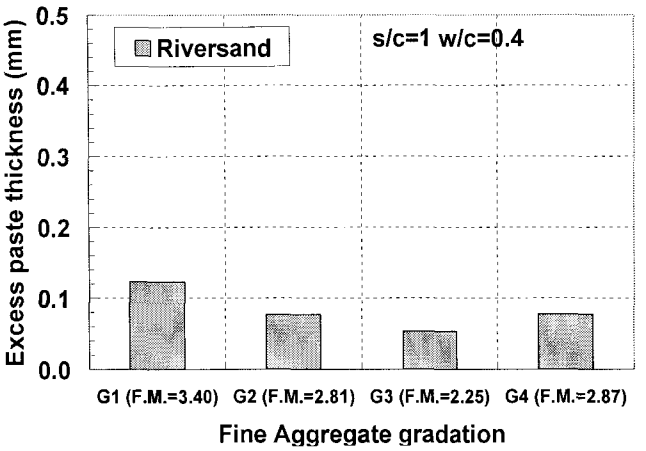

(b) Graded sand

Figure 8-14 Calculated excess paste thickness of with different sand

Since mortar may have different aggregate sizes and gradation, the calculated excess paste thickness values are different when the aggregate size is different; thus, a nominal thickness was used to considering the effect from aggregate size. The nominal excess paste thickness is defined as the calculated excess paste thickness divided by the average radius of aggregate as (adopted from Oh et al., 1999):

$$t'_p = \frac{t_p}{r_{FA}} \qquad \textbf{Equation 8-32}$$

The calculated nominal excess paste thickness using uniform size aggregate and graded aggregate is shown in Figure 8-15. The results indicated that aggregate with higher angularity

(limestone) has a much lower calculated nominal excess paste thickness than aggregate with lower angularity (riversand). Results in Figure 8-15 (b) clearly illustrated that with same kind of fine aggregate (riversand), mortar with graded fine aggregate has significantly higher nominal excess paste thickness (around 0.4 to 0.8) compared to those with uniform size fine aggregate (around 0.2 to 0.3). This is due to the smaller size of aggregate particles filling up the space between uncompacted void of relative bigger size of particles. This phenomenon can explain why mortars with better-graded aggregate have better flow.

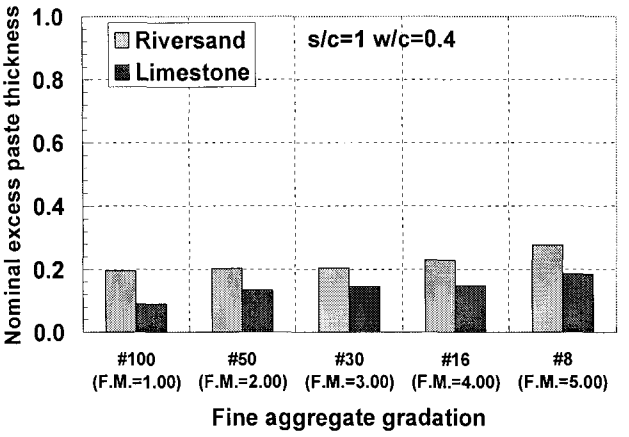

(a) Single-sized sand

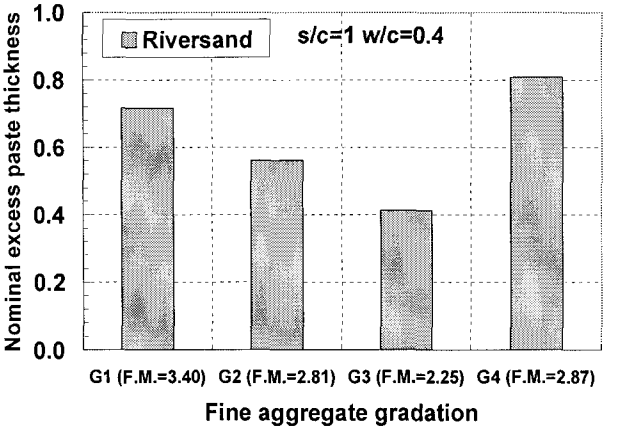

(b) Graded sand

Figure 8-15 Calculated nominal excess paste thickness with different gradation of sand

According to the equations of effect of spacing on composite rheology (Equations 8-17 and 8-18) and the definition of the nominal excess paste thickness (Equation 8-32), the yield

stress and viscosity of the mortar contributed from spacing can be directly calculated by the nominal excess paste thickness according to the following two equations:

$$\tau_{0m}{}^{o} / \tau_{0p} = 1 + 1/t_p' \qquad \textbf{Equation 8-33}$$

$$\eta_m{}^{o} / \eta_p = 1 + 1/t_p' \qquad \textbf{Equation 8-34}$$

Where t_p' is the calculated normal excess paste thickness, τ_{0p} and η_p are the yield stress and viscosity of paste respectively, which was obtained from Equation 5-1 and 5-2.

It is necessary to point out that the since calculation of surface area of aggregate is underestimated because of the assumption of the spherical shape of particles, further study is still necessary to improve the calculation by introduction of some shape factors using tools such as image analysis (Rao et al., 2000). However, the effect of aggregate shape was not as significant as expected because the size of the aggregate particle used in calculation was actually overestimated due to the fact of the spherical assumption. In the calculation, each particle was assumed to fit on every side of a single sieve mesh opening, which resulted in a larger aggregate and counteract to the effects on the calculated surface area. This statement is consistent with Heitzman (2005)'s research that the effect of aggregate shape is not very sensitive in calculating asphalt film coating thickness.

8.3.2 Mortar Rheology Analysis

The derived terms related to yield stress and viscosity contributed by the mortar coated on spherical particles ($\tau_0{}^{o}$ and η^{o} from equation 8-33 and 8-34), together the yield stress and viscosity contributed from the direct friction of aggregate particles ($\tau_0{}^{\Delta}$ and η^{Δ} from equation 8-20 and 8-21) are used in finalize the concrete rheology model. In order to study the statistical significance of different parameters, linear regressions using the logarithm values of input and output parameters were used. A stepwise regression method with significance level of 0.05 was applied in statistical analysis (details regarding the statistical analysis method and terminology can be found in Appendix VIII). The parameters of the nominal

excess paste thickness and the calculated paste rheological parameters from identical w/c according to Equation 5-1 and 5-2 were used in these models.

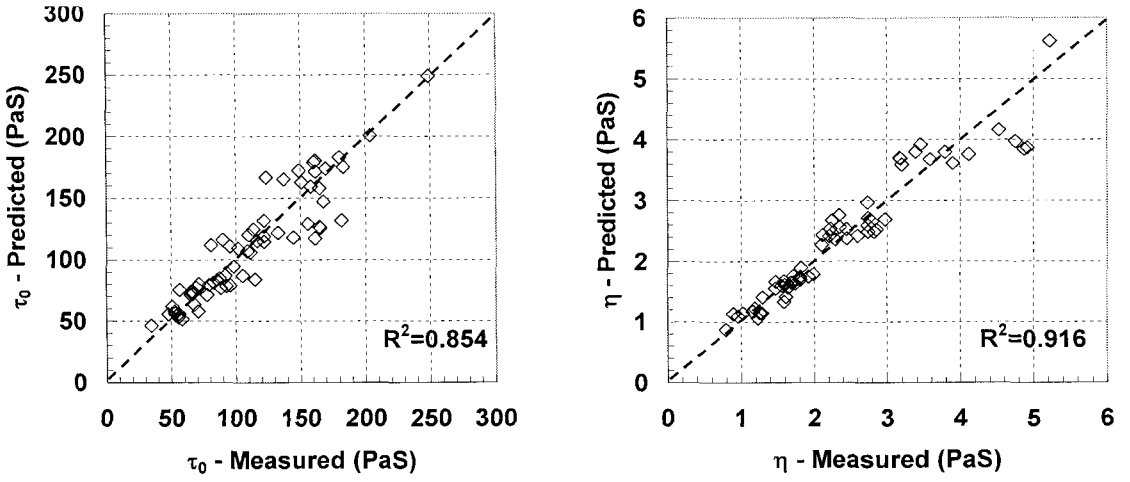

(a) Yield stress (b) Viscosity

Figure 8-16 Prediction for mortar rheological parameter

Results shown in Figure 8-16 indicate that the predicted and measured viscosity and yield stress have good agreement, with R^2 value of 0.92 and 0.85 respectively. It is necessary to point out that when the s/c increases to 3, the amount of paste in mortar is not enough to fill up the space between aggregate. This results in a negative calculated excess paste thickness, in which case the proposed model is no longer valid. Also, when the volume fraction of fine aggregate is high, several of the mortar mixes did not perform like liquid; additionally, strong segregation or rough mixes which can not flow well were observed. The rheology test of these mixes also showed very inconsistent results, which indicated they were not suitable for rheometer test. Due to these problems, the author did not these test results of mortar with negative calculated excess paste thickness in the analysis within this section. Based on the developed measurement results and parameters, the regression model equations for predicting mortar viscosity and yield stress are:

$$\eta_m = 2.04\eta_p^{0.649}(1+1/t_p')^{0.0823} \qquad \textbf{Equation 8-35}$$

$$\tau_{0m} = 5.29\tau_{0p}^{0.676}(1+1/t_p')^{0.116} \qquad \textbf{Equation 8-36}$$

Results indicated that with the increase of paste viscosity and yield stress, viscosity and yield stress of mortar increase respectively, which was expected because rheological performance of suspension in mortar is different. On the other hand, the yield stress and viscosity of mortar also decrease when nominal excess paste thickness increases, due to the increasing coating thickness of aggregate which the increases the distance between aggregate particles and thus provides the mortar with better flowability.

Table 8-1 ANOVA for prediction of mortar yield stress

Source	DF	Sum of Squares	Mean Square	F-Ratio	p-value
$\ln[\tau_{0_p}(1+1/t_p')]$	1	10.12	10.12	416.9	<.0001
$\ln(1+1/t_p')$	1	7.02	7.02	289.2	<.0001
Error	60	1.46	0.243		
C. Total	62	11.61			<.0001

Table 8-2 ANOVA for prediction of mortar viscosity

Source	DF	Sum of Squares	Mean Square	F-Ratio	p-value
$\ln[\eta_p(1+1/t_p')]$	1	11.305	11.305	962.1	<0.0001
$\ln(1+1/t_p')$	1	8.367	8.367	712.1	<0.0001
Error	60	0.705	0.01175		
C. Total	62	12.26			<.0001

According to the analysis results for mortar yield stress modeling in Table 8-1, the F-ratio of the term $ln[\tau_{0p}(1+1/t_p')]$ and $ln(1+1/t_p')$ is 416.9 and 289.2 respectively, with corresponding p-values smaller than 0.0001. According to the analysis of variance (ANOVA) table for the linear regression analysis results for mortar viscosity modeling in Table 8-2, the F-ratio of the term $ln[\eta_p(1+1/t_p')]$ and term $ln(1+1/t_p')$ is 962.1 and 712.1 respectively, with corresponding p-values smaller than 0.001. The residual versus prediction curve did not show any clear pattern, which indicates that the regression is appropriate. The statistical analysis indicated that the effect of both t_p' and η_p (or τ_{0p}) are statistically significant, with the significance level 0.05, because the p-value in the models are both less than 0.05. Factors

relating to friction ($Tan\Phi_{FA}$) was not found to be statistical significant (p-value much larger than 0.05), which is consistent with previous ANN analysis in section 8.1.1. This may be caused by the fact that the calculated excess paste thickness is interrelated to the aggregate friction angle, which might conceal the statistical significance of the effect from aggregate friction.

8.4 Concrete Rheology Modeling

8.4.1 Excess Mortar Thickness

Based on the previous mentioned two-phase theory by Topcu and Kocataskin (1995), concrete can be considered as a composite with coarse aggregate and mortar, if the mortar is considered as a uniform suspension according to two-phase theory. The idea of calculation of the excess paste thickness (Oh et al., 1999) was extended to calculate the excess mortar thickness. As shown in Figure 8-17, it is necessary to have sufficient coating between coarse aggregates to minimize the friction between them and hence to attain high workability on concrete.

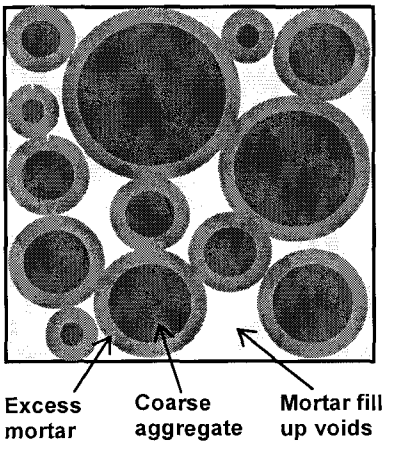

Figure 8-17 Definition of excess mortar thickness

Using a similar approach as used when calculating the excess paste thickness, the total volume of mortar can be divided into two portions, in which one part is the mortar in between voids among aggregates and the other part is the excess mortar, which covers the

coarse aggregate particles and separates them from contact with each other. The volume of the excess mortar can be calculated according to:

$$V_{em} = V_m - V_{cm} \qquad \textbf{Equation 8-37}$$

In this equation V_{em} is the volume of the excess mortar (mm^3), V_{cm} is volume of mortar in between voids (mm^3), and V_m is the total volume of mortar (mm^3).

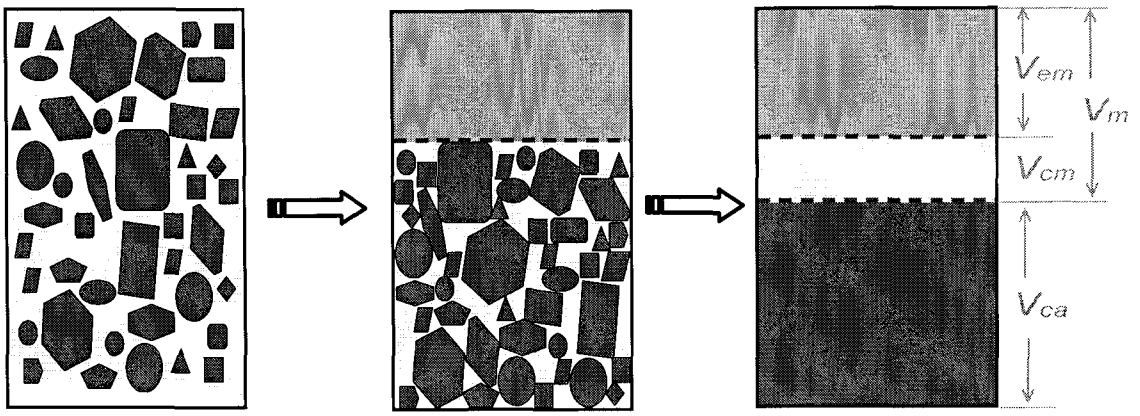

Figure 8-18 Calculation of excess mortar volume

According to Figure 8-18, the volume of mortar can be calculated as:

$$V_m = (W_w + W_c + W_{FA}) / \gamma_m \qquad \textbf{Equation 8-38}$$

In this equation W_w is the weight of water (g), W_c is the weight of cement (g), W_{FA} is the weight of fine aggregate (g), and γ_m is the density of mortar (g/mm^3) (which can normally be assumed to be $2.5x10^{-3} g/mm^3$ (Mindess et al., 2003)). Assuming the weight of cement is one gram, the weight of the water, sand W_{FA} and coarse aggregate W_{CA} can be calculated according to the mix design by times the w/c and coarse aggregate-to-cement ratio (CA/c).

According to the definition, the uncompacted void can be expressed as:

$$V_{n-CA} = \frac{V_{v-CA}}{V_{v-CA} + W_{CA} / \gamma_{CA}} \qquad \textbf{Equation 8-39}$$

In this equation W_{CA} is the weight of coarse aggregate (g), $V_{v\text{-}CA}$ is the volume of void between coarse aggregate (mm^3) and γ_{CA} is density of coarse aggregate (g/mm^3), which can be calculated according to the specific gravity at SSD condition from section 4.2.1 ($\gamma_{CA} = G_{sb\text{-}CA} x 10^{-3} g/mm^3$). Equation 8-39 can be expressed with the following:

$$V_{v-CA} = \frac{V_{n-CA} W_{CA} / \gamma_{CA}}{1 - V_{n-CA}} \qquad \textbf{Equation 8-40}$$

In this equation the spaces between the coarse aggregate particles are filled up with mortar, so $V_{v\text{-}CA}$ will be the same as V_{cm} in equation 8-37. Assuming the aggregate material is spherical and according to the density of coarse aggregate γ_{CA}, the number of coarse aggregate particles of different sizes can be calculated as:

$$N_{CA} = \frac{W_{CA} / \gamma_{CA}}{\frac{4\pi}{3} r_{CA}^{\ 3}} \qquad \textbf{Equation 8-41}$$

In this equation N_{CA} is the number of coarse aggregate particles at an individual size and r_{CA} is the average radius of coarse aggregate on individual sieves (mm), which can be calculated according to the average of the sieve size where aggregate lies in between:

$$r_{CA} = \frac{D_{\min} + D_{\max}}{4} \qquad \textbf{Equation 8-42}$$

In this equation D_{min} is the maximum sieve size that the aggregate can not pass through and D_{max} is the minimum sieve size through which the aggregate can pass. For example, the average size on 3/8" sieve can be calculated according to the size of 3/8" sieve ($D_{min} = 9.5mm$) and 1/2" sieve ($D_{max} = 12.5mm$), which will be 5.5mm.

For graded coarse aggregate, the average radius of particles can be calculated by the weighted average of particle size on number of particles:

$$r_{G-CA} = \frac{\sum N_{i-CA} r_{i-CA}}{\sum N_{i-CA}} \qquad \textbf{Equation 8-43}$$

The surface area of the coarse aggregates can be calculated by the number of aggregate times the area of the individual aggregate surface using:

$$S_{CA} = N_{CA} \times 4\pi r_{CA}^{2} \qquad \textbf{Equation 8-44}$$

In this equation S_{CA} is the surface area of coarse aggregate (mm^2). For graded coarse aggregate, the surface area can be calculated by summing up surface area at different aggregate size:

$$S_{G-CA} = \sum N_{i-CA} \times 4\pi r_{i-CA}^{2} \qquad \textbf{Equation 8-45}$$

In this equation N_{i-CA} is the number of coarse aggregate in certain size and r_{i-CA} is the average radius of coarse aggregate in certain size.

According to the assumption that each particle will be covered with same thickness of mortar, the excess mortar thickness can then be calculated by dividing the volume of excess mortar by the surface area:

$$t_m = \frac{V_{em}}{S_{CA}} \qquad \textbf{Equation 8-46}$$

Figure 8-19 illustrates the calculated results of excess mortar thickness of concrete with the same mix design but different sizes of coarse aggregate. The calculated excess mortar thickness decrease with the increase of volume content as expected because of the reducing of the available amount of mortar. It can also be found that with the increase of the dimension of coarse aggregate, the excess mortar thickness will be significantly increased because of the decreasing of surface area, which requires less mortar to coat the surface of coarse aggregate. No significant different of the calculated excess mortar thickness by using single size or graded aggregate was found. The graded aggregate resulted in a higher excess mortar thickness comparing to smaller size aggregate (#4), but lower excess mortar thickness comparing to larger size aggregate (3/4").

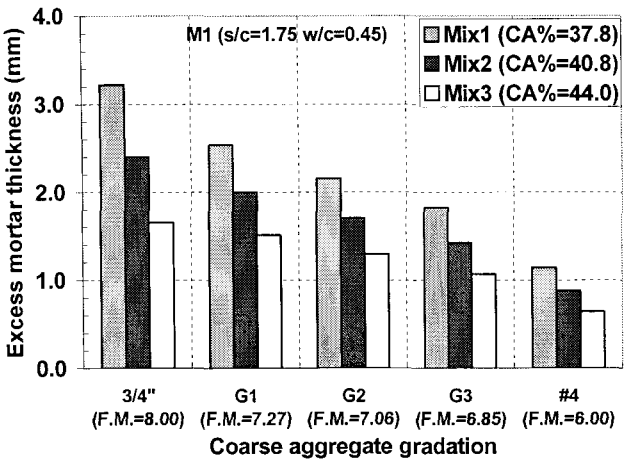

Figure 8-19 Calculated excess mortar thickness with different coarse aggregate

The nominal excess mortar thickness can be calculated by dividing the excess mortar thickness with the average radius of coarse aggregate r_{CA}:

$$t'_m = \frac{t_m}{r_{CA}} \qquad \textbf{Equation 8-47}$$

The results of the calculated nominal excess mortar thickness were shown in Figure 8-20. Results indicated that concretes with graded aggregate have higher nominal excess mortar thickness, which is because of the lower uncompacted void content of the aggregate resulting in greater amounts of excess mortar. Also, higher coarse aggregate content results in lower nominal excess mortar thickness, which is because more of the mortar volume will be required corresponding to a higher volume fraction of aggregate. Results also showed that the size of chosen single size aggregate in do not result in significant different normal excess mortar thickness value as the excess mortar thickness shown in Figure 8-19. However, the decrease of the excess mortar thickness with the decrease of the aggregate size as illustrated in Figure 8-19 indicated that using smaller size of aggregate will result in a lower coating thickness. This means aggregate have more chance to contact with each other and have more contribution on the friction force inside concrete, which explained why using smaller size of aggregate generally sometimes result in concrete with higher yield stress and viscosity value.

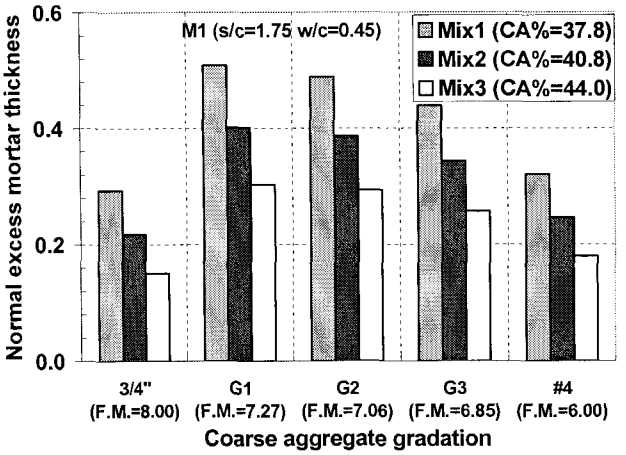

Figure 8-20 Calculated nominal excess mortar thickness with different gradation of coarse aggregate

According to Equations 8-17 and 8-18, the rheology of the concrete contributed from spacing can be directly calculated by the nominal excess mortar thickness as:

$$\tau_{0c}{}^{o} = \tau_{0m}(1+1/t_m') \qquad \textbf{Equation 8-48}$$

$$\eta_c{}^{o} = \eta_m(1+1/t_m') \qquad \textbf{Equation 8-49}$$

Where t_m' is the calculated normal excess mortar thickness, τ_{0m} and η_m are the yield stress and viscosity of mortar respectively, which was obtained from Table A-4.

8.4.2 Concrete Rheology Analysis

Similar to the study in mortar rheology, statistical models using the developed theoretical parameters related to mortar coating and coarse aggregate friction were developed for the prediction of concrete rheological properties as well as for evaluation of the degree that these factors influenced the concrete rheological behavior.

The derived term related to yield stress and viscosity contributed by the mortar coated on spherical particles ($\tau_0{}^{o}$ and η^{o} from equation 8-48 and 8-49), together the yield stress and viscosity contributed from the direct friction of aggregate particles ($\tau_0{}^{\Delta}$ and η^{Δ} from equation 8-20 and 8-21) are used in finalize the concrete rheology model. In order to study the rheology of concrete, linear regression using the logarithm values of input and output

parameters was used. A linear regression analysis with possible parameters that may affect the rheology was performed with stepwise regression analysis with significance of 0.05.

A model with the term of yield stress from coating $\tau_{0m}(1+1/t_m')$ and friction $tan(\phi_{CA})$ as shown in Equation 8-50 was found to have a strong correlation with the yield term (interception G) from concrete rheology measurement.

$$G = 0.00138[\tau_{0m}(1+1/t_m')]^{1.35}[Tan\phi_{ca}]^{-1.83} \qquad \textbf{Equation 8-50}$$

Equation 8-50 shows that with the increasing of mortar yield stress τ_{0m}, the yield term (interception G) of concrete increases. When excess mortar thickness, the interception also increases because of the increasing of spacing. It was also found from the ANOVA table (Table 8-3) that the F-ratio of this term is 149.3, corresponding to a p-value less than 0.0001, which indicates that the factor of $\tau_{0m}(1+1/t_m')$ is significant in a 0.05 significance level. The F-ratio of the parameter $tan(\phi_{CA})$ is 3.80, corresponding to a p-value slightly higher than 0.05, indicating that the effect from aggregate friction is still significant. It was observed that the estimated parameter for $tan(\phi_{CA})$ have negative effect, indicating that (providing all of the other parameters are fixed) with the increase of aggregate friction angle, the concrete yield value decreases. This was not explainable by the previously described theory of rheology contributed from friction. This phenomena might caused by the interaction of the calculated excess mortar thickness and friction. Since the uncompacted void content used in Equation 8-40 is directly related to the friction angle, a higher friction angle will result in a higher void content of the aggregate, and the effects of void content conceals the effect from aggregate friction and results in a the negative effect parameter. Analysis on the sensitive of effect from different factors shown from the ANN analysis (Figure 8-4) demonstrated that when the friction angle of the aggregate increases, it had a positive effect on the yield term of rheology. The interaction between these two terms used in statistical analysis resulted in an unexpected expression of the terms. However, the involvement of the friction angle term did improve the model, although the physical meaning can not be directly explained. The problem might be solved by using different kinds of aggregate from other sources which have significantly different friction angles.

Table 8-3 ANOVA for prediction of concrete yield parameter

Source	DF	Sum of Squares	Mean Square	F-Ratio	p-value
$\ln[\tau_{0m}(1+1/t_m')]$	1	6.897	6.897	149.3	<.0001
$\ln[\tan(\Phi_{ca})]$	1	0.176	0.176	3.80	0.0653
Error	20	0.924	0.0462		
C. Total	22	7.863			<.0001

The analysis of the viscosity term (slope H) of the concrete rheology test as shown in Equation 8-51 indicates that the viscosity of concrete not only related to the nominal mortar thickness and friction angle of the coarse aggregate but that it is also related to the volume fraction of coarse aggregate, in agreement with the research from Kurokawa et al. (1996) as shown in Equation 2-18.

$$H = 9.125[\eta_m(1+1/t_m')]^{0.3907}\left[(V_{ca}\%)^{1.446}(Tan\phi_{ca})^{0.00535}\right] \qquad \textbf{Equation 8-51}$$

ln[η_m(1+1/t_m'), *ln[V_{ca}%xtan(Φ_{ca})]* and *ln[tan(Φ_{ca})]* have F-ratios of 23.89, 9.38 and 11.98 respectively, corresponding to p-value all less than 0.05, which indicates that all three parameters have statistical significant effects on the concrete viscosity term. Results shown in Figure 8-21 of a prediction with R^2 value of 0.88 and a p-value of model less than 0.0001 indicates a very good prediction. The residual versus prediction curve also did not show any clear pattern. Results indicate that both the terms from spacing and from aggregate friction have significant effects on the viscosity of concrete.

Table 8-4 ANOVA of prediction of concrete viscosity parameter

Source	DF	Sum of Squares	Mean Square	F-Ratio	p-value
$\ln[\eta_m(1+1/t')]$	1	0.129	0.129	23.89	0.0001
$\ln[V_{ca}\% \times \tan(\phi_{ca})]$	1	0.0505	0.0505	9.38	0.0064
$\ln[\tan(\phi_{ca})]$	1	0.0645	0.0645	11.98	0.0026
Error	19	0.102	0.00539		
C. Total	22	1.115			<.0001

Results shown in Figure 8-21 indicate that the predicted and measured interception and slope of concrete rheology test are in strong agreement, with an R^2 value of 0.86 and 0.88 respectively. The P-value for the model are less than 0.001, the residual versus prediction curve also did not show clear pattern, which indicates that the regression is appropriate.

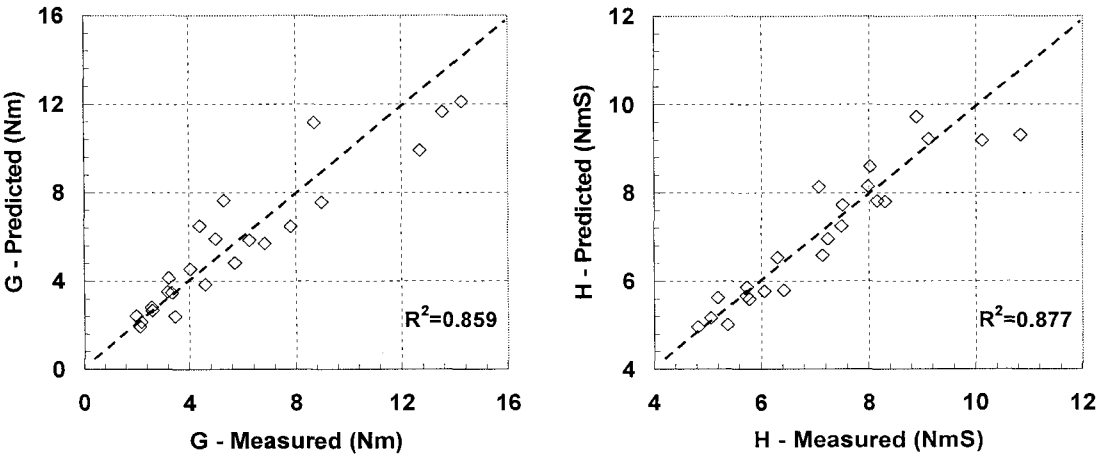

(a) Yield term **(b) Viscosity term**

Figure 8-21 Prediction for concrete rheological parameters

8.5 Summary

According to the initial study using ANN methods, the effects of aggregate on mortar and concrete rheology, including type, size, gradation, and content, were systematically considered. Results showed that aggregate proportion, void content, friction, together with the rheology of paste and mortar all showed important effects on mortar and concrete rheological parameters. Theoretical parameters relating to aggregate spacing and friction were obtained and studied based on microstructure of concrete and mechanics accordingly. Statistical tool was use to finalize the rheology model with these developed theoretical parameters as well as for evaluation of the degree that these factors influenced the mortar and concrete rheological behavior.

According to the newly developed models, the parameters including rheology of suspension, nominal paste or mortar thickness and tangent of aggregate friction can be successfully used

to predict the mortar and concrete rheology. Results and modeling from this chapter proved that mortar and concrete rheology contributed from both spacing and friction. The newly developed models were found to be more rational and practical compared to the previous models. The developed models can be used to analyze the effects of aggregate on mortar and concrete rheology. Also, the models have great potential to be used to design mortar and concrete with desirable rheology parameters.

CHAPTER 9. SUMMARY AND CONCLUSIONS

9.1 Summary

In this study, the rheological behavior of paste, mortar, and concrete have been investigated using rotational rheometers. Type I Portland cement was used as the cement, limestone was used as the coarse aggregate, riversand and limestone were used as the fine aggregate. A total of 10 cement paste mixes, 136 mortar mixes and 23 concrete mixes were evaluated. Different variables relating to the effects of aggregate - including proportion, type, size, and gradation on mortar and concrete rheology - were quantitatively studied. The relationships of the rheology tests with standard slump tests and flow table tests were discussed.

Based on the test data, models were developed for predicting the mortar and concrete rheological properties as well as for evaluating the factors that influence mortar and concrete rheological behavior. Based on the two-phase theory and excess paste theory, the excess paste thickness of fine aggregate, excess mortar thickness of coarse aggregate and aggregate friction were calculated and chosen as the major parameters in study. The rheology models were then obtained using these parameters according to statistical regression analysis. Unlike the previous models, the effects of aggregate on mortar and concrete rheology were systematically considered in the present models. The newly developed models were found to be more rational and practical comparing to the previous models.

9.2 Findings

The major findings of this study are included as the following:

1. Aggregate Characterization

- Aggregate gradation, shape, and surface texture can be simply characterized by the measurement of uncompacted voids between the aggregate particles. Generally, aggregate with higher uncompacted void content provides mortar and concrete with a lower flow.

- Friction between aggregate particles can be characterized by a newly developed friction angle test. The increase of aggregate friction angle generally increases the yield stress and viscosity of cementitious materials.

2. Effects of Aggregate on Mortar and Concrete Rheology

- Aggregate with lower uncompacted void content generally reduces mortar or concrete yield stress and viscosity. Graded aggregate can considerably reduce yield stress and viscosity of mortar and concrete because of the reduced void content.
- Irregular shape and rough-surface aggregates have higher uncompacted void contents and higher friction angles than round and smooth-surface aggregates. Fine aggregate with a high friction angle (limestone) results in higher yield stress and viscosity mortar compared to low friction angle fine aggregate (riversand).
- For a given aggregate content, finer aggregate normally provides mortar and concrete with higher yield stress and viscosity.
- Increasing the amount of aggregate content results in larger values of yield stress and viscosity of mortar and concrete because of the decrease in the thickness of the paste or mortar coating on the aggregate particles.

3. Modeling Study

- Excess paste or mortar thickness can be estimated according to the aggregate uncompacted void content and mix design. Mortar and concrete with larger amounts of excess paste or greater mortar thickness has a lower yield stress and viscosity.
- Parameters used in the model can be obtained through mix design and aggregate properties with simple test such as uncompacted void and friction angle. The models were found to be more rational and practical comparing to the previous models.
- The rheology of the matrix (paste or mortar), relative thickness of paste or mortar, and aggregate friction were considered as the major parameters in the newly developed models.

- The developed models can be used to analyze the effects of aggregate on mortar and concrete rheology. They can also be used to design mortar and concrete with desirable rheological parameters.

4. Test Methods

- Standard tests, including the mortar flow table test and the concrete slump test, were compared with the rheometer test results. The combination of the slump and flow table test results may provide engineers with sufficient information on the rheological behavior of cementitious materials.

9.3 Research Limitations and Recommendations

In the present study, some assumptions were made in the concrete rheology model development. These assumptions shall be re-evaluated and/or modified to improve the models in future study.

In the calculations of the surface area and excess paste or mortar thickness, aggregate particles were assumed to be spheres, and effect of aggregate shape was not directly considered in the models. Also, the portion of concrete rheology decided by spacing and from aggregate friction was not able to study independently because of the limitation of test equipment. A comparison of aggregate versus same aggregate with voids filled by mortar (i.e. concrete with the corresponding mix design) performed by direct shear or triaxial test may be used to study the contribution from aggregate friction in concrete rheological performance, which should be helpful to further improve the model.

The mixtures of mortar and concrete were assumed to perform uniformly under deformation in the calculation of rheology parameters, which might not be practical since material at different locations might deform differently. A computer simulation may be applied to imitate the flow pattern of materials inside the mixture.

The yield stress and viscosity for concrete used in the present research are not available due to the difficulty of the simulation of exact flow behavior in the concrete rheometer test (the viscosity parameter (H) and yield parameter (G) were calculated instead). It is necessary to develop reference materials in order to get absolute rheological parameters and improve the accuracy of concrete rheometers. The standard reference material using plastic spheres and oil-based system to simulate concrete mixtures in order to compare different concrete rheometers is currently under discussion by ACI committee 236A.

In the present research, the effects of chemical admixtures and SCMs on the rheological performance of cementitious materials were not considered. It is necessary to consider the effect on the rheological properties of cement paste on a wider range in the rheology model, since different admixtures are more often used in current concrete.

Due to the limitation of time and source of materials, the accuracy, reliability, and reproducibility of model was restricted because of the relative small amount of data. A larger series of measurements and materials with a broader range of properties have to be tested in order to improve the validity of model. Additional data including the field data, assuming that the aggregate property parameters and mix designs are available, can improve the accuracy and wider applicable range of the model by setting up a bigger data base.

REFERENCES

ACI Committee 116, (2000). "*Cement and concrete terminology*", ACI 116R-00, ACI Manual of Concrete Practice, Detroit, MI

Aiad, I., (2003). "Influence of time addition of superplasticizers on the rheological properties of fresh cement pastes", *Cement and Concrete Research,* Vol. 33, No. 8, pp. 1229-1234

Aiad, I.; Abd El-Aleem, S.; and El-Didamony, H., (2002). "Effect of delaying addition of some concrete admixtures on the rheological properties of cement pastes", *Cement and Concrete Research,* Vol. 32, No. 11, pp. 1839-1843

Amer, N.; Delatte, N.; and Storey, C., (2004). "Using gyratory compaction to investigate density and mechanical properties of roller-compacted concrete", *Journal of the Transportation Research Board*, Transportation Research Record 1834, pp. 77-84

Amziane, S.; Ferraris, C. F.; and Koehler, E. P., (2005). "Measurement of workability of fresh concrete using a mixing truck", *Journal of Research of the National Institute of Standards and Technology*, Vol. 110, No. 1, pp. 55-66

API Specification 10A, (2002). "*Specification for cements and materials for well cementing*", API/ANSI/ISO 10426-1-2001, Washington D.C.

Asphalt Institute, (1989). "*The Asphalt Handbook*", Manual Series No. 4 (MS-4) 1989 Edition

Assaad, J.; Khayat, K. H.; and Daczko, J., (2004). "Evaluation of static stability of self-consolidating concrete", *ACI Materials Journal,* Vol. 101, No. 3, pp. 207-215

Assaad, J.; Khayat, K. H.; and Mesbah, H., (2003). "Assessment of thixotrophy of flowable and self-consolidating concrete", *ACI Materials Journal,* Vol. 100, No. 2, pp. 99-107

ASTM C29/C29M-97 (Reapproved 2003), (American Association of State Highway and Transportation Officials Standard AASHTO No.: T19/T19M), (2003). "*Standard test method for bulk density ("unit weight") and voids in aggregate*", Annual Book of ASTM Standards, Vol. 04. 02

ASTM C33-03, (2003). "*Standard specification for concrete aggregates*", Annual Book of ASTM Standards, Vol. 04. 02

ASTM C 39/C 39M-01 (2003). "*Standard test method for compressive strength of cylindrical concrete specimens*", Annual Book of ASTM Standards, Vol. 04. 02

ASTM C125-03, (2003). "*Standard terminology relating to concrete and concrete aggregates*", Annual Book of ASTM Standards, Vol. 04. 02

ASTM C127-01, (2003). "*Standard test method for density, relative density (specific gravity), and absorption of coarse aggregate*", Annual Book of ASTM Standards, Vol. 04. 02

ASTM C128-01, (2003). *Standard test method for density, relative density (specific gravity), and absorption of fine aggregate*", Annual Book of ASTM Standards, Vol. 04. 02

ASTM C138/C138M-01, (2002). "*Standard test method for density (unit weight), yield, and air content (gravimetric) of concrete*", Annual Book of ASTM Standards, Vol. 04.02

ASTM C143/C143M-00, (2002). "*Standard test method for slump of hydraulic-cement concrete*", Annual Book of ASTM Standards, Vol. 04.02

ASTM C150-02, (2002). "*Standard specification for Portland cement*", Annual Book of ASTM Standards, Vol. 04.01

ASTM C192/C192M-00, (2002). "*Standard practice for making and curing concrete test specimens in the laboratory*", Annual Book of ASTM Standards, Vol. 04.02

ASTM C230/C230M-98, (2003). "*Standard specification for flow table for use in tests of hydraulic cement*", Annual Book of ASTM Standards, Vol. 04. 01

ASTM C305-99 (American Association State Highway and Transportation Officials Standard AASHTO No. T162), (2003). "*Standard practice for mechanical mixing of hydraulic cement pastes and mortars of plastic consistency*", Annual Book of ASTM Standards, Vol. 04. 01

ASTM C778-02, (2003). "*Standard specification for standard sand*", Annual Book of ASTM Standards, Vol. 04. 01

ASTM C1252-98, (2003). "*Standard test methods for uncompacted void content of fine aggregate (as influenced by particle shape, surface texture, and grading)*", Annual Book of ASTM Standards, Vol. 04. 02

ASTM C1437-01, (2003). "*Standard test method for flow of hydraulic cement mortar*", Annual Book of ASTM Standards, Vol. 04. 02

Atzeni, C.; Massidda, L.; and Sanna, U., (1985). "Comparison between rheological models for Portland cement pastes", *Cement and Concrete Research*, Vol. 15, No. 3, pp. 511-599

Bager, D. H.; Mette, R.; and Rune, M. J., (2004). "Rheology of self-compacting mortars - Influence of particle grading", *Nordic Concrete Research*, No. 26

Banfill, P. F. G., (2003). "The rheology of fresh cement and concrete – A review", *Proc 11th International Cement Chemistry Congress, May 2003, Durban*

Banfill, P. F. G.; Xu, Y.; and Domone, P. L. J., (1999). "Relationship between the rheology of unvibrated fresh concrete and its flow under vibration in a vertical pipe apparatus", *Magazine of Concrete Research*, Vol. 51, No. 3, pp. 181-190

Banfill, P. F. G. (1994). "Rheological methods for assessing the flow properties of mortar and related materials", *Construction and Building Materials*, Vol. 8, No. 1, pp. 43-50

Banfill, P. F. G.; and Saunders, D. C., (1981). "On the viscometric examination of cement pastes", *Cement and Concrete Research*, Vol. 11, No. 3, pp.363-370

Barrioulet, M.; and Legrand, C., (1991). "Diphasic semi-empiric model for the rheological behavior of vibrated fresh concrete", *In:* P. F. G. Banfill, Ed., *Rheology of fresh cement and concrete: proceeding of the international conference*, E & FN Spon, pp. 343-351

Barnes, H. A.; Hutton, J. F.; and Walters, K., (1989). "An introduction to rheology", Elsevier Science Publishers B. V.

Bartos, P., (1992). "*Fresh concrete – properties and tests*", Elsevier Science Publishers B. V.

Bhatty, J. I.; and Banfill, P. F. G., (1982). "Sedimentation behaviour in cement pastes subjected to continuous shear in rotational viscometers", *Cement and Concrete Research*, Vol. 12, No. 1, pp. 69-78

Bilgil, A.; Ozturk, B.; and Bilgil, H., (2005). "A numerical approach to determine viscosity-dependent segregation in fresh concrete", *Applied Mathematics and Computation,* Vol. 162, No. 1, pp. 225-241

Bloem, D.L.; and Gaynor R. D., (1963). "Effects of aggregate properties on strength of concrete", *Journal of the American Concrete Institute*, pp. 1429-1454

Bonen, D.; and Shah, S. P., (2005), "Fresh and hardened properties of self-consolidating concrete", *Progress in Structural Engineering and Materials*, Vol. 7, No. 1, pp. 14-26

Bosiljkov, V. B., (2003). "SCC mixes with poorly graded aggregate and high volume of limestone filler", *Cement and Concrete Research*, Vol. 33, No. 9, pp. 1279-1286

Bui, V. K.; Montgomery, D.; Hinczak, I.; and Turner, K., (2002a). "Rapid testing method for segregation resistance of self-compacting concrete", *Cement and Concrete Research,* Vol. 32, No. 9, pp. 1489-1496

Bui, V. K.; Akkaya, Y.; and Shah, S. P., (2002b). "Rheological model for self-consolidating concrete", *ACI Materials Journal*, Vol. 99, No. 6, pp. 549-559

Çelik, T.; and Marar, K., (1996). "Effects of crushed stone dust on some properties of concrete", *Cement and Concrete Research,* Vol. 26, No. 7, pp. 1121-1130

Chang, C.; and Powell, R. L., (1994). "Effect of particle size distributions on the rheology of concentrated bimodal suspensions", *Journal of Rheology*, Vol. 38, No. 1, pp. 85-98

Chia, K. S.; and Zhang, M. H., (2004). "Effect of chemical admixtures on rheological parameters and stability of fresh lightweight aggregate concrete", *Magazine of Concrete Research*, Vol. 56, No. 8, pp. 465-473

Coussot, P.; and Piau, J. M., (1995). "Large-scale field coaxial cylinder rheometer for the study of the rheology of natural coarse suspensions", *Journal of Rheology*, Vol. 39, No. 1, pp. 105-124

Cry, M.; Legrand, C.; and Mouret, M., (2000). "Study of the shear thickening effect of superplasticisers on the rheological behavior of cement pastes containing or not mineral additives", *Cement and Concrete Research*, Vol. 30, No. 9, pp. 1477-1483

Das, B. M., (1995). "*Principles of foundation engineering*", 3rd Edition, PWA Publishing Company

De Larrard, F., (1999). "*Concrete mixture proportioning – A scientific approach*", E & FN Spon

De Larrard, F.; Ferraris, C. F.; and Sedan, T., (1998). "Fresh concrete: A Herschel-Bulkley material", *Materials and Structures*, Vol. 31, No. 211, pp. 494-498

De Larrard, F.; Hu, C.; Sedran, T.; Szitkar, J.; Joly, C. M.; Claux, F.; and Derkx, F., (1997). "A new rheometer for soft-to-fluid fresh concrete", *ACI Materials Journal*, Vol. 94, No. 3, pp. 234-243

Denis, A.; Attar, A.; Breysse, D.; and Chauvin, J. J., (2002). "Effect of coarse aggregate on the workability of sandcrete", *Cement and Concrete Research,* Vol. 32, No. 5, pp. 701-706

Dilek, U.; and Leming, M. L., (2004). "Relationship between particle shape and void content of fine aggregate", *Cement, Concrete and Aggregates*, Vol. 26, No. 1, pp. 14-20

Domone, P. L. J.; Xu, Y.; and Banfill, P. F. G., (1999). "Developments of the two-point workability test for high-performance concrete", *Magazine of Concrete Research,* Vol. 51, No. 3, pp. 171-179

Faroug, F.; Szwabowski, J.; and Wild, S., (1999). "Influence of superplasticizers on workability of concrete", *Journal of Materials in Civil Engineering*, Vol. 11, No. 2, pp. 151-157

Ferraris, C. F.; and Brower, L. E., (2004). "*Comparison of concrete rheometers: International tests at MB (Cleveland OH, USA) in May, 2003*", NISTIR 7154

Ferraris, C. F.; and Brower, L. E., (2001). "*Comparison of concrete rheometers: International tests at LCPC (Nantes, France) in October, 2000*", US Department of Commerce and National Institute of Standards and Technology

Ferraris, C. F.; Obla, K. H.; and Hill, R., (2001). "The influence of mineral admixtures on the rheology of cement paste and concrete", *Cement and Concrete Research,* Vol. 31, No. 2, pp. 245-255

Ferraris, C. F., (1999). "Measurement of the rheological properties of high performance concrete: State of the art report", *Journal of Research of the National Institute of Standards and Technology*, Vol. 104, No. 5, pp. 461-477

Ferraris, C. F.; and de Larrard, F., (1998). "*Testing and modeling of fresh concrete rheology*", NISTIR 6094

Ferraris C. F.; and Gaidis J. M., (1992). "Connection between the rheology of concrete and rheology of cement paste", *ACI Materials Journal*, Vol. 89, No. 4, pp. 388-393

Flatt, R. J.; Martys, N.; and Bergstrom, L., (2004). "The rheology of cementitious materials", *MRS Bulletin*, Vol. 29, No. 5, pp. 314-318

Garboczi, E. J.; Martys, N.S.; Saleh, H. H.; and Livingston, R. A., (2001). "Acquiring, analyzing, and using complete three-dimensional aggregate shape information", *Aggregates, Concrete, Bases, and Fines, 9th Annual Symposium, Proceedings, Center for Aggregates Research. April 22-25, 2001, Austin, Texas*

Geiker, M. R.; Brandl, M.; Thrane, L. N.; Bager, D. H.; and Wallevik, O., (2002a). "The effect of measuring procedure on the apparent rheological properties of self-compacting concrete", *Cement and Concrete Research*, Vol. 32, No. 11, pp. 1679-1850

Geiker, M. R.; Brandl, M.; Thrane, L. N.; and Nielsen, L. F., (2002b). "On the effect of coarse aggregate fraction and shape on the rheological properties of self-compacting concrete", *Cement, Concrete, and Aggregate*, Vol. 24, No. 1, pp. 3-6

Gjorv, O. E., (1998). "Workability: a new way of testing", *Concrete International*, Vol. 20, No. 9, pp. 57-60

Golaszewski, J.; and Szwabowski, J., (2004). "Influence of superplasticizers on rheological behaviour of fresh cement mortars", *Cement and Concrete Research*, Vol. 34, No. 2, pp. 235-248

Grunewald, S., (2004). "*Performance-based design of self-compacting fibre reinforced concrete*", Thesis (PhD), Delft University

Hackley, V. A.; and Ferraris, C. F., (2001). "*The use of nomenclature in dispersion science and technology*", Special Publication 960-3, NIST

Heitzman, M., (2005). "*Development of new film thickness models for hot mix asphalt – achieving HMA mixture durability*", Thesis (PhD), Iowa State University

Ho, D. W. S.; Sheinn, A. M. M.; Ng, C. C.; and Tam, C. T., (2002). "The use of quarry dust for SCC applications", *Cement and Concrete Research*, Vol. 32, No. 4, pp. 505-511

Hobbs, D. W., (1976). "Influence of aggregate volume concentration upon the workability of concrete and some predictions from the viscosity - elasticity analogy", *Magazine of Concrete Research*, Vol. 28, No. 97, pp. 191-202

Hu, C.; and de Larrard, F., (1996). "The rheology of fresh high performance concrete", *Cement and Concrete Research*, Vol. 26, No. 2, pp. 283-294

Hu, C.; de Larrard, F.; and Gjorv, O. E., (1995). "Rheological testing and modelling of fresh high performance concrete", *Materials and Structures/Materiaux et Constructions*, Vol. 28, No. 175, pp. 1-7

Hu, J.; and Wang. K, (2005). "Effects of aggregate on flow properties of mortar", *Proceedings of the 2005 Mid-Continent Transportation Research Symposium, Ames, Iowa, August 2005*

Illston J. M.; and Domone P. L. J., (2001). "*Construction materials – their nature and behavior*", 3rd ed., Spon Press, London and New York

Jamkar, S. S.; and Rao, C. B. K., (2004). "Index of aggregate particle shape and texture of coarse aggregate as a parameter for concrete mix proportioning", *Cement and Concrete Research,* Vol. 34, No. 11, pp. 2021-2027

Jiang, W.; and Roy, D. M., (1993). "Microstructure and flow behavior of fresh cement paste", *Materials Research Society Symposium Proceedings*, Vol. 289, pp. 161-166

Jones, T. E. R.; and Taylor, S., (1977). "Mathematical model relating the flow curve of a cement paste to its water/cement ratio", *Magazine of Concrete Research*, Vol. 29, No. 101, pp. 207-212

Kamal, H. K., (1998). "Viscosity-enhancing admixtures for cement-based materials - An overview", *Cement and Concrete Composites,* Vol. 20, No. 2-3, pp. 171-188

Kantro, D. L., (1980). "Influence of water-reducing admixtures on properties of cement paste – A miniature slump test", *Cement, Concrete, and Aggregates*, Vol. 2, No. 2, pp. 95-102

Kennedy, C.T., (1940). "The design of concrete mixes", *Proceedings of the American Concrete Institute*, Vol. 36, pp. 373-400

Khayat, K. H.; Saric- Coric, M.; and Liotta, F., (2002). "Influence of thixotropy on stability characteristics of cement grout and concrete", *ACI Materials Journal*, Vol. 99, No. 3, pp. 234-241

Khayat, K. H.; and Yahia, A., (1997). "Effect of Eelan gem-high-range water reducer combinations on rheology of cement grout", *ACI Materials Journal*, Vol. 94, No.5, pp. 365-372

Kleinbaum, D. G.; Kupper, L. L., Muller, K. E., and Nizam, A., (1998). "*Applied regression analysis and other multivariable methods*", Duxbury Press

Koehler, E. P.; Bodenlos, K. D.; and Fowler, D. W., (2004). "Development of an energy-based approach to workability characterization", *12th Annular Symposium Proceedings, International Center for Aggregate Research, Denver, Colorado, April 4-7, 2004*

Koehler, E. P.; and Fowler, D. W., (2004). "*Development of a portable rheometer for fresh Portland cement concrete*", ICAR Report 105-3F, International Center for Aggregates Research, The University of Texas at Austin

Koehler, E. P.; and Fowler, D. W., (2003). "*Summary of concrete workability test methods*", ICAR Report 105-1, International Center for Aggregates Research, The University of Texas at Austin

Kosmatka, S, H.; Kerkhoff, B.; and Panarese, W. C., (2002). "*Design and control of concrete mixture*", 14th ed., Portland Cement Association

Krstulovic, P.; and Juradin, S., (1999). "Modeling of fresh concrete behavior under vibration", *International Journal for Engineering Modeling*, Vol. 12, No. 1, pp. 43-51

Kurokawa, Y.; Tanigawa, Y.; Mori, H.; and Nishinosono, K., (1996). "Analytical study on effect of volume fraction of coarse aggregate on Bingham's constants of fresh concrete", *Transactions of the Japan Concrete Institute*, Vol. 18, pp. 37-44

Kwan, A. K. H.; Mora, C. F.; and Chan, H. C., (1999). "Particle shape analysis of coarse aggregate using digital image processing", *Cement and Concrete Research,* Vol. 29, No. 9, pp. 1403-1410

Labouret, S.; Looten-Baquet, I.; Bruneel, C.; and Frohly, J., (1998). "Ultrasound method for monitoring rheology properties evolution of cement", *Ultrasonics,* Vol. 36, No. 1-5, pp. 205-208

Lachemi, M.; Hossain, K. M. A.; Lambros, V.; Nkinamubanzi, P. C.; and Bouzoubaâ, N., (2004a). "Self-consolidating concrete incorporating new viscosity modifying admixtures", *Cement and Concrete Research*, Vol. 34, No. 6, pp. 917-926

Lachemi, M.; Hossain, K. M. A.; Lambros, V.; Nkinamubanzi, P. C.; and Bouzoubaâ, N., (2004b). "Performance of new viscosity modifying admixtures in enhancing the rheological properties of cement paste", *Cement and Concrete Research,* Vol. 34, No. 2, pp. 185-193

Lambe, T. W., (1969). *"Soil mechanics",* John Wiley & Sons, New York

Lei, W.; and Struble, L.J., (1997). "Microstructure and flow behavior of fresh cement paste", *Journal of the American Ceramic Society*, Vol. 80, No. 8, pp. 2021-2028

Li, Z.; Ohkubo, T.-A.; and Tanigawa, Y., (2004a). "Yield model of high fluidity concrete in fresh state", Journal of Materials in Civil Engineering, Vol. 16, No. 3, pp. 195-201

Li, Y.; Zhou, S.; Yin, J.; and Gao, Y., (2004b). "The effect of fly ash on the fluidity of cement paste, mortar, and concrete", *In:* K. Wang, Ed. *International Workshop on Sustainable Development and Concrete Technology, Beijing, China, May 20-21, 2004,* CTRE

Lyman, O. R., (1993). "*An introduction to statistical methods and data analysis*", 4th ed., Duxbury Press

Malhotra, V. M., (1964). "Correlation between particle shape and surface texture of fine aggregates and their water requirement", *Materials Research & Standard*, December, pp.656-658

Mammoli, A. A., (2002). "Towards a reliable method for predicting the rheological properties of multiphase fluids", *Engineering Analysis with Boundary Elements*, Vol. 26, No. 9, pp. 747-755

Martys, N. S., (2005). "Study of a dissipative particle dynamics based approach for modeling suspensions", *Journal of Rheology*, Vol. 49, No. 2, pp. 401–424

Martys, N. S.; and Ferraris, C. F., (2003). "Simulation of SCC flow", *First North American Conference on the Design and Use of Self-Consolidating Concrete, November 12-13, 2002,* pp.27-30

Mehta, P. K.; and Monteiro, P. J. M., (1993). "*Concrete - structure, properties and materials*", 2nd ed., Prentice Hall

Mindess, S.; Young, J. F.; and Darwin, D., (2003). "*Concrete*", 2nd ed., Prentice Hall

Mora, C. F.; Kwan, A. K. H.; and Chan, H. C., (1998). "Particle size distribution analysis of coarse aggregate using digital image processing", *Cement and Concrete Research,* Vol. 28, No. 6, pp. 921-932

Mori, H.; and Tanigawa, Y., (1992). "Simulation methods for fluidity of fresh concrete", *Memoirs of the School of Engineering, Nagoya University,* Vol. 44, No. 1, pp. 71-134

Murata, J.; and Kikukawa, H., (1992). "Viscosity equation for fresh concrete", *ACI Materials Journal*, Vol. 89, No. 3, pp. 230-237

Nachbaur, L.; Mutin, J. C.; Nonat, A.; and Choplin, L., (2001). "Dynamic mode rheology of cement and tricalcium silicate pastes from mixing to setting", *Cement and Concrete Research,* Vol.31, No. 2, pp. 183-192

Nehdi, M.; and Rahman, M. A., (2004). "Estimating rheological properties of cement pastes using various rheological models for different test geometry, gap and surface friction", *Cement and Concrete Research,* Vol. 34, No. 11, pp. 1993-2007

Nehdi, M.; El Chabib, H.; and El Naggar, H. M., (2001). "Predicting performance of self-compacting concrete mixtures using artificial neural networks", *ACI Materials Journal*, Vol. 98, No. 5, pp. 394-401

Nehdi, M.; Mindess, S.; and Aïtcin, P. C., (1998). "Rheology of high-performance concrete: Effect of ultrafine particles", *Cement and Concrete Research,* Vol. 28, No. 5, pp. 687-697

Nehdi, M.; and Mindess, S., (1996). "Applicability and significance of rheometric tests for rheology of fluid and self-leveling high-strength concrete", *Transportation Research Record*, No. 1574, pp. 41-48

Nichols, F. P. Jr., (1982). "Manufactured sand and crushed stone in Portland cement concrete", *Concrete International: Design and Construction*, Vol. 4, No. 8, pp. 56-63

Noguchi, T.; Oh, S.G.; and Tomosawa, F., (1999). "Rheological approach to passing ability between reinforcing bars of self-compacting concrete", *RILEM International Symposium on Self-Compacting Concrete, 1999, University of Tokyo*

Oh, S. G.; Noguchi, T.; and Tomosawa, F., (1999). "Toward mix design for rheology of self-compacting concrete", *RILEM International Symposium on Self-Compacting Concrete, 1999, University of Tokyo*

Ouchi, M.; Edanarsu, Y.; Ozawa, K.; and Okamura, H., (1999). "Simple evaluation method for interaction between coarse aggregate and mortar's particles in self-compacting concrete", *Transactions of the Japan Concrete Institute*, Vol. 21, pp. 1-6

Papo, A.; and Piani, L., (2004a). "Flow behavior of fresh Portland cement pastes", *Particulate Science and Technology*, Vol. 22, No. 2, pp. 201-212

Papo, A.; and Piani, L., (2004b). "Effect of various superplasticizers on the rheological properties of Portland cement pastes", *Cement and Concrete Research*, Vol. 34, No. 11, pp. 2097-2101

Papo, A., (1988). "Rheological models for cement pastes", *Materials and Structures*, Vol. 21, No. 121, pp. 41-46

Park, C.K.; Noh, M.H.; and Park, T.H., (2005). "Rheological properties of cementitious materials containing mineral admixtures", *Cement and Concrete Research*, Vol. 35, No. 5, pp. 842-849

Pashias, N.; and Bogera, D. V., Summers J.; and Glenister D. J., (1996). "A fifty cent rheometer for yield stress measurement", *Journal of Rheology*, Vol. 40, No. 6, pp. 1179-1189

Perret, S.; Palardy, D.; and Ballivy, G., (2000). "Rheological behavior and setting time of microfine cement-based grouts", *ACI Materials Journal*, Vol. 97, No. 4, pp. 472-478

Persson, A. L., (1998). "Image analysis of shape and size of fine aggregates", *Engineering Geology,* Vol. 50, No. 1-2, pp. 177-186

Petit, J. Y.; Wirquin, E.; and Duthoit, B., (2005). "Influence of temperature on yield value of highly flowable micromortars made with sulfonate-based superplasticizers", *Cement and Concrete Research,* Vol. 35, No. 2, pp. 256-266

Petrou, M.; Wan, B.; Gardala-Maria, F.; Kolli, V. G.; and Harries, K., (2000a). "Influence of mortar rheology on aggregate settlement", *ACI Materials Journal*, Vol. 97, No. 4, pp. 479-485

Petrou, M. F.; Harries, K. A.; Gadala-Maria, F.; and Kolli, V. G., (2000b). "A unique experimental method for monitoring aggregate settlement in concrete", *Cement and Concrete Research*, Vol. 30, No. 5, pp. 809-816

Pfeuffer, M.; and Kusterle, W., (2001). "Rheology and rebound behaviour of dry-mix shotcrete", *Cement and Concrete Research,* Vol. 31, No. 11, pp. 1619-1625

Popovics, S., (1982). "*Fundamentals of Portland cement concrete: A quantitative approach - Vol. 1: Fresh concrete*", John Wiley & Sons, Inc.

Powers, T. C., (1968). "*The properties of fresh concrete*", John Wiley & Sons, Inc.

Quiroga, P. N.; and Fowler, D. W., (2004). "*The Effect of aggregates characteristics on the performance of Portland cement concrete*", ICAR Report 104-1F, International Center for Aggregates Research, The University of Texas at Austin

Rao, C.; Tutumluer, E.; and Kim, I. T.; (2002). "Quantification of coarse aggregate angularity based on image analysis", *Transportation Research Record*, Vol. 1787, No. 02-3124, pp. 117-124

Ravindrarajah, S. R.; Siladyi, D.; and Adamopoulos, B., (2003). "Development of high-strength self-compacting concrete with reduced segregation potential", *In:* O. Wallevik and *I.* Nielsson, Eds. *Proceedings of the 3rd International RILEM Symposium , Reykjavik, Iceland, 17-20 August 2003,* RILEM Publications, pp. 530-532

Ritchie, A. G. B., (1962). "The triaxial testing of fresh concrete", *Magazine of Concrete Research*, Vol. 14, No. 40, pp. 37-41

Roshavelov, T., (2005). "Prediction of fresh concrete flow behavior based on analytical model for mixture proportioning", *Cement and Concrete Research*, Vol. 35, No. 5, pp. 831-835

Rosquoet, F; Alexis, A.; Kjelidj, A.; and Phelipot, A., (2003). "Experimental study of cement grout: Rheological behavior and sedimentation", C*ement and Concrete Research*, Vol. 33, No. 5, pp. 713-722

Roussel, N.; Stefani, C.; and Leroy, R., (2005). "From mini-cone test to Abrams cone test: measurement of cement-based materials yield stress using slump tests", *Cement and Concrete Research*, Vol. 35, No. 5, pp. 817-822

Roy, D. M.; and Asaga, K., (1979). "Rheological properties of cement mixes: III The effects of mixing procedures on viscometric properties of mixes containing superplasticizer", *Cement and Concrete Research*, Vol. 9, No. 6, pp. 731-739

Rudzinski, L., (1984). "Effect of fly ash on the rheological behavior of cement pastes", *Materiaux et Constructions, Materials and Structures*, Vol. 17, No. 101, pp. 369-373

Saak, A. W.; Jennings, H. M.; and Shah, S. P., (2004). "A generalized approach for the determination of yield stress by slump and slump flow", *Cement and Concrete Research*, Vol. 34, No. 3, pp. 363-371

Saak, A. W.; Jennings, H. M.; and Shah, S. P., (2001). "New methodology for designing self-compacting concrete", *ACI Materials Journal*, Vol. 98, No. 6, pp. 429-439

Safawi, M. I.; Iwaki, I.; and Miura, T., (2004). "The segregation tendency in the vibration of high fluidity concrete", *Cement and Concrete Research,* Vol. 34, No. 2, pp. 219-226

Schowalter, W. R.; and Christensen, G., (1998). "Toward a rationalization of the slump test for fresh concrete: Comparisons of calculations and experiments", *Journal of Rheology*, Vol. 42, No. 4, pp. 865-870

Schramm, G., (1994). "*A practical approach to rheology and rheometry*", 1994, Gebrueder HAAKE GmbH

Shaughnessy, R. III; and Clark, P. E., (1988). "The rheological behavior of fresh cement pastes", *Cement and Concrete Research*, Vol. 18, No. 3, pp. 327-341

Shikata, T., (2001). "Viscoelastic behavior of ideal bimodal suspensions", *Chemical Engineering Science*, Vol. 56, No. 9, pp. 2957-2966

Smith, M. R.; and Collis, L., (2001). "*Aggregates – sand, gravel and crushed rock aggregates for construction purposes*" 3rd ed., The Geological Society London

Struble, L. J.; and Jiang, Q., (2004). "Effects of air entrainment on rheology", *ACI Materials Journal,* Vol. 101, No. 6, pp. 448-456

Struble, L. J.; Puri, U.; and Ji, X., (2001). "Concrete rheometer", *Advances in Cement Research*, Vol. 13, No. 2, pp. 53-63

Struble, L. J.; Szecsy, R.; Lei, W.; and Sun, G., (1998). "Rheology of cement paste and concrete", *Cement, Concrete, and Aggregate,* Vol. 20, No. 2, pp. 269-277

Struble, L. J.; and Lei, W., (1995). "Rheological changes associated with setting of cement paste", *Advanced Cement Based Materials,* Vol. 2, No. 6, pp. 224-230

Struble, L.; and Sun, G., (1995). "Viscosity of Portland cement paste as a function of concentration viscosity of Portland cement paste as a function of concentration", *Advanced Cement Based Materials,* Vol. 2, No. 2, pp. 62-69

Su, N.; Hsu, K.; and Chai, H., (2001). "A simple mix design method for self-compacting concrete", *Cement and Concrete Research*, Vol. 31, No. 12, pp. 1799-1807

Svermova, L.; Sonebi, M.; and Bartos, P. J. M., (2003). "Influence of mix proportions on rheology of cement grouts containing limestone powder", *Cement and Concrete Composites,* Vol. 25, No. 7, pp. 737-749

Tang, C.; Yen, T.; Chang, C.; and Chen, K., (2001). "Optimizing mixture proportions for flowable high-performance concrete via rheology tests", *ACI Materials Journal*, Vol. 98, No. 6, pp. 493-502

Tanigawa, Y.; and Mori, H., (1989). "Analytical study on deformation of fresh concrete", *Journal of Engineering Mechanics*, Vol. 115, No. 3, pp. 493-508

Tanigawa, Y.; Mori, H.; Tsutsui, K.; and Kurokawa, Y., (1986). "Simulation of deformation of fresh concrete by visco-plastic finite element analysis", *Transactions of the Japan Concrete Institute*, Vol. 8, pp. 57-64

Tattersall, G. H., (1991). "Workability and quality control of concrete", E & FN Spon

Tattersall, G. H.; and Banfill, P. F. G., (1983). "*The rheology of fresh concrete*", Pitman Publishing Inc.

Tattersall, G. H., (1976). "*The workability of concrete*", Viewpoint Publication, Cement and Concrete Association, Wexham Springs, Slough

Tattersall, G. H., (1973). "The rationale of a two-point workability test", *Magazine of Concrete Research*, Vol. 25, No. 84, pp. 169-172

Topcu, I. B.; and Kocataskin, F., (1995). "A two-phase composite materials approach to the workability of concrete", *Cement and Concrete Composites*, Vol. 17, No. 4, pp. 319-325

Vom Berg, W., (1979). "Influence of specific surface and concentration of solids upon the flow behavior of cement pastes", *Magazine of Concrete Research*, Vol. 31, No. 109, pp. 211-216

Wallevik, J. E.; and Wallevik, O. H., (1998). "Effect of eccentricity and tilting in coaxial cylinder viscometers when testing cement paste", *Nordic Concrete Research*, Vol. 18

Wallevik, O. H.; and Gjorv, O. E., (1990). "Modification of the two-point workability apparatus", *Magazine of Concrete Research*, Vol. 42, No. 152, pp. 135-142

Wang, K.; and Hu J., (2005). "Use of a moisture sensor for monitoring the effect of mixing procedure on uniformity of concrete mixtures", *Journal of Advanced Concrete Technology*, Vol. 3, No. 3

Wang, K.; Schlorholtz, S. M; Hu, J.; and Zhang, S., (2005). "Investigation into flow property measurements of low-slump concrete using vibrating slope apparatus (VSA)", *ASTM International Journal*, Vol. 2, No. 5

Williams, D. A.; Saak, A. W.; and Jennins, H. M., (1999). "The influence of mixing on the rheology of fresh cement paste", *Cement and Concrete Research*, Vol. 29, No. 9, pp. 1491-1496

Wills, M. H., Jr., (1967). "How aggregate particle shape influences concrete mixing water requirement and strength", *Journal of Materials*, Vol. 2, No. 4, pp. 843-865

Winslow, D. N., (1987). "Rate of absorption of aggregates", *Cement, Concrete and Aggregates*, Vol. 9, No. 2, pp. 154-158

Wong, G. S.; Alexander, A. M.; Haskins, R.; Poole, T. S.; Malone, P. G.; and Wakeley, L., (2001). "*Portland cement and concrete rheology and workability*," Final Report (FHWA-RD-00-025), U.S. Department of Transportation, Federal Highway Administration

Xie, Y.; Liu, B.; Yin, J.; and Zhou, S., (2002). "Optimum mix parameters of high-strength self-compacting concrete with ultrapulverized fly ash", *Cement and Concrete Research*, Vol. 32, No. 3, pp. 477-480

Yahia, A. and Khayat, K. H., (2001). "Analytical models for estimating yield stress of high-performance pseudoplastic grout", *Cement and Concrete Research,* Vol. 31, No. 5, pp. 731-738

Yang, M.; and Jennings, H. M., (1995). "Influences of mixing methods on the microstructure and rheological behavior of cement paste", *Advanced Cement Based Materials,* Vol. 2, No. 2, pp. 70-78

Yen, T.; Tang, C.; Chang, C.; and Chen, K., (1999). "Flow behaviour of high strength high-performance concrete", *Cement and Concrete Composites,* Vol. 21, No. 5-6, pp. 413-424

Zain, M. F. M.; Safiuddin, M.; and Yusof, K. M., (1999). "A study on the properties of freshly mixed high performance concrete", *Cement and Concrete Research*, Vol. 29, No. 9, pp. 1427-1432

APPENDIX. I FINE AGGREGATE SPECIFIC GRAVITY AND ABSORPTION

ASTM C128 specified the test method to determine the bulk density and the absorption of aggregate (after 24 hours in water) on the basis of the weight of SSD fine aggregate and apparent specific gravity. Since it is very difficult to have every batch of mortar mixed with SSD sand, OD sand was used in mortar mixing. Considering aggregate can absorbed a significant amount of water in the first several minutes after contact with it (Winslow, 1987), a modified method from ASTM C128 was therefore applied to estimate the absorption of fine aggregate within the first ten minutes, which is approximately the time from aggregate contact with water to completing the mortar rheology measurement. Notably, within the time period of five to ten minutes, no detectable additional amount of water absorption within the fine aggregate used in present study was found through measurement.

Figure A-1 Fine aggregate specificity gravity and absorption

In this modified method, the OD fine aggregate was place into the pycnometer (as shown in Figure A-1), in stead of the SSD aggregate. The estimation of absorption of fine aggregate within the first ten minutes is described below:

1. Measured the weight (around 800 grams) of OD sand and recorded the weight as Wt_s (g)

2. Calculated the volume of sand V_s (cm^3) according to specific gravity $G_{sb(OD)}$ calculated through ASTM C128 based on:

$$V_s = Wt_s / G_{sb(OD)} \times cm^3 / g \qquad \textbf{Equation A-1}$$

3. Placed the weighted sand into the pycnometer, filled it with water, and removed all the air bubbles by rolling, inverting and agitating the pycnometer
4. Measured the weight the pycnometer when it was full of water and sand and recorded the weight as Wt_{s+w} (g)
5. Calculated the weight of water including the absorbed amount of water by weight according to:

$$Wt_{w1} = Wt_{w+s} - Wt_s \qquad \textbf{Equation A-2}$$

6. Calculated the weight of water (excluding the absorbed amount of water) by volume times the density of water according to:

$$Wt_{w2} = (V_{py} - V_s) \times 1(g / cm^3) \qquad \textbf{Equation A-3}$$

7. Calculated the absorption based on the difference of the calculated Wt_{w1} (g) and Wt_{w2} (g) as:

$$Abs\% = (Wt_{w1} - Wt_{w2}) / Wt_s \times 100 \qquad \textbf{Equation A-4}$$

This calculated aggregate absorption is different from the aggregate absorption from ASTM C128, which reflected the aggregate absorption capacity. As shown in Figure 4-1, the calculated absorption from equation A-4 indicated the absorption of aggregate in the first ten minutes *(AbsAct%),* which is a little bit lower than the absorption earned according to ASTM C128 *(AbsTot%).*

The w/c were calculated by considering the amount of water absorbed into the aggregate. The modified w/c can be calculated according to:

$$w/c = (w/c)_{OD} - s/c \times Abs_{Act}\% \qquad \textbf{Equation A-5}$$

In this equation *w/c* is the actual water-to-cement ratio of mortar (in the period of mortar rheological test), $(w/c)_{OD}$ is the w/c calculated based on OD fine aggregate, s/c is the sand-to-cement ratio of mortar, and $Abs_{Act}\%$ is the absorption of fine aggregate within testing period (ten minutes).

The rates of water absorption were found to vary with size and type of aggregates. Results also showed that the actual absorption in the rheological testing period (*AbsAct%* as shown in Figure 4-1) was always a little lower than total absorption ability of aggregate (*AbsTot%* as shown in Figure 4-1). Most of the aggregates used in present research take in around 60% to 80% of their 24 hours uptake of water within the first several minutes.

APPENDIX II. CEMENT PASTE RHEOMETER TEST

Previous research found that by choosing a different rheology testing procedure, the shear stress versus shear rate curve might behave differently (Geiker et. al., 2002a). For example, the flow curves from the measurement might turn from linear to nonlinear, such as shown in Figure A-2. When the w/c of the cement paste are relative high (0.50 or 0.60), the shear rate and shear stress curve will not show linear behavior as expected from Bingham behavior. Specifically, when shear rates are higher than $70s^{-1}$, the slope will increase significantly, which indicates that more force is required to increase the flow rate in cement paste. This phenomenon may be caused by the flow current interference inside the measurement container because of the much higher flowability and liquid-like behavior of the cement paste.

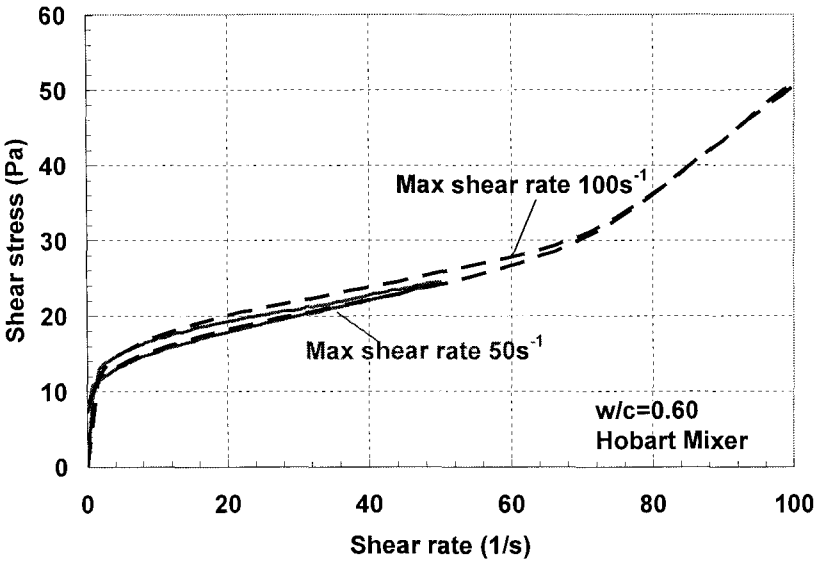

Figure A-2 Rheology test result from different test procedures

Results also illustrated that although the flow behavior is different at higher shear rate range, the downward part of the flow curves still fit very well with the results of flow curves when the shear rate is relatively low. In order to get consistent results, a maximum shear rate of $50s^{-1}$ instead of $100s^{-1}$ was therefore used for rheology test of cement paste.

APPENDIX III. CEMENT PASTE MINI-SLUMP CONE TEST

The mini-slump cone test was original developed by Kantro (1980) for evaluating the influence of WR on workability of cement paste. The test method had been successfully used to estimate the effect of different admixtures (Svermova et. al., 2003) and to evaluate the loss of workability with time (Kantro, 1980). The mini-slump cone test was found to be very efficient on evaluating the effect of chemical and mineral admixtures because the study object is neat cement pastes, which make the test more sensitive than slump test of concretes.

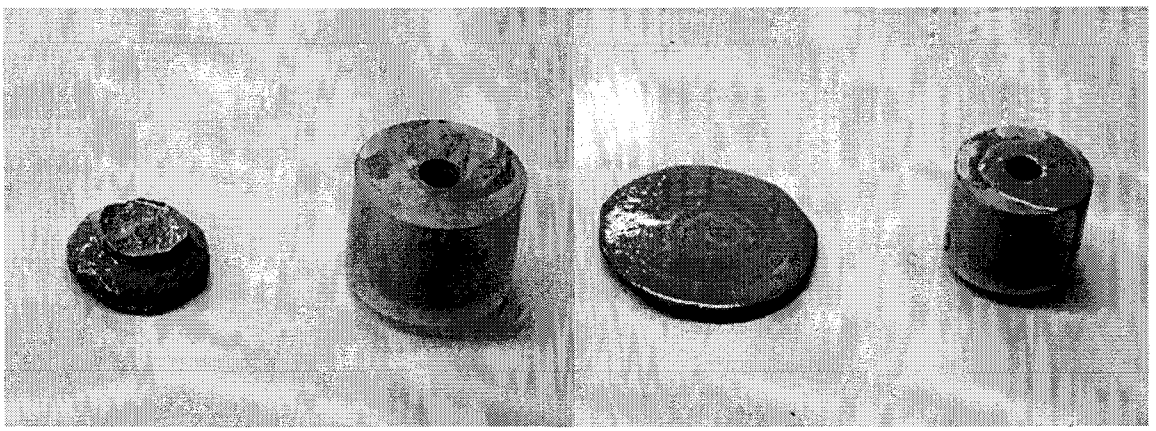

(a) Paste with low flowability **(b) Paste with high flowability**

Figure A-3 Mini-slump cone test

The mini-slump cone was performed similarly to the slump test. The resulting paste pat areas rather than heights are measured, and the results are expressed as the percentage of flow. As shown in Figure A-3, different paste may show different shapes of paste cone and different flow percentages. The procedure described below was used to estimate the flow of different cement in this research:

1. Put mini-slump cone on leveled and clean table surface,
2. Pour the paste into the mini-slump corn carefully, avoiding any run-offs on the slides,
3. Strike off the excess paste remaining on the top of the mini-slump cone with the spatula,
4. Lift the mini-slump cone vertically upward smoothly,

5. Use the calipers to measure the spread of the paste once the paste has stopped flowing (take the average of three diameter readings in different directions), and
6. Calculate the %Flow according to:

$$\%Flow = 100(S - D)/D \qquad \textbf{Equation A-6}$$

where S is the spread of the paste (mm) and D is the bottom diameter inside the mini-slump cone (mm).

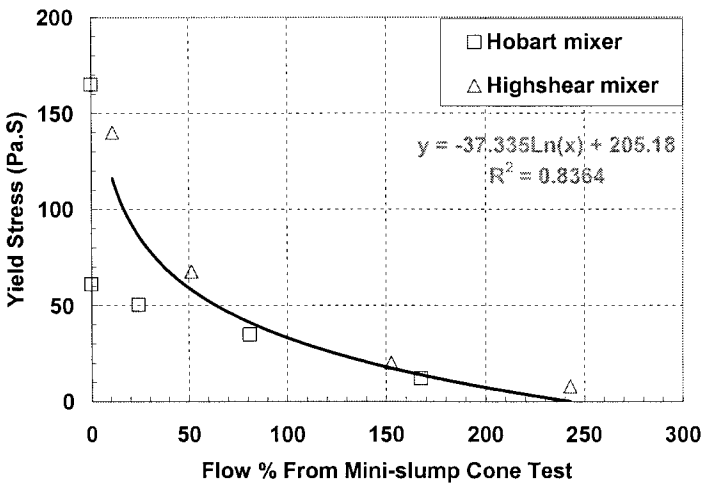

(a) Relationship with yield stress

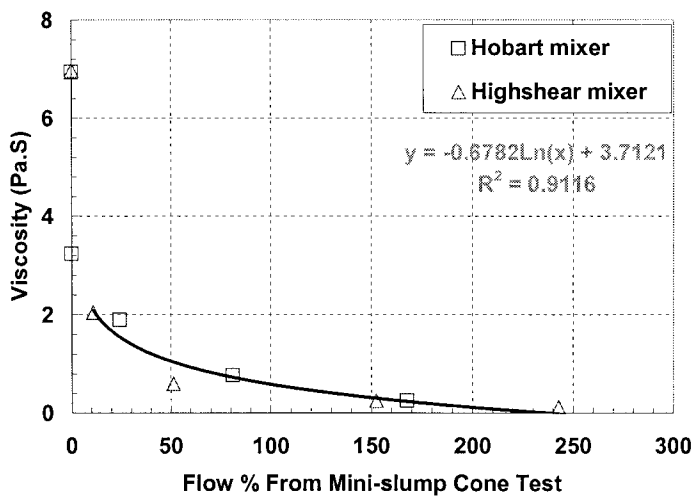

(b) Relationship with viscosity

Figure A-4 Comparison of mini-slump test results with rheological parameters

In the present study, the mini-slump cone test was performed in addition to the paste rheology test for different kinds of cement paste. The results showed that, as expected, cement paste with higher w/c would show higher flow percentage.

The comparison between flow percentage from the mini-slump cone test and the rheological parameters were also made. Results as shown in Figure A-4 indicate that the flow percentage from the mini-slump cone test can by some means be correlated to both viscosity and yield stress of cement paste, which indicates that when the mini-slump cone test is properly performed; the test result can be used to reflect the rheology behavior of the cement paste. Previous research by the author indicated that the flow from the mini-slump cone test have very strong correlations with the viscosity of the cement paste. This phenomenon was demonstrated clearly when different chemical admixtures were added, because the behavior of the paste is significantly different when different admixtures are added. However, in cement pastes with just different w/c, this difference cannot be clearly observed. This part of the research will not be described further in this dissertation.

APPENDIX IV. MODIFIED MORTAR FLOW TABLE TEST

The flow percentage of mortar was measured by the flow table test according to ASTM C1437, where the flow was determined by the spread diameter from a standard sample at certain amount of drops (25 drops) of flow table (Figure A-5). The spread diameter generally increases as the flow table drops, which is cause by the vibration generated from the drop which can overcome the yield stress inside mortar mixture. In general, a larger flow percentage indicated a better flowability of mortar.

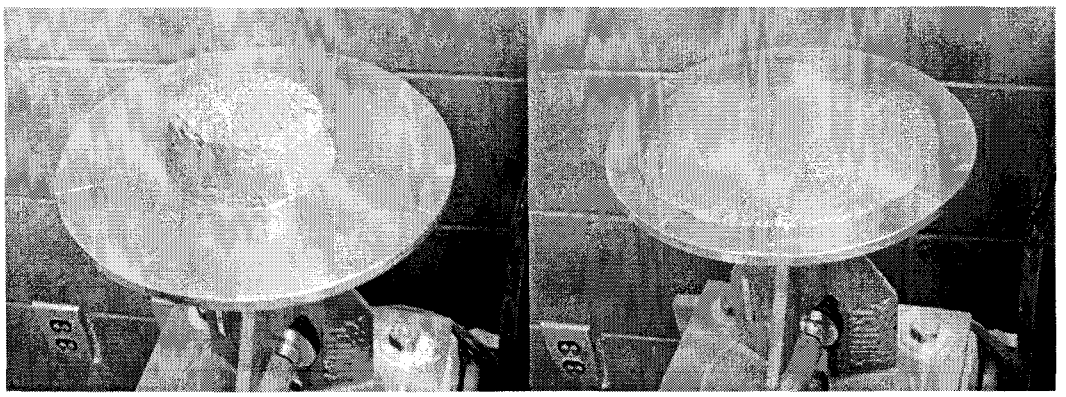

(a) Beginning of test **(b) End of test**

Figure A-5 Flow table test

The flow table test was original designed to determine the water content needed for a cement paste sample to obtain a given flow spread of 110±5 %. The test is performed with a standard flow table after the table drops 25 times. In the present research, a modified flow test was used. Instead of keeping the flow constant by varying the water content, the w/c and the s/c were change according to the design for each series of tests, and the resulting flows were then measured. The mortar sample was placed on the same flow table and subjected to 25 drops, and then the spread diameter of the sample was measured. The flowability of the mortar was expressed as a flow percentage - the percentage of the spread diameter over the original bottom diameter of the sample. Since the flow table has a limited diameter, some of the mortar with good flowability will flow off the flow table after fewer than 25 drops.

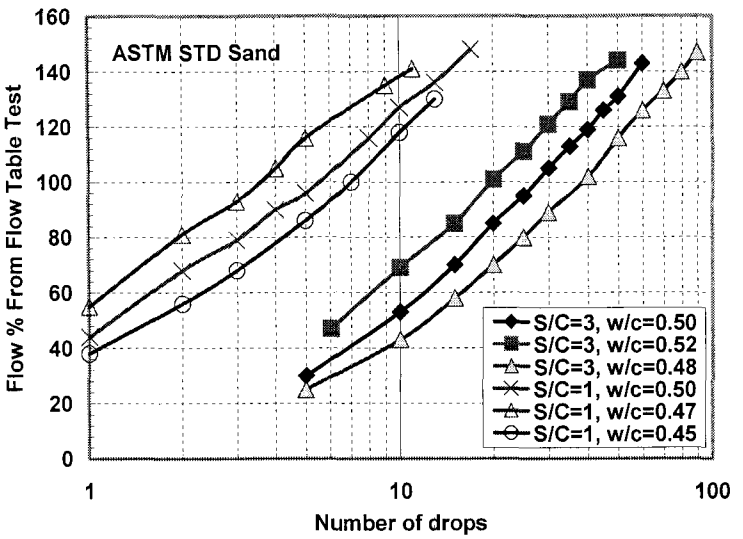

Figure A-6 Number of drops versus flow percentage of flow table test (adopted from Hu and Wang, 2005)

According to the previous research of the author (Figure A-6), the flow percentages have a linear relationship with drop numbers in a certain range using a logarithm scale. A series of tests using standard sand with different fine aggregate content and different w/c were performed. According to the study of the relationship between drop number and flow percentage over 40 batches of different mortar as shown in Figure A-7, a relationship as shown in the following equation can be obtained through regression:

$$F_{25} = F_t + 46.779(\ln 25 - \ln t) \qquad \textbf{Equation A-7}$$

where t is the drop number of flow table, F_{25} is the flow percentage of mortar at 25 drops, and F_t is the flow percentage of mortar at t drops. This flow table calibration curve as shown in Figure A-6 has a very high R square value of 0.98 and statistical analysis showed that the relationship is statistically significant.

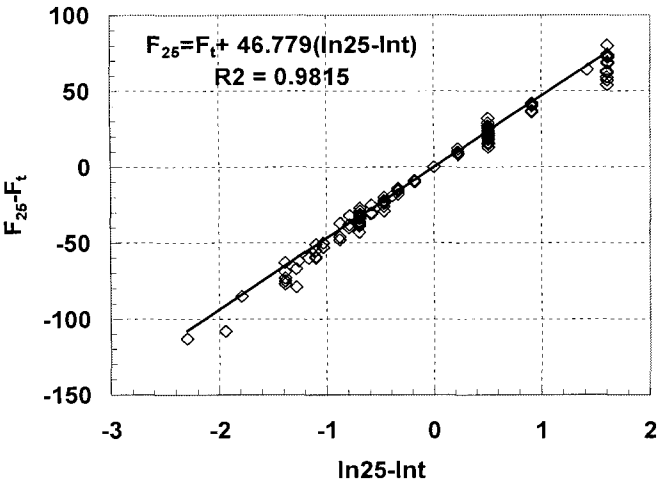

Figure A-7 Flow percentages for different drops number

The calibration of the flow table tests showed that the number of drops in the flow table test have a strong correlation with flow percentage. This relationship can be used to estimate the flow percentage value when the flowability is very high (flow percentage larger than 150%, which can not be measure through a regular flow table test). In the test of mortar with high flowability, which can be only performed less than 25 drops, the flow percentage of mortar was measured before the mortar flows out from the flow table. The flow number was then recorded, and the flow percentage calculated according to the above equation. This modified flow table test had been successfully applied to study the effect of w/c, content, type, size and gradation of fine aggregate on mortar workability (Hu and Wang, 2005).

APPENDIX V. MORTAR RHEOLOGY TEST RESULTS

Table A-1 Mortar rheology test results at s/c=1*

Riversand					Limestone				
Sand	w/c	η	τ_0	Flow %	Sand	w/c	η	τ_0	Flow %
S100	0.40	2.22	144.7	126	L100	0.40	2.80	164.7	113
S100	0.45	1.48	95.9	145	L100	0.45	1.80	115.2	132
S100	0.50	0.96	55.5	161	L100	0.50	0.90	56.0	149
S50	0.35	4.12	161.9	106	L50	0.36	4.92	160.7	108
S50	0.40	2.25	122.0	134	L50	0.41	2.44	121.9	129
S50	0.45	1.60	88.5	147	L50	0.46	1.69	79.4	143
S50	0.50	1.23	58.5	149	L30	0.35	4.75	180.3	117
S30	0.35	4.87	183.3	101	L30	0.40	2.74	132.7	132
S30	0.40	2.86	161.5	133	L30	0.45	1.81	83.0	153
S30	0.45	1.72	92.8	149	L16	0.35	3.46	161.7	116
S16	0.35	3.79	149.0	124	L16	0.40	2.35	110.0	141
S16	0.40	2.83	116.7	141	L16	0.45	1.59	71.7	153
S16	0.45	1.74	69.7	149	L8	0.35	3.39	170.0	111
S8	0.30	5.23	248.8	78	L8	0.40	2.74	89.9	138
S8	0.35	3.18	123.7	104	L8	0.45	1.62	68.0	153
S8	0.40	2.60	80.8	119					
G1	0.35	3.90	158.4	136					
G1	0.40	2.45	109.0	140					
G1	0.45	1.65	66.6	162					
G2	0.35	3.58	150.9	119					
G2	0.40	2.21	101.8	145					
G2	0.45	1.66	65.9	157					
G3	0.35	3.18	137.4	129					
G3	0.40	2.12	95.4	141					
G3	0.45	1.56	66.0	158					
G4	0.35	3.20	165.1	118					
G4	0.40	2.29	111.4	135					
G4	0.45	1.47	65.1	154					

*Yield stress (τ_0) with the unit of Pa, viscosity (η) with the unit of Pa·S

Table A-2 Mortar rheology test results at s/c=2*

Riversand					Limestone				
Sand	w/c	η	τ_0	Flow %	Sand	w/c	η	τ_0	Flow %
S100	0.46	2.80	173.6	88	L100	0.50	2.40	152.7	88
S100	0.51	1.92	129.3	121	L100	0.55	1.96	116.8	109
S100	0.56	1.40	68.2	138	L100	0.60	1.56	101.6	135
S100	0.61	0.82	41.2	158	L50	0.51	2.36	140.8	115
S50	0.41	2.44	226.2	77	L50	0.56	1.64	77.2	139
S50	0.46	2.33	122.3	116	L50	0.61	1.01	44.0	156
S50	0.51	1.68	89.7	146	L30	0.45	2.43	157.1	88
S50	0.56	0.98	51.5	143	L30	0.50	1.75	99.3	125
S30	0.40	3.70	220.2	64	L30	0.55	1.17	59.6	141
S30	0.45	1.96	155.5	131	L16	0.46	2.19	139.5	95
S30	0.50	1.46	91.0	131	L16	0.51	1.44	76.2	126
S30	0.55	0.94	52.9	147	L16	0.56	0.83	59.6	146
S16	0.36	3.86	241.0	81	L8	0.41	3.41	131.7	89
S16	0.41	3.83	189.5	116	L8	0.46	1.93	100.7	120
S16	0.46	2.10	113.7	144	L8	0.51	1.23	55.6	135
S16	0.51	1.59	77.9	144					
S8	0.36	4.53	203.9	87					
S8	0.41	2.97	122.0	125					
S8	0.46	1.92	92.2	141					
S8	0.51	1.29	71.1	150					
G1	0.40	2.25	165.6	119					
G1	0.45	1.81	85.7	137					
G1	0.50	1.03	48.0	155					
G2	0.40	2.35	181.7	113					
G2	0.45	1.99	105.7	138					
G2	0.50	1.16	52.7	153					
G3	0.40	2.74	168.1	114					
G3	0.45	1.82	98.5	143					
G3	0.50	1.19	50.9	150					
G4	0.40	2.75	155.9	118					
G4	0.45	1.72	87.8	140					
G4	0.50	1.26	53.0	149					
STD	0.45	2.22	100.0	129					
STD	0.50	1.30	56.7	140					
STD	0.55	0.80	34.8	155					

*Yield stress (τ_0) with the unit of Pa, viscosity (η) with the unit of Pa·S

Table A-3 Mortar rheology test results at s/c=3*

Riversand					Limestone				
Sand	w/c	η	τ_0	Flow %	Sand	w/c	η	τ_0	Flow %
S100	0.61	0.09	0.0	53	L100	0.66	2.28	182.8	92
S100	0.66	0.31	9.0	81	L100	0.71	2.05	94.6	104
S100	0.71	1.30	29.5	121	L100	0.78	1.80	104.7	114
S50	0.56	1.33	53.8	70	L50	0.56	0.57	34.5	46
S50	0.61	1.24	32.2	104	L50	0.61	1.75	107.2	76
S50	0.66	1.23	35.2	137	L50	0.66	1.89	98.8	98
S30	0.46	0.34	14.0	49	L30	0.56	2.39	172.7	53
S30	0.51	1.98	112.3	76	L30	0.61	2.13	135.5	92
S30	0.56	1.86	81.3	113	L30	0.66	1.52	89.7	112
S30	0.61	1.30	61.5	132	L16	0.46	0.00	0.0	83
S16	0.46	3.92	186.3	55	L16	0.51	3.75	174.7	69
S16	0.51	1.96	123.7	83	L16	0.56	2.07	119.9	70
S16	0.56	1.29	80.6	121	L8	0.46	NA	NA	50
S8	0.41	4.23	289.6	71	L8	0.51	NA	NA	83
S8	0.46	2.31	162.7	94	L8	0.56	NA	NA	105
S8	0.51	1.23	155.9	126					
G1	0.45	2.11	125.9	128					
G1	0.50	1.46	82.8	130					
G1	0.55	0.91	47.7	155					
G2	0.45	2.20	179.2	92					
G2	0.50	1.94	114.6	134					
G2	0.55	1.31	53.5	149					
G3	0.50	0.67	151.9	94					
G3	0.55	1.59	94.2	122					
G3	0.60	1.06	49.4	149					
G4	0.45	2.64	174.2	86					
G4	0.50	1.61	111.1	121					
G4	0.55	1.24	49.1	142					

*Yield stress (τ_0) with the unit of Pa, viscosity (η) with the unit of Pa·S

APPENDIX VI. RHEOLOGY OF MORTAR INSIDE CONCRETE

The concrete in the present study was designed to have three groups of mixtures with the same mortar properties (same s/c and w/c for mortar as indicated in Table 3-3). However, as shown in Figure A-8, the rheological parameters of mortar sieved through concrete vary significantly even within same group, which indicated that the mortar sieved from concrete have different rheological properties with the same design mortar mix through standard mixing method using the Hobart mixer. The phenomenon is probably caused by the changes in the internal structure of mortar through the hand sieving process, which further resulted in very different rheology parameters.

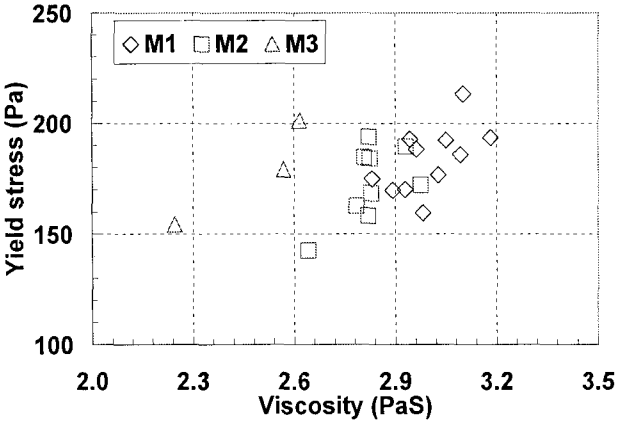

Figure A-8 Rheological parameters of mortar sieved from concrete

In the modeling study in chapter 8, the rheology parameters of mortar mixed with the Hobart mixer as shown in Table A-4 (all symbols are the same as in Table 3-3), in stead of the mortar sieved through concrete were used in the calculation.

Table A-4 Mortar rheology parameters from standard mortar mixing.

Mortar	Concrete	s/c	w/c	Yield stress (Pa)	Viscosity (PaS)
M1	Mix1, Mix2, and Mix3	1.75	0.45	70.1	1.55
M2	Mix4, Mix5, and Mix6	2.21	0.45	106.0	1.93
M3	Mix7, Mix8, and Mix9	2.60	0.50	119.7	1.96

APPENDIX VII. ARTIFICIAL NEURAL NETWORK ANALYSIS

Artificial neural network (ANN) modeling is inspired by the biological structure of neurons and the internal operation of human brain. Neural networks consist of multiple layers of many interconnected linear or nonlinear processing units operating in parallel fashion. Among all artificial neural network architectures, the back-propagation model is the most commonly used structure.

Multi-layer networks use a variety of learning techniques, and the most popular among them is back-propagation. The back-propagation model is normally composed of a network of elements as shown in Figure A-9. It is most useful for feed-forward networks (networks that have no feedback, or simply, that have no connections that loop). The term is an abbreviation for "backwards propagation of errors". Back-propagation requires that the transfer function used for the units (sometimes called neurons) be differentiable.

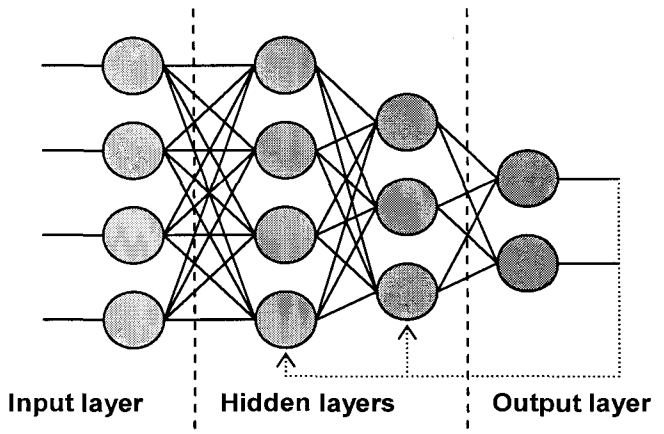

Figure A-9 Typical neural network element arrangement

The network shown is known as a fully connected network and every possible connection from a node in one layer is made to nodes in the next layer. More complex networks can be constructed that contain feedback and have the ability to better model dynamic responses.

The equations for calculating terms in the hidden layers and the output layer use non-linear relationships (Equation A-8 to A-10 were adopted from Nehdi et al., 2001). The output from a given node, *j*, in a network is given in terms of inputs to that node by:

$$U_j^l = \sum_{i=1}^{n} W_{ji}^l X_i^{l-1} + \theta_j^l \qquad \textbf{Equation A-8}$$

In this equation U_j^l is the current output state of the *j-th* processing element in layer *l*, W_{ji}^l is the weight on the connection joining the *i*-th element in layer *l-1* to the *j*-th element in layer *l*, θ_j^l is a threshold value assigned to neuron *j* in layer *l*, and X_i^{l-1} is the input coming from neuron *i* in layer *l-1* to neuron j in layer *l*.

The net input U_j^l is then modified by an activation function *f* to generate an output value Y_j^l as given by:

$$Y_j^l = f(U_j^l) \qquad \textbf{Equation A-9}$$

where *f* is traditionally a hyperbolic tangent, sigmoid, or sine function.

A continuous nonlinear sigmoid function is commonly used as an activated function in ANN because it meets the differentiability requirement needed in the back-propagation algorithm, and it is represented by:

$$f_j^l = \frac{1}{1+e^{-(U_j^l-\theta_j^l)}} \qquad \textbf{Equation A-10}$$

The weights, *W*, in the equation can be thought of as modeling memory. They are the weighting parameters in the equation system formed by the network and are fitted to allow the output of the neural network to produce the proper outputs. Neural networks are trained to produce proper outputs. This process sets the weighting parameters W_{ji}^l and is similar to performing a regression analysis. The neural network, formulated in the above fashion, creates a set of non-linear equations that are combined in a way in which the parameters can

be readily found. With this view, a process that can be modeled with a simple linear regression analysis should not require the more complex neural network approach. In addition, a neural network model is a form of multi-variable non-linear regression analysis.

In the modeling for mortar rheology, five different factors were selected as the input layer, which covered the mix design of mortar and the properties of the aggregate used. The five factors used are: s/c, w/c, the fineness modulus, the friction angle and the uncompacted void content of fine aggregate. A trial-and-error approach was adopted rules to determine the architecture of a back-propagation neural network. After trying several network architectures, one hidden layer with three hidden parameters was used for the present study.

As mentioned in chapter 7, the rheology test has a limitation when the aggregate percentage is high because the material can not perform liquid like anymore. In this research, the mortar with the calculated excess paste thickness less than zero was not included in the modeling analysis. Only 63 sets of data were used in the analysis, instead of all 136 sets.

Two different ANN analyses were performed in mortar rheology study, one is with all the 63 set of data as training data, the relative degree of importance of different input factors were evaluated through this study as shown in Figure 8-2. In addition to that, another ANN study was performed by randomly select around 80% of the data set as training data, and the rest 20% of the data set as testing data in order to evaluate the validity of the ANN model. The actual-to-predicted values of the mortar rheology parameters from these two ANN analyses are shown in Figure A-10 (Figure A-10 (a-1), (b-1) and (c-1) showed the results from analysis from all data sets, Figure A-10 (a-2), (b-2) and (c-2) showed the results from analysis from the selected training and testing data sets). Results showed that a relative high R^2 value was found through the model, which indicated that this model can capture the relationship between the input parameters and output. It was also observed that there was no dramatically decrease of the coefficient of correlation by using the testing set to evaluate the validity of the model, which indicated that the ANN analysis is appropriate .The model can be successful used to predict the rheology of mortar from the original mix design and aggregate properties.

Similar to mortar, six different parameters were selected as the input layer in the modeling for concrete rheology, which covered the mix design of concrete and the properties of the aggregate used. The six parameters used are: CA%, FA/c, w/c, the fineness modulus, the friction angle and the uncompacted void content of coarse aggregate. A trial-and-error approach was adopted in selecting the architecture of neural network. After trying several network architectures, one hidden layer with three hidden parameters was used for the present study.

Two different ANN analyses were performed in concrete rheology study, one is with all the 23 set of data as training data, the relative degree of importance of different input factors were evaluated through this study as shown in Figure 8-4. In addition to that, another ANN study was performed by randomly select around 80% of the data set as training data, and the rest 20% of the data set as testing data in order to evaluate the validity of the ANN model. The actual-to-predicted values of the concrete rheology parameters from these two ANN analyses are shown in Figure A-11 (Figure A-11 (a-1), (b-1) and (c-1) showed the results from analysis from all data sets, Figure A-11 (a-2), (b-2) and (c-2) showed the results from analysis from the selected training and testing data set). Results showed that a relative high R^2 value was found through the model, which indicated that this model can capture the relationship between the input parameters and output. It was also observed that although the coefficient of correlation by using the testing set to evaluate the validity of the model decrease, consider the relative small testing set and training set, the model is considered to be acceptable. The model still has potential to be used to predict the rheology of concrete from the original mix design and aggregate properties.

Results from the ANN analysis of the mortar and concrete rheology study showed that the purpose of evaluating the relative importance degree of different factors on mortar and concrete rheology was fulfilled. The ANN analysis can be successfully used to evaluate the degree of importance of different factors related to mix design and material properties on mortar and concrete rheology. The analysis in this section also indicated that ANN has potential be used to design concrete with desirable rheology properties, because it can make predictions directly from the mix design, which might be very helpful in practical use. The

designer can modify the mix design or aggregate gradation according to the desire workability parameters through this tool. The ANN model considered almost all of the parameters which might affect the rheology of concrete, including the mix design and aggregate properties, factors that were not considered by most of the other models described in Chapter 2. However, the size of the data set for using in the ANN analysis is still relative small, which limited the validity of the model. A successful ANN model still requires additional experiment data, especially material with aggregates of different properties from various sources.

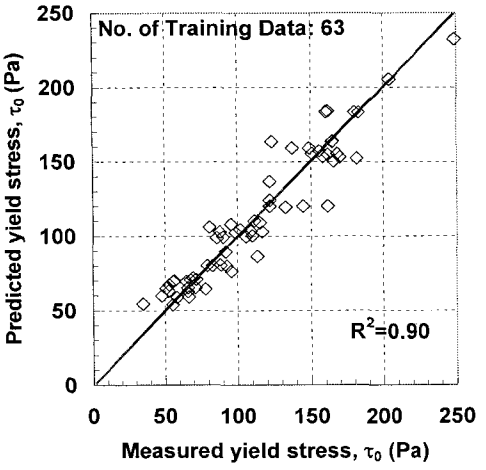

(a-1) Yield stress, all data

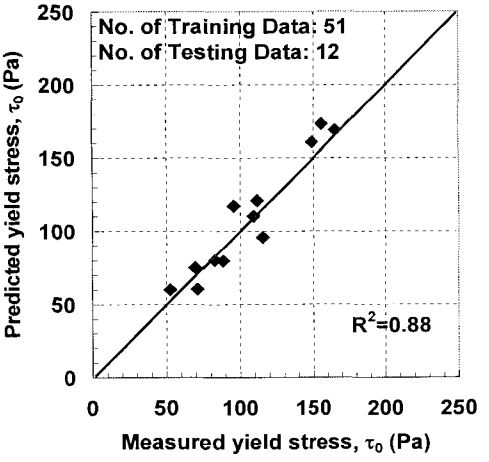

(a-2) Yield stress, testing data

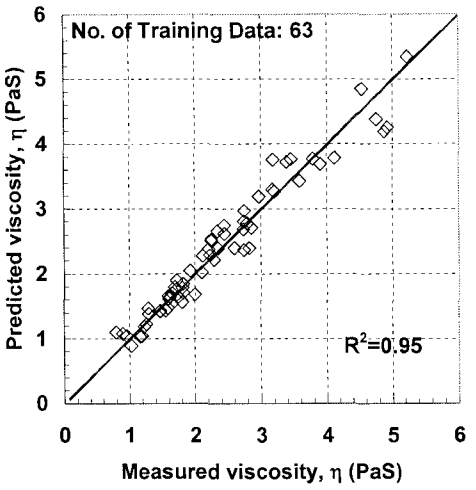

(b-1) Viscosity, all data

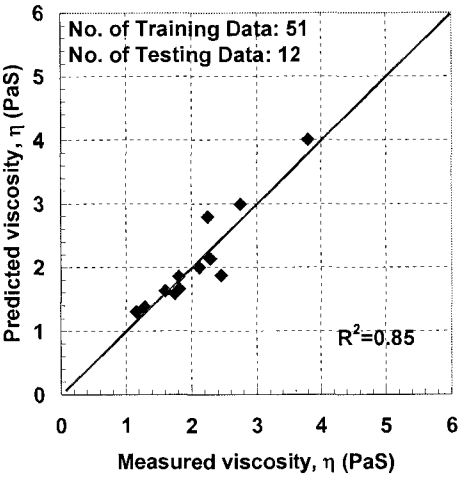

(a-2) Viscosity, testing data

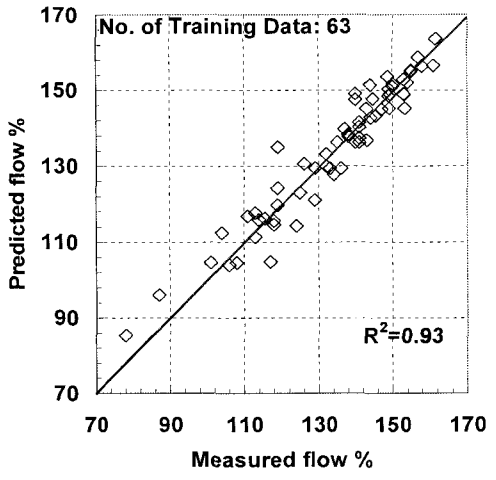

(c-1) Flow %, all data

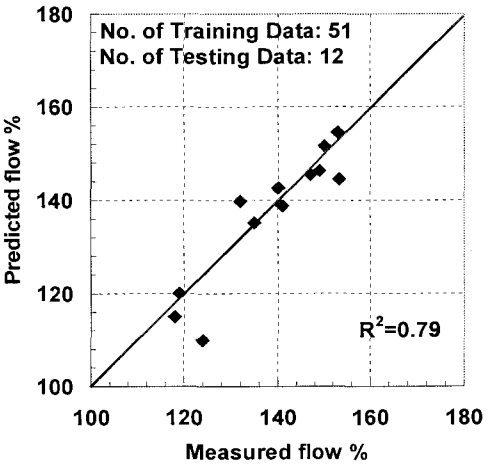

(c-2) Flow %, testing data

Figure A-10 Prediction of mortar rheological properties using ANN analysis

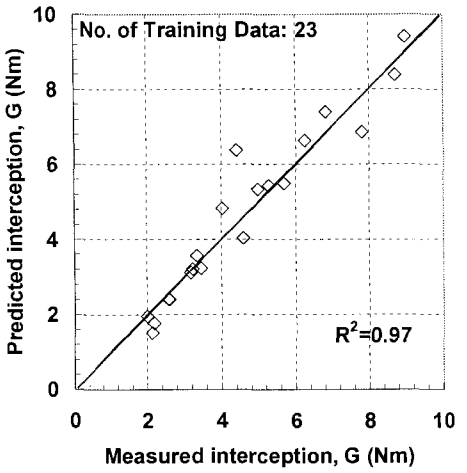

(a-1) Yield term, all data

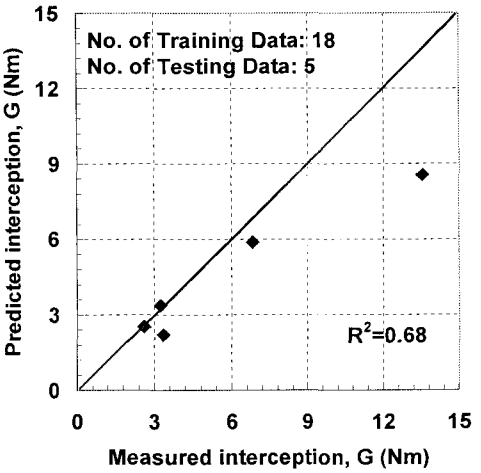

(a-2) Yield term, testing data

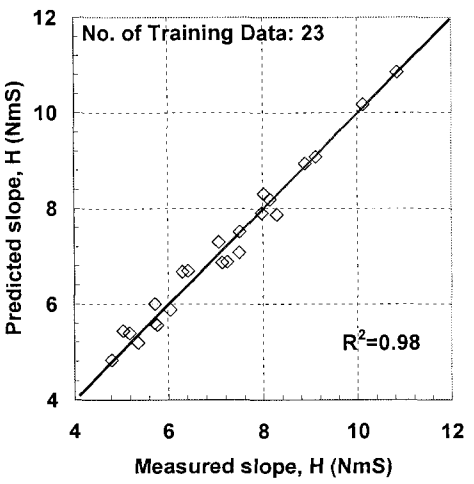

(b-1) Viscosity term, all data

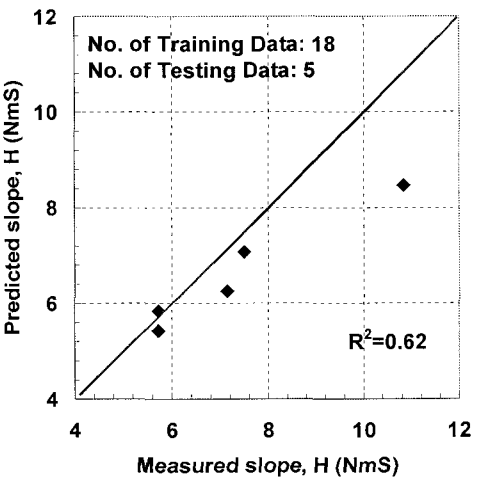

(a-2) Viscosity term, testing data

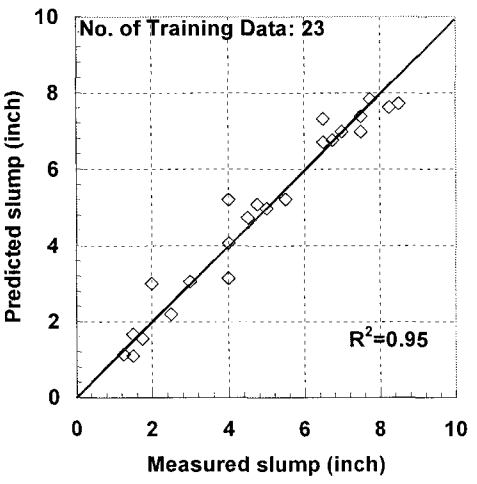

(c-1) Slump, all data

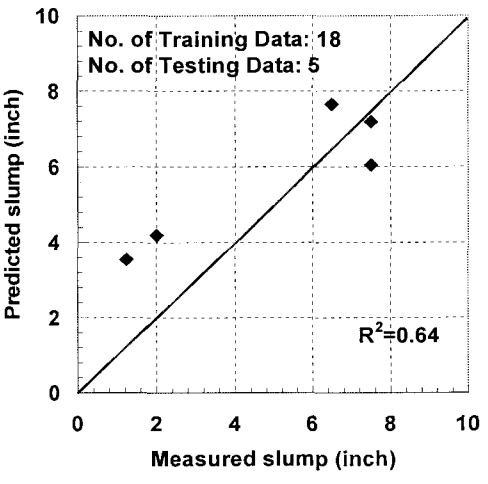

(c-2) Slump, testing data

Figure A-11 Prediction of concrete rheological properties using ANN analysis

APPENDIX VIII. REGRESSION ANALYSIS

Regression analysis was used as major tool to establish the rheology model based on the developed theoretical parameters. Some commonly-used statistical regression analysis terms are briefly described below (all equations and figures in this section are after Lyman, 1993 and Kleinbaum et al., 1998).

(1). Least Squares Method

The lease squares method is used to determine the best fitting line that minimizes the sum of the squares of the length of the vertical line segments drawn from the observed data points to the fitted line as shown in Figure A-12. The smaller the deviation of observed values, the closer the best fitting line to the data.

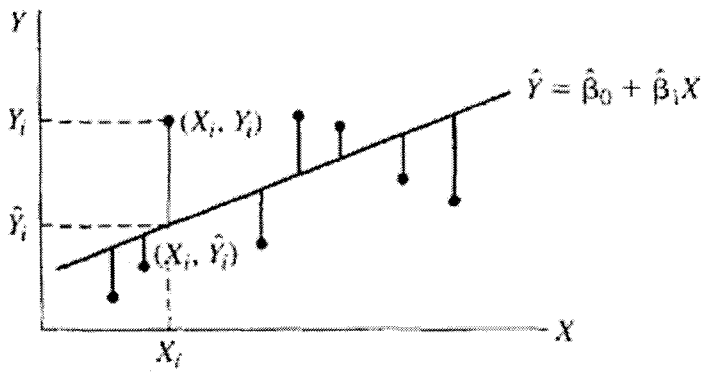

Figure A-12 Deviation of observed points from the fitting regression line (adopted from Kleinbaum et al., 1998)

The sum of the square of distance is given by:

$$\sum_{i=1}^{n}(Y_i - \hat{Y}_i)^2 = \sum_{i=1}^{n}(Y_i - \hat{\beta}_0 - \hat{\beta}_1 X_i)^2 \qquad \textbf{Equation A-11}$$

In this equation Y_i is the observed value, $\hat{Y}_i$ is the estimated value at X_i based on the fitted line, $\hat{\beta}_0$ is the intercept of the fitted line and $\hat{\beta}_1$ is the slope of the fitted line.

The least square solution is to find the $\hat{\beta}_0$ and $\hat{\beta}_1$ for which the sum of square is a minimum value. This minimum sum of the squares is called the sum of squares due to errors (or sum of square error, SSE). As long as these two parameters are determined, the best fitting line is fixed.

(2) Correlation Coefficient

The correlation coefficient is used to estimate how two random variables are linearly associated in a sample. The sample correlation coefficient is defined as:

$$r = \frac{\sum_{i=1}^{n}(X_i - \overline{X})(Y_i - \overline{Y})}{\sum_{i=1}^{n}(X_i - \overline{X})^2 \sum_{i=1}^{n}(Y_i - \overline{Y})^2} \qquad \textbf{Equation A-12}$$

Here r is a dimensionless quantity with values range from -1 to 1. The larger the $|r|$ is, the stronger the relation is. If r is 1 or -1, it means the linear association between X and Y is perfect. An $|r|$ value range from 0.85 to 1 is generally agreed to indicate a strong relationship, while $0.5 \leq |r| \leq 0.85$ means moderate relationship and $|r| < 0.5$ indicates weak relationship.

R^2 value measures the strength of the linear relationship between X and Y. If X is not used at all, the best predictor in this case would be the sample mean of the Y ($\overline{Y}$). The sum of the squares of deviations associated with the $\overline{Y}$ can be given by:

$$SSY = \sum_{i-1}^{n}(Y_i - \overline{Y})^2 \qquad \textbf{Equation A-13}$$

If the X is used to predict the Y, the sum of square due to errors is given by:

$$SSE = \sum_{i-1}^{n}(Y_i - \hat{Y}_i)^2 \qquad \textbf{Equation A-14}$$

The square of the sample correlation coefficient R^2 is given:

$$R^2 = \frac{SSY - SSE}{SSY}$$ **Equation A-15**

Therefore, R^2 gives the proportionate reduction in the sum of the squares of vertical deviations due to the use of the fitted line $\hat{Y} = \hat{\beta}_0 - \hat{\beta}_1 X$ instead of $\overline{Y}$. The larger the value of R^2, the greater the reduction in SSE is and the stronger the linear relationship between X and Y. For example, a R^2 = 0.80 means 80% of the variation in Y can be explained with the help of X.

(3). Test for significance

In order to take the uncertainties of using a sample into account and to assess whether the fitted line helps to predict Y, it is necessary to test statistical hypotheses about the unknown parameters in the fitted line.

For the fitted line $\hat{Y} = \hat{\beta}_0 - \hat{\beta}_1 X$, the estimators $\hat{\beta}_0$ and $\hat{\beta}_1$ are normally distributed with respect to β_0 and β_1. These estimators together with the estimates of their variance can be used to test statistics based on the t distribution as shown in Figure A-13.

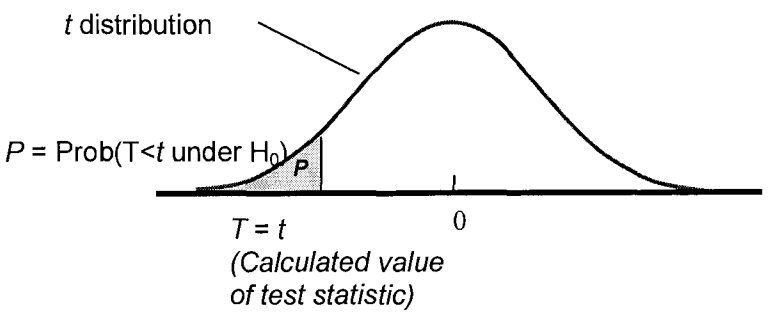

Figure A-13 Explanation of the definition of p-value

In the present study, the null hypothesis is that the mean of the estimator is zero, and the significance level is 0.05. More specifically, to test the null hypothesis H_0: $\beta_1=0$, the test statistic used in expressed as:

$$t = \frac{\hat{\beta}_1}{S_{\hat{\beta}_1}}$$ **Equation A-16**

In this equation $S_{\hat{\beta}_1}$ is the standard error of the estimated parameter $\hat{\beta}_1$, and t is the t-ratio of test hypotheses. The t-ratio of estimators $\hat{\beta}_0$ can be calculated in similar way.

The test statistic has the t distribution with n-2 degrees of freedom when H_0 is true. Another generally used parameter is F-ratio, which is the traditional test statistic to test that the term effect is zero. Base on the calculated t-ratio or F-ratio, the p-value can be found from the table of percentiles of the t distribution or F distribution. If there is no relationship between X and Y, the probability of getting a similar sample is equal to p-value. The p-value can be used to determine whether to reject or accept the null hypothesis. If the p-value is smaller than 0.05, the null hypothesis can generally been rejected, which means the X does help to predict Y in 0.05 significance level.

The ANOVA table conducted using JMP statistic analysis software was used to provide overall summary of multiple regression analysis in the present study, which gives the information of the significance level of different parameters used in modeling.

(4). Stepwise Method

In the present study, several possible parameters can be used in the statistical model. The stepwise regression method was conducted in this dissertation using JMP statistic analysis software, which gives a stepwise regression for a single continuous or categorical y and all types of effects. The significance level of choosing the parameter used in present research is 0.05. The model has all possible statistical significant parameters (with a p-value less than 0.05) and the highest R^2 value was chosen as the final models in stepwise regression analysis.

(5). Linear Regression use Logarithm Parameters

The significance analysis generally can only be performed in linear regression, which is not suitable for the present modeling study. A linear regression using logarithm parameters was therefore applied. The logarithm values of the input and output parameters instead of the original values were used in the regression analysis. The following equation can be obtained:

$$\ln Y = A + B\ln X_1 + C\ln X_2 \qquad \textbf{Equation A-17}$$

In this equation X_1 and X_2 are the estimated terms and A, B, and C are the parameter estimates from regression analysis. Equation A-17 can be transformed into a regression equation as shown in Equation A-18, while the significance level of different parameters X_1 and X_2 can still be calculated according to the linear regression analysis.

$$Y = e^{A} X_1^{\,B} X_2^{\,C} \qquad \textbf{Equation A-18}$$

ACKNOWLEDGEMENTS

I would like to express my deepest gratitude to my major advisor, Dr. Kejin Wang, for her support, advice, and direction during this study. I am also very grateful for Dr. James Cable, Dr. Halil Ceylan, Dr. Kristen Constant, Dr. Brian Coree, and Dr. David White's time and efforts on serving my Ph.D. committee and providing valuable comments on my dissertation.

Ideas, helps and supports provided by Zhi Ge, Sunghwan Kim, Ping Lu, Michael Heitzman and Ha Pham are also essential for me to complete my study and research. The following individuals have provided valuable contributions in helping me to finish the experiments: Ben Hermanson, Longjie Hong, Gang Lu, Tyson Rupnow, and Shihai Zhang. All tests in presented study were performed at the Portland Cement Concrete (PCC) Pavement and Materials Research laboratory, Iowa State University. I like to acknowledge the technicians of PCC lab Bob Steffes, Heath Gieselman, Bryan Zimmerman, and Jeremy McIntyre for their assistance in the lab.

I would like to express my gratitude to my wife, Yaoling, this work would not have been possible without the support and encouragement of her. I want to thank my parents, family and friends for the support they provided.

Ames, November 2005